

**EVALUATION OF THE EFFECTS OF SOLAR ULTRAVIOLET
RADIATION ON THE GROWTH OF *VIBRIO CHOLERAE* AND ON
THE SECRETION OF THE CHOLERA TOXIN**

by

CORNELIUS CANO SSEMAKALU

submitted in accordance with the requirements for

the degree of

MASTER OF SCIENCE

in the subject

LIFE SCIENCE

at the

UNIVERSITY OF SOUTH AFRICA

SUPERVISOR: PROF M PILLAY

CO- SUPERVISOR: DR E BARROS

PROF SR MAGANO

NOVEMBER 2010

DEDICATION

For my wonderful Mother (Nakimbowa Catherine),
Whose love, humility, creativeness and perseverance
Shows no boundaries

DECLARATION

I, Ssemakalu Cano Cornelius hereby declare that Evaluation of the effects of Solar Ultraviolet Radiation on the growth of *Vibrio cholerae* and on the secretion of the cholera toxin is my own work and that all the sources that I have used or quoted have been indicated and acknowledged by means of complete references. The thesis has not been submitted or will not be submitted to a university or any institution for the award of a degree.

Signed (Author)

Date

Signed (Supervisor)

Date

Signed (Co-supervisor)

Date

ABSTRACT

Cholera is a water-borne disease that continues to ravage resource poor communities around the world especially those in developing countries. The disease is caused by *Vibrio cholerae* microorganisms whose natural habitat is the aquatic ecosystem. It is believed that this microorganism prior to becoming the primary cause of cholera acquired virulence factors expressed by two separate genetic elements. These genetic elements are known as VPI Φ and CTX Φ were acquired in that order for known physiological reasons. However only *V. cholerae* in possession of the CTX genetic element are capable of causing cholera disease. At present only two serotypes are known to have the ability to cause cholera and these are *V. cholerae* serotypes O1 and O139.

SODIS (Solar disinfection) is an extremely low cost refined technology that can be used for the disinfection of water especially in areas where there is a considerable amount of sunshine. Although this technology is a composite of various factors the underlying principle is the use of solar ultraviolet radiation (SUVR). The preliminary target of SUVR is the cytoplasmic membrane and this was confirmed by flow cytometric analysis. The consequences of leaky cytoplasmic membrane include cellular death to the microorganism as well as an increase in cholera toxin secretion.

The main objective of this study was to investigate the effect of solar ultraviolet radiation on the growth of *V. cholerae* and on the secretion of cholera toxin and to provide supporting information for the use of SODIS in South Africa while observing the possible role that climate may play in the onset of cholera disease.

The initial part of the study evaluated the culturability, biomass increase and cholera toxin secretion in both a nutrient poor and a nutrient rich media by two toxigenic and one non toxigenic strain of *V. cholerae*. A series of pH and temperature combinations were used to achieve this objective. The result revealed that the microorganisms survived in both media. An increase in biomass was observed for all the bacteria grown in the nutrient rich media whereas in the poor nutrient media the bacteria remained culturable but no increase in biomass was observed. Interestingly lower temperatures seemed to provide more optimal growth conditions while high temperature on most occasions favoured cholera toxin secretion, in both media.

The second part of the study required the exposure of the microorganisms to SUVR. A SODIS approach was used with a few modifications. The *V. cholerae* strains were exposed to solar radiation during all the seasons of the year. Evaluation of the viability, the increase in biomass and the detection of cholera toxin secretion was determined after each exposure to solar radiation. The results seem to suggest that the effect of SUVR depended on the season of the year, the nature of the media, strain, solar conditions and in the duration of solar exposure, in no particular order. The secretion of cholera toxin was mainly dependent on the media used, the season of the year and on the serotype of the strain.

This study represents the first report on the evaluation of SUVR for the disinfection of water under South African conditions (Pretoria area) during all seasons of the year with variations in solar radiation levels and temperature. Furthermore what actually happened to *V. cholerae* during solar exposure in terms of cell morphology, cell viability and secretion of cholera toxin is also reported and this can give an insight of the possible role that SUVR may play in the onset of cholera.

The main recommendation emanating from this study is the sensitisation of communities worldwide about the capacity that, SUVR carries to lighten the burden of communicable water borne diseases especially, in resource limited areas through the implementation of SODIS.

ACKNOWLEDGEMENTS

My deepest gratitude goes to my supervisors, Prof. Michael Pillay and Dr. Eugenia Barros for their invaluable support, encouragement, mentorship and input throughout the entire duration of this degree.

I would like to acknowledge the Mandela Rhodes Foundation's (MRF) for awarding me the prestigious Mandela Rhodes Scholarship which is an embodiment of the Pan African Vision for a United Africa of which I am a firm believer.

I would like to thank the University of South Africa (UNISA) for its research support and providing me with this opportunity as well as the Council for Scientific and Industrial Research (CSIR) Biosciences for providing the project, the environment and use of their research facilities.

I would like to thank my dearest family and friends Thomas Mataka, Makonde Kutama, Tsepang Majara, Col. Tim Terry, Charlotte Mashaba, Magambo Mwiza Gloria and Dr. Eunice Ubomba-Jaswa. Thank you for your unquantifiable moral support and encouragement.

I would like to thank anyone else whom I could have inadvertently missed for your support.

ABBREVIATIONS AND ACRONYMS

WHO	World Health Organisation
TCP	Toxin Coregulated Pilus
ACF	Accessory Colonization Factors
CT	Cholera Toxin
CTB	Cholera Toxin B
CTA	Cholera Toxin A
SODIS	Solar Disinfection
EPEC	Entropathogenic <i>Escherichia coli</i>
SUVR	Solar Ultra Violet Radiation
UVR	Ultra Violet Radiation
PET	Polyethylene Terephthalate
UVA	Ultra Violet A
UVB	Ultra Violet B
UVC	Ultra Violet C
DNA	Deoxyribonucleic Acid
RNA	Ribonucleic Acid
nm	Nanometres
NER	Nucleotide Excision Repair
PER	Photoenzymatic Repair
FCM	Flow cytometry
cFDA	Carboyfluorescien diacetate
FDA	Fluorescein diacetate
CTC	5-Cyano-2,3-ditolyl tetrazolium
CFDA-AM	5-Carboxyfluorescein diacetate; acetoxymethyl ester
PCR	Polymerase Chain Reaction
NCTC	National Collection of Type Cultures

LB	Luria Broth
DWA	Department of Water Affairs
OD	Optical Density
PBS	Phosphate Buffered Saline
GInaFiT	Gearaerd and Van Impe inactivation model fitting tool
RMSE	Root Mean Sum of Squared Errors
CFU	Colony Forming Units
ml	Millilitres
CSIR	Centre for Scientific and Industrial Research
HRP	Horse reddish peroxidise
TMB	Tetramethylbenzidine
BSA	Bovine Serum Albumin
EB	Ethidium Bromide
PI	Propidium Iodide
Sybr Green I	Sybr Green I
NRE	Natural Resources and Environment
DMSO	Dimethylsulfoxide
CPD	Cyclobutane pyrimidine dimers

TABLE OF CONTENT

DEDICATION	I
DECLARATION	II
ABSTRACT	III
ACKNOWLEDGEMENTS	V
ABBREVIATIONS AND ACRONYMS	VI
TABLE OF CONTENT	VIII
LIST OF FIGURES	XII
LIST OF TABLES	XV
CHAPTER 1	1
1 BACK GROUND AND LITERATURE REVIEW	1
1.1 Introduction	1
1.2 Cholera Disease and <i>Vibrio cholerae</i>	1
1.2.1 Virulence and Pathogenicity of <i>Vibrio cholerae</i>	2
1.2.1.1 Cholera Toxin.....	3
1.3 An Overview of Cholera Disease	4
1.4 Solar Disinfection of Water.....	5
1.5 Solar Ultraviolet Radiation.....	7
1.5.1 Factors Influencing Aquatic and Terrestrial SUVR on Earth	7
1.5.2 The Effects of SUVR on Biological Molecules or Systems	9
1.5.2.1 Absorption Characteristics of Major Biomolecules	9
1.5.2.2 The Action Spectra and Photoproducts	9
1.5.2.3 SUVR Damaged DNA Repair Mechanisms.....	10
1.5.3 Effects of UVA on Biological Systems	11
1.5.4 Effects of UVB on Biological Systems	11
1.6 Flow Cytometry.....	12
1.6.1 Benefits/ Applications of Flow Cytometry in Microbiology	14
1.6.2 Cellular viability and activity assessment using FCM.....	15
1.6.3 Different approaches for assessing viability using flow cytometry	15
1.6.3.1 Membrane Integrity	15

1.6.3.2	Membrane Potential.....	16
1.6.3.3	Membrane Function.....	16
1.6.3.4	Metabolic activity.....	17
1.6.3.5	Respiratory activity	17
1.7	Viable But Non-Culturable States	17
1.7.1	Induction of VBNC.....	19
1.7.2	“Dangers” surrounding VBNC	19
1.8	Modelling of Bacterial Survival	20
1.8.1	GInaFiT Modelling	20
1.8.1.1	Log-linear model covering shape I survivor curves	21
1.8.1.2	Log-linear model with shoulder and/or tailing covering shapes I, II, III and IV survivor curves	22
1.8.1.3	The Weibull type models’ covering shapes I, VI and VIII survivor curves.....	22
1.8.1.4	The biphasic models covering shapes I, II, IV and VII survivor curves	23
1.9	Significance and Purpose of the Study	23
1.10	Aims and Objectives.....	24
CHAPTER 2		25
2	MATERIALS AND METHODS.....	25
2.1	Bacterial Strain	25
2.2	Resuscitation of the Bacterial Strains.....	25
2.3	Determination of Growth Curves	26
2.3.1	Preparation of Growth Media	26
2.3.1.1	Growth curve of <i>V. cholerae</i> in LB	26
2.3.1.2	Growth Kinetics of <i>V. cholerae</i> in LB.....	26
2.3.2	Growth curve of <i>V. cholerae</i> in Ground Water.....	27
2.3.2.1	Modelling of <i>V. cholerae</i> survival in Ground water using the GInaFiT tool 27	
2.4	Sample Preparation Prior and Enumeration after SUVR Exposures.....	27
2.5	Solar Ultra Violet Radiation measurement.....	28
2.6	Cholera Toxin Determination using ELISA.....	29
2.6.1	Ganglioside G _{M1} Cholera Toxin Assay.....	29
2.7	Flow cytometric Analysis.....	30

2.7.1	Preparation of <i>V. cholerae</i> for Flow Cytometry	30
2.7.2	Flow-cytometric measurements	30
2.7.3	Data analysis	31
CHAPTER THREE		32
3	RESULTS.....	32
3.1	Growth Properties of <i>Vibrio cholerae</i>	32
3.2	Effect of the pH of LB and Temperature on the Growth of <i>V. cholerae</i>	32
3.2.1	Growth of the O1 Serotype	32
3.2.2	Growth of the O139 Serotype	34
3.2.3	Growth of the 1009 strain	36
3.3	Effect of the pH of Ground Water and Temperature on the Growth of <i>V. cholerae</i>	39
3.3.1	Ground Water at 25°C.....	39
3.3.2	Ground Water at 30°C.....	41
3.3.3	Ground Water at 37°C.....	43
3.4	Optimal growth Conditions	46
3.4.1	Growth of <i>V. cholerae</i> in Luria Broth.....	46
3.4.1.1	Growth Rate and Relative Increase in Biomass of <i>V. cholerae</i> in LB	47
3.4.2	Growth of <i>V. cholerae</i> in Ground water	49
3.5	Solar Ultraviolet Radiation.....	51
3.6	SUVR and Temperature Pattern.....	51
3.7	Exposure of <i>V. cholerae</i> to SUVR	53
3.7.1	SUVR Exposures during Spring	54
3.7.1.1	Ground water	55
3.7.1.2	LB.....	57
3.7.2	SUVR Exposures during Summer	59
3.7.2.1	Ground water	60
3.7.2.2	LB.....	62
3.7.3	SUVR Exposures during Autumn.....	64
3.7.3.1	Ground water	65
3.7.3.2	LB.....	67
3.7.4	SUVR Exposures during Winter.....	69
3.7.4.1	Ground water	70

3.7.4.2	LB.....	72
3.8	Flow Cytometric Analysis.....	75
3.8.1	Optimization of flow cytometry for <i>Vibrio cholerae</i>	75
3.8.1.1	Staining properties of the fluorescent dyes	75
3.8.1.2	Staining Characteristics of the Single Dyes	76
3.8.1.2.1	Sybr Green I Staining	76
3.8.1.2.2	Carboxyfluorescein diacetate Treatment.....	77
3.8.1.2.3	Propidium Iodide Staining.....	79
3.8.1.2.4	Ethidium Bromide Staining.....	81
3.8.1.3	Staining Characteristics of Dye Mixtures.....	82
3.8.1.3.1	Sybr Green and Propidium Iodide	82
3.8.1.3.2	Sybr Green I and Ethidium Bromide.....	84
3.8.1.3.3	Carboxyfluorescein diacetate and Propidium Iodide	85
3.9	Flow cytometric analysis of solar radiated samples.....	87
3.9.1	Flow cytometric analysis of solar exposed <i>V. cholerae</i> in ground water	88
3.9.2	Flow cytometric analysis of solar exposed <i>V. cholerae</i> strains in LB	98
CHAPTER 4		106
4	GENERAL DISCUSSION AND CONCLUSION	106
4.1	Growth of <i>V. cholerae</i> and Toxin Secretion under Laboratory Conditions	107
4.2	Growth of <i>V. cholerae</i> and Toxin Secretion during Exposures to Solar Radiation	108
4.3	Conclusion.....	111
4.4	Recommendations	112
References.....		113

List of Figures

Figure 1: Types of inactivation curves.....	22
Figure 2: Relative increase in the biomass of <i>V. cholerae</i> serotype O1 grown at 37°C in LB.	33
Figure 3: Relative increase in the biomass of <i>V. cholerae</i> serotype O1 grown at 30°C in LB.	33
Figure 4: Relative increase in the biomass of <i>V. cholerae</i> serotype O1 grown at 25°C in LB.	34
Figure 5: Relative increase in the biomass of <i>V. cholerae</i> serotype O139 grown at 37°C in LB.	34
Figure 6: Relative increase in the biomass of <i>V. cholerae</i> serotype O139 grown at 30°C in LB.	35
Figure 7: Relative increase in the biomass of <i>V. cholerae</i> serotype O139 grown at 25°C in LB.	35
Figure 8: Relative increase in the biomass of <i>V. cholerae</i> strain 1009 grown at 37°C in LB.	36
Figure 9: Relative increase in the biomass of <i>V. cholerae</i> strain 1009 grown at 30°C in LB.	37
Figure 10: Relative increase in the biomass of <i>V. cholerae</i> strain 1009 grown at 25°C in LB.	37
Figure 11: Stack chart showing the highest relative increase in the biomass	38
Figure 12: Cholera toxin secretion by the virulent <i>V. cholerae</i> serotypes.	39
Figure 13: Inactivation curves of <i>V. cholerae</i> serotypes.....	40
Figure 14 (a): Inactivation curves of <i>V. cholerae</i> serotypes.....	42
Figure 15: Inactivation curves of <i>V. cholerae</i> serotypes	44
Figure 16: Cholera toxin secretion by the virulent <i>V. cholerae</i> serotypes.	46

Figure 17:Growth curves of the <i>V. cholerae</i> serotypes.....	47
Figure 18: Bar and line graph showing the relative increase in biomass and relative growth rates.	48
Figure 19: The best GInaFiT model describing the survival of <i>V. cholerae</i> serotype O1.	49
Figure 20: The best GInaFiT model describing the survival of <i>V. cholerae</i> serotype O139. .	50
Figure 21: The best GInaFiT model describing the survival of <i>V. cholerae</i> strain 1009.....	50
Figure 22: Daily maximum levels.....	52
Figure 23: Inactivation kinetics of solar exposed <i>V. cholerae</i>	56
Figure 24: The effect of SUVR on the release of cholera toxin	57
Figure 25: Representative growth curves of solar exposed <i>V. cholerae</i>	58
Figure 26: The effect of SUVR on the secretion of cholera toxin	59
Figure 27: Inactivation kinetics of solar exposed.....	61
Figure 28: The effect of SUVR on the production and release of cholera toxin.....	62
Figure 29: Representative growth curves of solar exposed.....	63
Figure 30: The effect of SUVR on the release of cholera toxin.....	64
Figure 31: Inactivation kinetics of solar exposed.....	66
Figure 32: The effect of SUVR on the production and release of cholera toxin.....	67
Figure 33: Representative growth curves of solar exposed.....	68
Figure 34: The effect of SUVR on release of cholera toxin.....	69
Figure 35: Inactivation kinetics of solar exposed.....	71
Figure 36: The effect of SUVR on the release of cholera toxin.....	72

Figure 37: Inactivation kinetics of solar exposed.....	73
Figure 38: The effect of SUVR on the release of cholera toxin.....	74
Figure 39: Flow cytometry histograms of compensated settings.	76
Figure 40: Flow cytometry histogram and dot plots.	77
Figure 41: Flow cytometric histograms and gated dot plots.	78
Figure 42: Flow cytometric histograms and gated dot plots.	80
Figure 43: Flow cytometry histograms as well as gated dot plots	82
Figure 44: Flow cytometry histograms and dot plots.....	83
Figure 45: Flow cytometry histograms and dot plots.....	85
Figure 46: Flow cytometry histograms and dot plots.....	86
Figure 47: Flow cytometric analysis of green florescence histograms.	89
Figure 48: Flow cytometric analysis of green florescence histograms.	90
Figure 49: Histograms of green fluorescence intensity.....	94
Figure 50: Histograms of green fluorescence intensity.....	97
Figure 51: Flow cytometric analysis of green florescence histograms.	99
Figure 52: Flow cytometric analysis of green florescence histograms.	100
Figure 53: Smoothed density plots FL1, $520 \pm 30\text{nm}$ (GRN fluorescence); SSC (Side Scatter) resulting from the flow cytometric analysis.	102
Figure 54: Smoothed density plots FL1, $520 \pm 30\text{nm}$ (GRN fluorescence); SSC (Side Scatter) resulting from the flow cytometric analysis	105

List of Tables

Table 1: Bacteria used for this Study	25
Table 2: Growth rates and doubling times of LB grown <i>V. cholerae</i> at 37°C pH 8.5	48
Table 3 : Showing the GInaFiT modelling of <i>V. cholerae</i> Strain Grown in Ground Water ...	49
Table 4: Mean and standard deviations for the different seasons	51
Table 5: The physiochemical properties of ground water	53
Table 6: SUVR, atmospheric conditions and temperature	55
Table 7: SUVR, atmospheric conditions and temperature	60
Table 8: SUVR, atmospheric conditions and temperature	65
Table 9: SUVR, atmospheric conditions and temperature	70

Chapter 1

1 Back ground and Literature Review

1.1 Introduction

According to the World Health Organisation (WHO), it is estimated that in every 8 seconds a child dies from a waterborne related disease and that more than five million people die from illnesses linked to consumption of unsafe drinking water or inadequate sanitation (Berney, Weilenmann, Simonetti, & Egli, 2006; McGuigan, Joyce, Conroy, Gillespie, & Elmore-Meehan, 1998; Safapour & Metcalf, 1999; WHO, 1996). Cholera is one of those waterborne diseases that have infected thousands of people leaving a large number of them dead. The weekly epidemiological record on cholera revealed a sharp increase in cholera cases during the year 2005 particularly in Africa and Asia (Osei & Duker, 2008; WHO, 2006). Even though the number of countries reporting on cholera cases has reduced globally, the actual number of cases is known to be much higher than that reported and continues to escalate (Kirschner et al., 2008). This could be attributed to underreporting and to inconsistencies in case definitions due to the lack of proper understanding of the standard definition of cholera. As a result some countries reported only laboratory confirmed cases even though various cholera cases have occurred according to WHO case definition they have been labelled as acute watery diarrhoea (WHO, 2006).

1.2 Cholera Disease and *Vibrio cholerae*

Cholera is a potentially epidemic and life-threatening secretory diarrhoea characterized by numerous, voluminous watery stools, often accompanied by vomiting, and resulting in hypovolemic shock and acidosis (Osei & Duker, 2008). This infection is caused by members of the species of a gram-negative microorganism known as *Vibrio cholerae* (*V. cholerae*) that exists naturally within aquatic environments (Merrell, Tischler, Lee, & Camilli, 2000). While other members of the genus may occasionally cause isolated outbreaks or milder diarrhoea, the majority of species are free living and not associated with the disease.

Both pathogenic and non-pathogenic *V. cholerae* strains are known to exist within the natural environment. Of the pathogenic ones, there are two serotypes, Inaba (AC) and Ogawa (AB), and two biotypes, classical and El Tor, both belonging to the toxigenic O group 1 that are

known to cause cholera (Aoki et al., 2009; Goel et al., 2008). *V. cholerae* O1 El Tor is known to be better adaptable to survive in the environment when compared to its counterpart, the classical biotype that is more toxigenic and responsible for the first six cholera pandemic that occurred in 1816, 1829, 1852, 1863, 1881, 1899 and 1961 ("Cholera - Wikipedia, the free encyclopedia," 2010). However, the last pandemic and or epidemic outbreaks (1967 to date) have been attributed to the El Tor biotype and which seems to have substituted the classical biotype. In addition, a constant evolution of the El Tor biotypes has been observed and is characterized by the production of a cholera toxin similar to that of the classical strains (Goel et al., 2008). On the other hand a new serogroup O139, also known as Bengal, has emerged. This serogroup is identifiable by the agglutination in O group 139 specific antiserum as well as the presence of a capsule (Aoki et al., 2009).

Once ingested through contaminated water or food, *V. cholerae* colonises the small intestine with subsequent production of the cholera toxin (Herz, Vimont, Padan, & Berche, 2003; Nackerdien, Keynan, Bassler, Lederberg, & Thaler, 2008; Srivastava, Fekete, & Chattoraj, 2006). Production of the cholera toxin causes the body to secrete large quantities of isotonic fluid by increasing the permeability of the vascular endothelium, thus enabling isotonic fluids to pass through the colon in abnormal amounts resulting in watery diarrhoea typical of cholera (Frost, 1976; Osei & Duker, 2008).

1.2.1 Virulence and Pathogenicity of *Vibrio cholerae*

Vibrio cholerae has evolved a sophisticated regulatory circuit to control the production of two key virulence factors that are responsible for the devastating cholera pandemics. These virulence factors are expressed by two separate genetic elements: CTX ϕ which expresses the cholera toxin genes and VPI ϕ which expresses the genes needed for toxin co-regulated pilus (TCP) production, accessory colonization factors (ACF) and the ToxT, TcpP, TcPI regulatory proteins. Once inside the *V. cholerae* these genetic elements are controlled by the ToxR regulatory cascade which is part of the microorganism's genome (Peterson, 2002).

Since TCP acts as the receptor for the CTX ϕ , ancestral *V. cholerae* ostensibly first acquired the VPI ϕ genetic element and then developed the ability to join its ToxT dependent regulatory circuit into the ToxR/ToxS system. Once the VPI ϕ system was established then *V. cholerae* acquired the CTX ϕ phage and placed its regulation under control of the ToxR/ToxT system (Peterson, 2002).

1.2.1.1 Cholera Toxin

Cholera Toxin (CT) is a multi-subunit ADP-ribosylating toxin that binds to the GM1 ganglioside found on intestinal epithelial cells. This toxin consists of a single cholera toxin A (CTA) subunit and five cholera toxin B (CTB) subunits both of which are encoded by the *ctx* operon on the CTX genetic element found on the CTX ϕ lysogenic filamentous phage (Peterson, 2002; Skorupski & Taylor, 1997). The single stranded 6.9kb CTX ϕ infects *V. cholerae* through TCP and survives as a prophage. The CTX ϕ genome is composed of two functionally distinct domains, the core that encodes the CT and phage morphogenesis genes and the RS2 regions that encodes the genes required for replication, integration and CTX ϕ regulation (Peterson, 2002).

Both subunits are produced in the bacterial cytoplasm and transported to the periplasm where with the help of the disulfide bond are folded and assembled into a 84-kDa heterohexameric AB₅ toxin complex (Aoki et al., 2009). This is eventually followed by the secretion of the toxin across the bacterial outer membrane into the extracellular space through a type II secretion mechanism. Once outside the bacterial cell, the CTB subunit through affinity binds to the ganglioside molecule of the target cells thus enabling the entry of CTA.

Although it is not clear how the subunits are transported across the bacterial cytoplasm, Aoki et al (2009) reported the presence of a nanotransportation system that is controlled by the pH of the environment. Nanotransportation is a phenomenon characterized by the intracellular transportation of bacterial proteins in response to an environmental stimulus (Aoki et al., 2009; Peterson, 2002)

The production of CT by the two biotypes occurs under different conditions. For instance, *in vitro* the classical biotypes require Luria Broth at a pH of 6.5 and temperature of 30°C to maximally produce CT. On the other hand the El Tor biotype needs to be grown in a bicarbonate environment without aeration followed by vigorous shaking to produce CT (Skorupski & Taylor, 1997). In addition the El Tor biotypes have distinct specific amino acid sequences for the CTB subunit. Mutations at positions 39 and 68 of the CTB protein sequence of the El Tor strains resulted in the production of CT similar to that produced by the classical biotype (Goel et al., 2008; Skorupski & Taylor, 1997).

1.3 An Overview of Cholera Disease

Cholera epidemics and pandemics have to a large extent been associated with unsanitary conditions, low urbanization and poverty (Herz et al., 2003; Srivastava et al., 2006). These factors are usually associated with densely populated communities close to surface waters from where cholera spreads to other communities based on their proximity (Osei & Duker, 2008; Srivastava et al., 2006). A typical but not limited scenario describing such a community would involve a water logged area with a forcibly created market or trading centre exhibiting high commercial activities (a landing site). Such areas particularly in Africa lack proper ablution facilities to accommodate the ever growing influx of traders and buyers. Consequently majority of the individuals resort to unhealthy practices such as urinating and defecating or disposal of faecal material into open gutters and open spaces, and as a result create unsanitary living conditions. These conditions enable the spread of cholera and other sanitary related diseases.

As much as cholera is associated with developing countries especially where hygiene is poor, there has been a global re-emergence of this disease in developed countries. Therefore it is important to consider that it does not necessarily require a major sanitary breakdown to cause a cholera outbreak as environmental, social and economical factors also have important roles to play (Frost, 1976; Kirschner et al., 2008; Osei & Duker, 2008). For instance, since global travel activities continue to intensify the possibility of *V. cholerae* penetrating developed countries through tourism and other activities cannot be excluded (Kirschner et al., 2008; WHO, 2006). In addition various water sources in developed countries such as Lake Neusiedler See in Europe and, surface water rivers, creeks, lakes and irrigation channels in the United States continue to serve as hot spots for migratory birds which have been associated with microbial import of specifically *V. cholerae* (Kirschner et al., 2008; Ogg, Ryder, & Jr, 1989). Finally the effects of climate change such as global warming and floods should not be ignored with regards to the re-emergence of cholera as increased temperatures favour the proliferation of pathogenic *Vibrio* strains in aquatic ecosystems while floods favour their transmission (Kirschner et al., 2008).

In an effort to solve cholera outbreaks and epidemics various measures such as immunization, construction of village hospitals, oral rehydration therapy and sanitary practices have been proposed, although their implementation still remains a global challenge (Echeverria, Harrison, Tirapat, & McFarland, 1983; WHO, 2006). However, cholera continues to

antagonise resource poor areas. This is mainly attributed to the difficulties such communities encounter when trying to access clean potable water that is mainly obtained from lakes, rivers, swamps and water-holes or small springs that are neither chlorinated nor exposed to any other form of sterilization. In addition, most of these waters are highly turbid and the material resource for filtering such waters is difficult to come by or costly if not both. Furthermore, disinfection of the water through boiling is impractical due to the scarcity of fuel (Ronán M. Conroy, Elmore-Meegan, Joyce, McGuigan, & Barnes, 1996; R. M. Conroy, Meegan, Joyce, McGuigan, & Barnes, 1999). Nevertheless emerging technologies such as solar disinfection (SODIS) using sunlight seems to serve as one solution to this problem (Boyle et al., 2008).

1.4 Solar Disinfection of Water

The spread of water-borne diseases through the consumption of faecally contaminated water still remains a major problem in developing countries. Solar radiation has been proposed as a means of treating contaminated water in areas with hot and sunny climates (Smith, Kehoe, McGuigan, & Barer, 2000). Sunshine was used by the ancient Indians to purify their water as early as 2000BC. Studies conducted by Downes and Blunt (1877) established the beneficial bactericidal effect of sunlight. This was supplemented by a study carried out by Acra et al (1989) and Conroy et al (1996) showing that the observed bactericidal effect was due to the long wave ultraviolet component of the sunlight. Since then studies such as those done on the Maasai community have emerged revealing the low risk of acquiring diarrhoeal disease associated with water treated through solar disinfection (SODIS) (Ronán M. Conroy et al., 1996; R. M. Conroy et al., 1999; R. M. Conroy, Meegan, Joyce, McGuigan, & Barnes, 2001; McGuigan et al., 1998). Studies have also shown that the risk of transmitting enteropathogenic *Escherichia coli* (EPEC) and viruses such as poliovirus and cysts known to survive in aquatic environments have been eliminated through SODIS treatment (Heaselgrave, Patel, Kilvington, Kehoe, & McGuigan, 2006; Ubomba-Jaswa, Boyle, & McGuigan, 2008). SODIS could serve as a means of emergency intervention against waterborne disease during times of crisis or at least until more permanent solutions can be put in place (Boyle et al., 2008).

SODIS can be defined as a process through which microbial contaminated water in a transparent vessel or container is disinfected or decontaminated through exposure to natural sunlight for 6 to 8 hours (Boyle et al., 2008; Heaselgrave et al., 2006; Navntoft, Ubomba-Jaswa, McGuigan, & Fernández-Ibáñez, 2008; Ubomba-Jaswa et al., 2008). The process

through which the disinfection occurs seems quite easy and straight forward. However, the mechanism through which it happens is a lot more complicated in that various factors such as solar ultraviolet radiation (SUVR), temperature, location and container or vessel used are major determinants of the outcome.

During SODIS treatment, bacterial inactivation occurs basically as a result of the synergistic effect between SUVR and an increase in water temperature (above 45°C) due to heat from the sun (Boyle et al., 2008; Navntoft et al., 2008; Ubomba-Jaswa et al., 2008). This disinfection or decontamination process is usually carried out in transparent containers such as those made out of glass or plastic, although polyethylene terephthalate (PET) bottles have found wider acceptance for this process in community studies (Boyle et al., 2008; Navntoft et al., 2008). This could be attributed to the cost and ease through which such bottles can be obtained compared to other transparent bottles made from other materials such as glass.

Efficient and effective bacterial inactivation is judged by the inability of the microorganisms to form colonies after SODIS treatments. It is, however, not quite clear if SODIS results in cellular lysis or in a viable but non-culturable bacterial state and most importantly if these cells retain infectivity (Smith et al., 2000). In addition, very few studies have assessed the effect of SODIS on biofilms as biofilms have been shown to confer chlorine resistance as a means of survival of the pathogenic *V. cholerae* O1 strain (J. G. Morris et al., 1996). Needless to say SODIS technology may hold the promise for the availability of microbiologically safe quality water for various disadvantaged and economically disabled communities. However, more work is required to define the parameters within which SODIS can be used.

SUVR also known as solar radiation is one of the greatest determinants of the SODIS process that is derived from natural sunlight. SUVR mainly consists of UVA whose wavelengths are in the range of 320nm to 400nm and UVB with wavelengths of 280nm to 320nm (Bailey, Neihof, & Tabor, 1983; Kramer, Baker, & Ames, 1988) as well as trace amounts of UVC with a wavelength less than 280nm. Natural factors such as adsorption and sedimentation influence the depth of light penetration. Usually clear environmental water consists of particulate matter of different sizes (Carlucci & Pramer, 1959; Navntoft et al., 2008). Microbes associate themselves with such particles and eventually settle at the bottom of the water body and accumulate in sediments. Hence, there is a greater number of bacteria in the sediment than there is in the over lying water. Therefore UVR is lethal to bacteria residing in

the shallow layers of the water reservoirs to a depth of about 3.3m if clear conditions exist (Bailey et al., 1983; Carlucci & Pramer, 1959; Fujioka, Hashimoto, Siwak, & Young, 1981).

1.5 Solar Ultraviolet Radiation

The sun plays a major role in our solar system providing the main source of energy for the continued existence of life on earth (Diffey, 1991). Its electromagnetic radiation is distributed over a wide range of wavelengths. Wavelengths shorter than 400nm are commonly known as the ultraviolet (UV) waveband whereas wavelengths longer than 700nm are known as infra-red radiation. Visible light on the other hand is composed of wave bands between 400nm and 700nm. According to the visible waveband, shorter wavelengths correspond to violet while longer wavelength corresponds to red. Similarly the UV waveband is sub-divided into three wavebands these being, UVA (320 to 400nm), UVB (280 to 320nm) and UVC (100-280nm) (Diffey, 1991; Parisi, 2005). However it is important to note that UVC does not reach the earth's surface because it is absorbed by the atmosphere. Of great interest to this study, is the amount of UV radiation from the sun that reaches the earth's surface [(henceforth referred to as Solar Ultra Violet Radiation (SUVR)]. As mentioned above SUVVR reaching the earth's surface is largely composed of UVA and UVB (Parisi, 2005; Qiu, Sundin, Chai, & Tiedje, 2004; WHO, 2002).

1.5.1 Factors Influencing Aquatic and Terrestrial SUVVR on Earth

The amount of SUVVR reaching the earth's surface is influenced by temporal, geographical and meteorological factors such as the sun's elevation, latitude, cloud cover and atmospheric conditions, altitude and last but not least the ground reflection (Diffey, 1991; Parisi, 2005; WHO, 2002).

The sun's elevation influences the amount of SUVVR reaching the earth's surface based on the distance between the sky and the sun due the time of the day. Thus SUVVR levels vary with the time of the day and time of the year. For instance 20 to 30% of the total daily SUVVR is received one hour either side of midday with 75% between 0900H and 1500H (Diffey, 1991; Qiu et al., 2004; WHO, 2002).

In terms of the latitude, SUVVR levels become higher as one gets closer to the equatorial regions. This is best expressed by the high levels of ultra violet index (UVI) measurements

from countries close to the equator (UVI 20) as compared to summer time values (UVI 8) in countries distant from the equator (Diffey, 1991; Diffey & Roscoe, 1990; WHO, 2002).

Cloud cover influences the amount of SUVR reaching the earth's surface in that the highest SUVR levels are experienced during cloudless skies. Nevertheless even with cloud cover SUVR levels could still be high. The atmosphere does provide an effective barrier against SUVR through UV scattering. For instance Rayleigh scattering still occurs even in the absence of clouds. This type of scattering is inversely proportional to the fourth power of the wavelength, and as a result leads to relatively higher scattering for shorter UVB, UVC wavelengths as compared to longer UVA and visible light wavelength (Parisi, 2005; WHO, 2002).

Altitude on the other hand influences the amount of SUVR because the higher the altitude the thinner the atmosphere and hence more UV is transmitted. As a result places on the Earth's surface below sea level are relatively poorer in UVB content than nearby sites at sea level (Diffey, 1991). In addition to that the ozone layer is responsible for barring the entry of radiation wavelengths less than about 290nm from reaching the earth's surface (Diffey, 1991). The reduction in the stratospheric ozone substantially increase fluxes of the most energetic and potentially damaging radiation such as UVB at the earth's surface (D. P. Morris et al., 1995).

Lastly the earth's environment reflects back some of the SUVR that reaches the earth's surface. Various ground surfaces contribute differently to the amount of SUVR reflected, for instance the grass, soil and water reflect less than 10% of the SUVR; fresh snow reflects as much as 80%; dry beach sand about 15% and 25% by the sea (Diffey, 1991; D. P. Morris et al., 1995; WHO, 2002). Water bodies to a certain point attenuate SUVR (Sinton, Finlay, & Lynch, 1999; Weinbauer, Wilhelm, Suttle, & Garza, 1997). But this phenomenon varies from one water body to another and greatly depends on the compositions of these water bodies mainly their dissolved organic carbon (Navntoft et al., 2008) and their altitude. Therefore lakes at higher altitudes experience higher maximum fluxes of incident SUVR (UVB increases 6% per 1000m above sea level) due to the reduced atmospheric attenuation ignoring the cloud cover (Diffey, 1991; D. P. Morris et al., 1995).

SUVR (280-400nm) has a pervasive and potentially damaging influence on both aquatic and terrestrial ecosystems. The damage sustained by biological systems due to SUVR exposure is highly dependent on wave length.

1.5.2 The Effects of SUVR on Biological Molecules or Systems

When biological molecules or systems are exposed to SUVR, a variety of outcomes is possible since the effectiveness of SUVR to produce a particular biological damage is wavelength dependent (Diffey, 1991; Joux, Jeffrey, Lebaron, & Mitchell, 1999). The biological effects are due to the amount of absorbed SUVR by the molecules of interest that is based on the action spectrum (Diffey, 1991). However, exposure to total sunlight has the most detrimental effect due to the synergistic action of combined wavelengths (Bailey et al., 1983).

The detrimental effects of SUVR on microorganisms are manifested by reduced DNA and protein synthesis, reduced exoenzymatic activity, reduced amino acid uptake, reduced oxygen consumption and lastly a decrease in bacterial abundance (Alonso-Sáez, Gasol, Lefort, Hofer, & Sommaruga, 2006; Elasri & Miller, 1999; Joux et al., 1999). Other biological structures such as the formation of exopolymers to a great extent reduce the amount of SUVR absorbed by biofilm forming microbes in the environment (Elasri & Miller, 1999).

1.5.2.1 Absorption Characteristics of Major Biomolecules

Nucleic acids are basically made up of nucleotide bases that act as chromophores. In deoxyribonucleic acid (DNA) and ribonucleic acid (RNA) these bases are purine derivatives adenine and guanine, and pyrimidine derivatives thymine, cytosine and uracil. Although the absorption spectra of the individual bases differ slightly, they commonly absorb at a maximum between 260 to 265nm and rapidly reduce absorption at longer wavelengths (Bailey et al., 1983; Diffey, 1991). Conversely proteins and DNA absorb most strongly in the UVB and UVC regions with absorption maxima of around 280nm. However, the absorbance of proteins is lower than that of nucleic acid solutions of equal concentration (Diffey, 1991). Finally the exposure of other biological molecules such as the porphyrins, carotenoids, steroids and quinines to SUVR usually results in serious biological consequences one of which is oxidation (Bailey et al., 1983; Diffey, 1991).

1.5.2.2 The Action Spectra and Photoproducts

An action spectrum could be defined as a plot showing the relative effectiveness of radiations of different wavelengths to produce a given biological effect. Therefore the action spectrum leading to the formation of a particular photoproduct would be similar to the absorption spectrum of the molecules responsible for the formation of that photoproduct. For example, the major photoproducts formed after the absorption of UVR by DNA are pyrimidine derivatives. Such photoproducts include cyclobutyl-type dimers also known as pyrimidine

dimers, pyrimidine adducts or spore photoproducts and lastly pyrimidine hydrates and DNA-protein cross-links (Diffey, 1991; Patrick & Rahn, 1976; Toth & Dose, 1976).

1.5.2.3 SUVR Damaged DNA Repair Mechanisms

Despite the fact that all biological systems from nano- to macro-systems are exposed to potentially harmful levels of SUVR, cellular protective mechanisms have evolved, that repair the damaged molecules. A number of different DNA repair mechanisms relevant to SUVR damage have been established and these include photoreactivation repair, nucleotide excision repair (NER), post replication repair and SOS repair (Arrage, Phelps, Benoit, & White, 1993; Diffey, 1991; Joux et al., 1999).

Photoreactivation repair or photoenzymatic repair (PER) is initiated through the binding of the photoreactivating enzyme to the UV-induced pyrimidine dimers in the dark. However, upon exposure to optical radiation between 330 and 600nm this complex dissociates resulting in the repaired DNA segment (Diffey, 1991; Joux et al., 1999; Qiu et al., 2004). PER is one of the most important repair mechanisms used by bacteria and has been shown to restore infectivity in natural communities of marine viruses (Alonso-Sáez et al., 2006; Weinbauer et al., 1997).

Nucleotide excision repair or dark repair is one of the fundamental repair mechanisms that take place in the dark or at night after diurnal exposure to sunlight. In brief the faulty region in one of the two strands of DNA is excised under enzymatic control and then subsequently replaced with normal nucleotides utilizing the complementary base-pairing information in the intact strand (Diffey, 1991; Joux et al., 1999; Xue & Nicholson, 1996).

Post replication repair on the other hand would correct SUVR damaged DNA through a replication process where gaps are left in the daughter strand opposite the damaged sites and eventually filled during DNA synthesis (Diffey, 1991).

SOS repair is not fully understood as yet. However, this mechanism is thought to have bypass systems that allow growth of the DNA chain across the damaged site of the thymine dimer. This is attained at the cost of fidelity of replication and a great deal of evidence indicates that SOS repair is the major cause of UV-induced mutagenesis (Diffey, 1991).

1.5.3 Effects of UVA on Biological Systems

The most energetic part of the SUVR entering the earth's atmosphere is UVA. Microbial motility in the environment is mainly due to UVA exposure through the formation of photosensitizers. Photosensitizers are formed when macromolecules absorb UVA in a process known as photo-oxidation; as a result the absorbed energy is transferred to oxygen leading to the formation of reactive oxygen species such as the superoxide radicals, hydroxyl radicals, hydrogen peroxide and singlet oxygen (Elasri & Miller, 1999; Navntoft et al., 2008; Qiu et al., 2004; Sinton et al., 1999).

Exposure of some microorganisms to UVA especially during their active stages of growth, results in irreversible damage to their catalase systems that renders them susceptible to damage from peroxide formation (Alonso-Sáez et al., 2006; Bailey et al., 1983). However, some microbes protect themselves from such action through the synthesis of enzymes such as alkyl hydroperoxide reductase (Bailey et al., 1983; Kramer et al., 1988; Sinton et al., 1999). In addition, UVA, through photo-oxidation, blocks the electron transport chain, induces damage to the cell membrane thus inactivating transport systems, interferes with metabolic energy production and causes single strand breaks in DNA (Berney et al., 2006). The presence of hydrogen bicarbonate ions in the environment serves as a means of protection for biological systems because bicarbonate ions act as photo absorbers limiting light penetration into bacterial suspensions (Navntoft et al., 2008). UVA has also been shown to reverse the detrimental effects conferred by UVB through the initiation of the PER mechanism (Joux et al., 1999). Generally UVA confers indirect damage to the DNA, protein and lipids through the formation of active reactive oxygen species (Joux et al., 1999).

1.5.4 Effects of UVB on Biological Systems

The depletion of the ozone layer has resulted in elevated levels of UVB reaching the earth's surface indirectly affecting both aquatic and terrestrial ecosystems (Bailey et al., 1983; Caldwell et al., 1998; Xue & Nicholson, 1996).

The general deleterious effects of UVB exposure include the indirect production of active oxygen species and free radicals, DNA damage, and partial inhibition of photosynthesis in plants. However, biological systems have developed protective mechanisms including radiation shielding due to structural or pigment changes and specific damage repair systems against these effects (Bailey et al., 1983; Caldwell et al., 1998; Joux et al., 1999).

Although the effects of UVB exposure on biological systems are mainly indirect, direct exposure to UVB often results in altered gene activity rather than damage. Therefore the effects of UVB radiation may be expressed through increased regulation rather than sustained damage (Bailey et al., 1983; Caldwell et al., 1998). This would explain the increase in pigment formation in most bacteria during laboratory exposure to artificial UVB.

The two most common UVB induced DNA lesions are the cyclobutane pyrimidine dimers (CPD) and photoproducts that are pyrimidine adducts such as pyrimidine pyrimidone. The accumulation of such lesions is lethal to microorganisms in that they could block DNA replication and transcription (Caldwell et al., 1998; Joux et al., 1999; Qiu et al., 2004). These lesions on the other hand differ from other DNA lesions because they require special enzymes that effectively remove them in the absence or presence of visible light at the favourable temperatures. In other words survival of microbes after exposure to UVB is largely due to these enzymes (Caldwell et al., 1998; Qiu et al., 2004).

Basically UVB causes both direct and indirect DNA damage due to the strong absorption of wavelengths below 320nm. However, insufficient exposure of some organisms to UVB might result in photoadaptation thereby increasing resistance to UVB and decreasing the rate of CPD accumulation during subsequent UVB irradiation periods (Joux et al., 1999).

1.6 Flow Cytometry

Flow cytometry (FCM) is a technique that uses scattered light for the rapid assessment of individual cells within a cellular population suspended in a stream of fluid. This technique enables quantitative and qualitative analysis of the distribution properties of individual cells within a sample (Bergquist, Hardiman, Ferrari, & Winsley, 2009; Hewitt, Caron, Nienow, & McFarlane, 1999). Although FCM is a dominant technique used in eukaryotic studies, its use in basic microbiology was limited due to factors such as the small bacterial size, problems associated with inadequate staining as well as the human factor. However, due to the advancements in optics and brighter spectrally diverse dyes this tool has emerged as a routine tool for microbiological research (Czechowska, Johnson, & van der Meer, 2008; Kamiya, Izumiyama, Nishimura, Mitchell, & Kogure, 2007; Steen, 2000).

In microbiology it is often important to determine the viability and the characteristics of the individual bacteria within a sample or a culture. In most laboratories this is commonly done by growing the bacterial sample in its favourable media followed by either microscopic

counting or colony forming unit counting, in the case of solid media. Various problems are, however, associated with these methods. Manual cell counts, for example, are tedious and to achieve statistical accuracy, an equal distribution of cells is required within a counting chamber- a situation quite difficult to achieve. It is also difficult to replicate ideal culture conditions for microbes from complex environments. Furthermore some microorganisms require a long time to be cultured. In addition, traditional culture methods often fail to detect stressed, sub-lethally injured, non-culturable or dead cells within a sample and can lead to partial or inconclusive results (Nebe-von-Caron, Stephens, Hewitt, Powell, & Badley, 2000).

Another method that is also used to determine cellular viability and replication of a bacterial sample is optical density (OD) where growth curves are generated by plotting OD readings versus time. This is, however, entirely based on the assumption that the size distribution or light scattering remains constant since OD, the product of cell number and size, is measured by light scattering. If for instance the cell size is decreasing as cell density increases the cell number as determined from the OD is automatically underestimated (Nebe-von-Caron et al., 2000). This would imply that the doubling time calculated from the OD measurements would be longer than it should. Furthermore, bacterial cells within a sample are not in the same growth state and often lead to different conclusions by researchers who rely on OD in bacterial cell cycle studies and related subjects (Steen, 2000).

As mentioned above it is very important to determine the viability and the characteristics of individual bacteria within a population at any given time so as to provide enough information for critical decision making. The use of classical microbiological methods, such as those mentioned above, has made it quite difficult to identify the state under which the microorganisms exist within a given sample at a given time. As a result a need for the rethinking of the definition of viability is apparent since some cells within a bacterial population undergo a state of viable but non-culturable (VBNC) or active but non-culturable (ABNC) conditions (Nebe-von-Caron et al., 2000; Sachidanandham, Gin, & Poh, 2005). The ABNC state of existence is believed to be a defensive mechanism exhibited by non-sporulating microorganisms when exposed to environmental stresses. Due to the ambiguous state of the environment and its microbial stressors (e.g. SUVR) it is quite difficult to cultivate microbes from environmental samples. This is because some of the cells within a given environmental sample may be metabolically active and capable of replicating while others may show the same characteristics but are incapable of replication. Others still may be dormant and non-active with injured permeabilised membranes or may be damaged to such

an extent that respiration is no longer possible (Czechowska et al., 2008). However, the ability to distinguish these different physiological states is important for assessing the growth and survival of pathogenic microbes in oligotrophic environments as well as the effects of toxic substances on these microbes. Such differentiations are not well addressed by conventional plating and counting techniques.

In an effort to overcome some of these problems researchers previously adopted a cellular synchronicity approach which was barely the case in the actual sense. The alternative to studying cells in synchronicity was to apply light or electron microscopy. However, data generated from these methods was largely qualitative. FCM on the other hand allowed for both the quantitative and qualitative assessment of cells at rates of several thousand cells per minute. The assessments were categorized according to intrinsic and extrinsic properties. Intrinsic properties can be studied by flow cytometry that includes light scattering measurements and do not require any form of staining reagents. This provides information with regards to cellular characteristics depending on the angles selected for the collection of the scattered light. For instance, light scattered in the forward direction (low angle) enables the estimation of the cellular size or protein content (Allman, Hann, Manchee, & Lloyd, 1992) while light scattered at wider angles provides information on the cellular shape and cytoplasmic granularity. It is for this reason that fluorescence measurements on unstained cells can be used to study photosynthetic pigment content or other cell associated auto fluorescence.

Unlike cells in the VBNC state there is documentation for protein formation in cells in the ABNC state. Emphasis has been focused on the membrane integrity of the cells as membranes are the major components primarily disturbed during the death process due to environmental stress. Taking this into consideration it would not be surprising to find that some of the adaptations undergone by the ABNC bacteria include cell wall toughening and nucleic acid condensation.

1.6.1 Benefits/ Applications of Flow Cytometry in Microbiology

Due to the problems and limitations associated with traditional methods used for the analysis of bacterial populations, direct optical detection methods such as flow cytometry have received increased popularity.

FCM offers a comprehensive means of detecting different kinds of bacteria within a given sample while discriminating the physiological states of the bacteria at the single-cell level at a given time. Contrary to that microbial detection methods that rely on replication are limited by the requirement to grow bacteria in an artificial environment and often results in inaccurate plate counts from natural samples. Since FCM allows the determination of cellular function it is possible to characterise the physiological state or degree of viability of bacteria through multiparametric or multi-colour flow cytometry analysis.

FCM offers better bacterial discrimination from other particles on the basis of nucleic acid staining using sample disaggregation and provides fast and reliable enumeration while minimising data artefacts due to post-sampling growth (Czechowska et al., 2008; Nebe-von-Caron et al., 2000).

FCM techniques offer a high throughput analysis of bacterial cells while maintaining the ability to determine the status of the cells at the single-cell level. This enables faster screening of bacterial material with a satisfactory degree of accuracy.

1.6.2 Cellular viability and activity assessment using FCM

The concept of viability assessment of bacterial cells, a key function in microbiology, has always been to elucidate the ability of bacteria to grow or multiply (Allen, Edberg, & Reasoner, 2004; Bartram, Cotruvo, Exner, Fricker, & Glasmacher, 2004). Although this has been done through the culturing of bacteria on nutrient rich media, it has been reported that only a small fraction of naturally occurring bacterial cells are actually culturable on such media and in addition some bacteria undergo dormant states of viability such as the VBNC or ABNC. Due to these findings more attention has been given to alternative approaches to assess viability and FCM is one of them.

1.6.3 Different approaches for assessing viability using flow cytometry

1.6.3.1 Membrane Integrity

This is probably one of the most explored approaches for determining viability without culturing. Flow cytometric analysis of the membrane integrity takes advantage of specific dyes that are retained and excluded by the bacterial membrane based on the size of the dye molecule. Dyes with small molecular sizes are capable of penetrating an intact cell membrane. However, if the membrane is damaged dyes with large molecular sizes can

penetrate the membrane and bind to the DNA (Czechowska et al., 2008; Nebe-von-Caron et al., 2000). The basic concept is that cells with severely damaged cell membranes are no longer viable although there are exceptions to this concept (Falcioni et al., 2008; Vives-Rego, Lebaron, & Nebe-von Caron, 2000). The most well-known dye for this application has been propidium iodide (PI). This dye is available commercially as an individual item or in combination with SYTO 9 as the so-called “live/dead” kit and can be used for both microscopy and FCM (Berney, Hammes, Bosshard, Weilenmann, & Egli, 2007). It should be noted that a combination of red and green fluorescence can result in yellow intermediates that render interpretation more difficult (Berney et al., 2007).

1.6.3.2 Membrane Potential

Membrane potential is basically the voltage difference between the interior and exterior of a cell. This phenomenon arises as a result of the actions of the ion channels, pumps and transporters that are part of the membrane fluid mosaic and whose sole responsibility is to maintain a constant ion concentration and transportation of cellular products in- and outside the cell. However, if a cell loses its cell membrane it automatically loses its membrane potential (Hewitt et al., 1999). The transportation and intracellular accumulation of stains such as DiBAC in bacterial cells requires the cell membrane to be depolarized (Berney et al., 2006; Hewitt et al., 1999). Therefore, stressed cells result in death, because depolarization of the cytoplasmic membrane caused inactivation of the metabolic pumps.

1.6.3.3 Membrane Function

Membrane function is usually indicative of the proper functioning of the bacterial membrane pumps. The use of membrane function as a target for FCM is effective in pure cultures but its applicability to natural communities/environments has not yet been shown. Ethidium bromide (EB) is the most widely used stain for assessing membrane functionality (Midgley, 1987). EB is known for its role in intercalating DNA during electrophoresis. This dye is very small and is capable of crossing an intact cell membrane; in active cells it is pumped out of the cell via a non-specific proton antiproton transport system (Midgley, 1987). If EB is combined with SYTO9 or SYBR green I (SGI) a quenching effect on the green fluorescence intensity is observed as soon as the red fluorescent dye enters the cells.

1.6.3.4 Metabolic activity

The metabolic activity of cells is demonstrated by the activities of enzymes such as dehydrogenases and esterases; they reveal the capacity of the microbe to synthesise the enzymes and the ability to maintain them in an active form.

Esterase is an intercellular enzyme common in most bacteria and it is supposed to remain active as long as the enzyme is protected from the environment (Vives-Rego et al., 2000). One of the common stains used for this purpose is carboxyfluorescein diacetate (cFDA). When cFDA is introduced into a metabolically active cell it undergoes hydrolysis within the cell by non-specific esterases liberating the fluorescent carboxyfluorescein (Czechowska et al., 2008; Nebe-von-Caron et al., 2000). Several stains are commercially available for the determination of the esterase activity. Some of these stains include cFDA, FDA and 5-carboxyfluorescein diacetate acetoxymethyl ester (CFDA-AM). However, one of the problems associated with this method is that enzymatic activity could still occur without the cell being viable, thus giving rise to false positives. So the use of fluorescent dyes and probes can enable the analysis of viable states beyond culturability (Hewitt et al., 1999).

1.6.3.5 Respiratory activity

For detection of respiratory activity a non-fluorescent stain is used. During the reaction this stain is reduced by a dehydrogenase enzyme to form insoluble fluorescent crystals. 5-cyano-2,3-ditolyl tetrazolium (CTC) is one of the most commonly used stains for discriminating between respiring and non-respiring cells (Czechowska et al., 2008).

Flow cytometry is rapidly becoming an important tool in the field of microbiology due to its ability to analyse microorganisms at both the community and single cell level. This tool facilitates the rapid acquisition of data as well as multi-parameter analyses. The increase in the availability and accessibility of fluorescent dyes over the past few years has advanced the applicability of this tool towards basic microbiology research. For this study, FCM will be used to investigate the effect of SUVR on the cytoplasmic membrane integrity of environmental and toxigenic *V. cholerae* strains.

1.7 Viable But Non-Culturable States

Exposure to SUVR might also lead to a state of viable but non-culturable (VBNC) cells. In the natural environment various Gram-negative and some Gram positive bacteria become unculturable when exposed to adverse growth conditions although they remain metabolically

active. The loss of culturability accompanied by the maintenance of the metabolic activity is considered to reflect entry of the cells into a viable but non-culturable (VBNC) state (Oliver, 2005). This physiological state describes the inability for a bacterial cell to grow on media that normally supports its growth under optimal laboratory conditions (Coutard et al., 2007; Oliver, 2005).

Cells entering a VBNC state often exhibit dwarfing, as well as major metabolic changes that include reductions in nutrient transport, respiration rates and macromolecular synthesis. Biosynthesis, however, does not cease but instead novel starvation and cold shock proteins are usually produced. Additionally ATP levels known to decline rapidly in dead and moribund cells, remain high in cells assuming a VBNC state. Furthermore, there is continued gene expression of cells in a VBNC state although it is not clear whether the reported genes are actually involved in the VBNC process (Oliver, 2005). Extensive modification of the cytoplasmic membrane fatty acid composition has also been described and reported to be essential for the continued membrane potential of cells undergoing the VBNC state (Oliver, 2005). VBNC cells are also known to possess an autolytic capability far higher than that of exponentially growing cells.

The linchpin for the hypothesis of the VBNC state is the demonstration of recovery of culturability of the VBNC cells. However, the recovery of culturability for such cells has long been debated as results from various studies have intimated that the culturable population may have been a result of very few cells remaining culturable. Nevertheless, other studies have concluded that non culturable bacteria should be able to revert to the culturable state, rather than undergo reductive cell division, characteristic of starved cells. Taking all the above into consideration an hypothesis was proposed to explain the recovery of culturability of VBNC that included the following: either all the bacteria in the original inoculum are in the VBNC state and are able to recover culturability by resuscitation, or only a few of the bacteria are VBNC, maintaining the ability to regrow, thereby mimicking resuscitation of the entire population (Coutard et al., 2007).

However, a few investigators have argued against the existence of a VBNC state in bacteria where much of their concern revolved around the terminology. For example, most investigators require that viability be indicated by colony development and in such case the phrase “viable but non-culturable” is an oxymoron.

1.7.1 Induction of VBNC

VBNC state can be induced by exposing cells to one or more forms of environmental stresses such as starvation, incubation outside the temperature range of growth, elevated osmotic concentration, oxygen concentration and exposure to white light (Oliver, 2005). These factors eventually result in a decline of colony forming units, although total cell counts generally remain fairly constant (Coutard et al., 2007; Oliver, 2005). In addition, various studies have shown that processes known to be bactericidal such as pasteurization and chlorination of waste water may instead invoke a VBNC state in bacteria (Oliver, 2005).

Cells can also continue to assume a VBNC state due to the plating medium. For instance, non-growing cells might produce free radicals such as hydrogen peroxide upon exposure to high nutrient and as a result prevent colony development on media (Oliver, 2005).

1.7.2 “Dangers” surrounding VBNC

A great number of pathogens and non-pathogens are known to exist in a VBNC state. The significance of this dormancy state has far reaching implications in medicine, in bioremediation, in the use of bacteria as faecal indicators and other biological studies where culturability is employed as the sole indicator for viability (Oliver, 2005; Xu et al., 1982). In terms of public health, microorganisms in a VBNC state pose a considerable threat because they cannot be detected by classical methods, especially in samples collected from stressful environments. For example, rods such as those of *Helicobacter pylori* can undergo a transition from rods to predominately non-culturable cocci as they enter the VBNC state (Coutard et al., 2007; Oliver, 2005). In addition, cells in such a state are capable of initiating an infection. For example the inoculation of VBNC *V. cholerae* into ligated rabbit ileal loops and its consumption by a human volunteer resulted in cholera with culturable *V. cholerae* (Oliver, 2005). Furthermore, cells in a VBNC state such as *H. pylori* have been observed to be resistant to antibiotics such as those used to treat ulcers and this could imply that the resurgence of ulcers due to this microbe may be initiated by the resuscitation of cells in a VBNC state after cessation of antibiotic treatment (Oliver, 2005).

It is quite evident that various bacteria, that are Gram-positive and Gram-negative, as well as pathogenic and non-pathogenic, are capable of existing in a VBNC state. Of greater importance is to understand the mechanisms involved in the initiation of infections in humans by cells in a VBNC state as cells in these state retain their virulence.

1.8 Modelling of Bacterial Survival

The modelling of bacterial survival curves continues to emerge as an important issue especially with the increased use of mild heat treatments of edible products which have to guarantee the safety of the products and also due to the increasing use of risk analysis aiming at a better control of food borne diseases (Albert & Mafart, 2005; Geeraerd, Herremans, & Van Impe, 2000).

In the past models were developed with the aim of predicting microbial growth in a constant and variable environment. This created a need for the generation of models describing microbial adaptation within such environments. The ground water used for this study is one of such environments.

With this objective in mind although various models have been proposed they were not used because of their specificity resulting in the inability to satisfy typical microbial survival curves (Albert & Mafart, 2005; Geeraerd et al., 2000). The majority of the microbial survival curves have a non-log-linear behaviour as well as a smooth initiation (shoulder) and saturation (tailing). A proper predictive survival model should be able to incorporate these phenomena so as to provide good parameter estimates for an accurate fit of the experimental data.

The shape of most microbial survival curves is the same as that of a typical survival curve described by Kalbfleish and Prentice (1980) and Lawless (2002) as failure time data (Albert & Mafart, 2005). In other words microbial survival curves are a representative of cumulative individual failure distributions. Taking all the above into account it should be noted that bacterial inactivation is not always the same simply because the individual bacterial failure time is unknown making it necessary to describe absolute populations and also incorporating tailing.

1.8.1 GInaFiT Modelling

GInaFiT (Geeraerd and Van Impe Inactivation Model Fitting Tool) is a freeware Add-in for Microsoft® Excel. This tool was created mainly to bridge the gap between people developing predictive modelling approaches and end-users especially those in the food industry who were either not familiar with using advanced non-linear regression analysis tools (Geeraerd, Valdramidis, & Van Impe, 2005).

GInaFiT is useful for testing nine different types of microbial survival models on user-specific experimental data relating the evolution of the microbial population with time. These nine model types include: (i) the classical log-linear curves, (ii) curves displaying a supposed shoulder before a log-linear decrease is apparent, (iii) curves displaying a supposed tail after a log linear decrease, (iv) survival curves displaying both shoulder and tailing behaviours, (v) concave curves, (vi) convex curves, (vii) convex/concave curves followed by tailing, (viii) biphasic inactivation kinetics, and finally (ix) biphasic inactivation preceded by a shoulder. Along with these models the tool automatically reports these statistical measurements: Standard Errors of the parameter values, the Sum of Squared Errors, the Mean Sum of Squared Errors and its Root, the R^2 and the adjusted R^2 . This tool can effectively assist the end user to communicate the performance of food preservation processes in terms of log cycles of reduction (Geeraerd et al., 2005).

The inactivation of vegetative bacterial cells, whether due to thermal or non-thermal means can exhibit one of the above mentioned models as illustrated in Figure 1 and are discussed below.

1.8.1.1 Log-linear model covering shape I survivor curves

The log-linear is a traditional way of describing microbial inactivation. In this model the total bacterial population is assumed to be equally sensitive to an antibacterial treatment and the death of an individual is dependent upon a random chance that a key target within it received sufficient treatment. Despite the worldwide use of this model a lot of deviations have been observed indicating that inactivation kinetics does not always follow the first order log-linear relationships (Geeraerd et al., 2005).

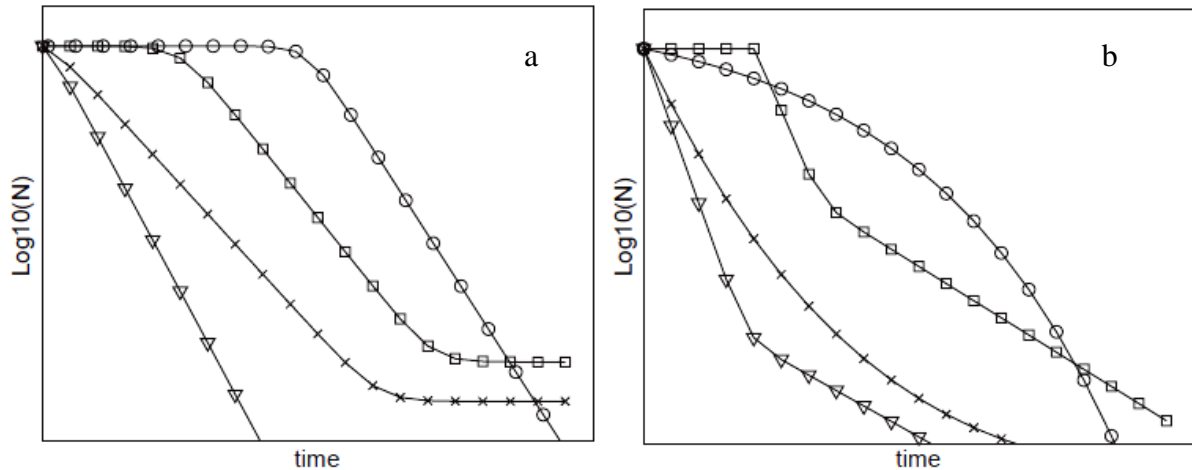


Figure 1: Types of inactivation curves in plot (a) linear (Δ , shape I), linear with tailing (x , shape II), sigmoidal-like (\square , shape III), linear with a preceding shoulder (o , shape IV). Plot (b) biphasic (Δ , shape V), concave (x , shape VI), biphasic with a shoulder (\square , shape VII), and convex (o , shape VIII) (Geeraerd et al., 2005).

1.8.1.2 Log-linear model with shoulder and/or tailing covering shapes I, II, III and IV survivor curves

These models take into consideration the physiological state of the cells, the specific inactivation rate and the residual population density and consist of three factors. The first factor demonstrates the log linear part of the inactivation curve which is also equivalent to the classical first-order inactivation kinetics discussed above. The second factor describes the shoulder effect based on the hypothesis of the presence of a pool of protective or critical component around each cell. In other words this pool is gradually destroyed. The third factor suggests the existence of a more resistant subpopulation that can be framed within the established mechanistic or vitalistic concepts (Cerf, 1977; Geeraerd et al., 2005). It is important to note that for this model tailing is considered for a population remaining constant in time or, otherwise stated, not undergoing any significant inactivation (Geeraerd et al., 2005).

1.8.1.3 The Weibull type models' covering shapes I, VI and VIII survivor curves.

The Weibull model when applied, describes microbial inactivation as the cumulative form of asymmetric Weibull probability density function for treatment resistances of individual microbial cells; however other distributions like the symmetric Fermi distribution are also possible. This modelling is based on different fundamental views with regards to microbial

inactivation in comparison with the models covered above. For this model if $p=1$, then δ (time unit) can be denoted as the time for the first decimal reduction where $p>1$ represents a convex shaped curve while $p<1$ represents a concave shaped curve (Albert & Mafart, 2005; Geeraerd et al., 2005).

1.8.1.4 The biphasic models covering shapes I, II, IV and VII survivor curves

This model when applied takes into account two major fractions one of which describes the initial population in a major subpopulation and the other an initial population in a minor subpopulation where in most cases it is more heat resistant than the previous one. This biphasic model can be used to describe survivor curves of shapes I, II and V. It can also be written under the form of two first order differential equations, if used for time-varying conditions, one representing the major subpopulation and the other representing the minor subpopulation. Biphasic inactivation curves have been observed in the framework of both thermal and non-thermal inactivation (Geeraerd et al., 2005).

1.9 Significance and Purpose of the Study

The background and literature review process brings to light some of the issues that enable the spread of cholera as well as the consequences this water borne disease causes most especially in developing nations. The sub-Saharan region in Africa has been shown to have the highest incidence of cholera disease compared to other regions in the world with developing countries (Gaffga, Tauxe, & Mintz, 2007).

Despite the effort that has been directed towards improving sanitation and hygiene, cholera and various other waterborne diseases continue to antagonise these resource poor communities. As a solution researchers have recommended the use of SODIS in communities lacking the appropriate resources to control the spread of cholera or any other water borne diseases. The recommendation for the use of SODIS has mainly been motivated by the cost and ease of use of this technology among other factors (Section 1.4 in the literature review).

However, this intervention together with hygiene and sanitation, although important, are not the only preventative measures as some of the factors leading to outbreaks are out of the scope of poor communities. One of these factors is climate. Very little is known about the role climatic factors play in the onset of cholera. In South Africa cholera incidences are known to occur during summer as opposed to winter and spring regardless of the sanitation

and hygienic state of the affected areas (Mugero & Hoque, 2001). Elsewhere, seasonal cholera outbreaks have been reported regardless of the limited preventative measures put into place.

1.10 Aims and Objectives

The aim of this study was to determine the effect that solar ultraviolet radiation has on the growth of *V. cholerae* and cholera toxin secretion so as to provide supporting information for the use of SODIS in the treatment of water. In addition, this study shares some light on the possible effect that climate may play in the onset of cholera disease.

The objectives of this study were:

- To evaluate the growth of *V. cholerae* and secretion of cholera toxin in a nutrient rich and nutrient poor environment under laboratory conditions.
- To evaluate the growth of *V. cholerae* and cholera toxin secretion in a nutrient rich and poor environment when exposed to sunlight and environmental temperature during the four seasons of the year as experienced in South Africa.
- To determine the possible effect of SUVR on the cytoplasmic membrane of the three *V. cholerae* strains used.
- To evaluate all the results generated in this study towards an understanding of how *V. cholerae* could be controlled by the effective use of solar radiation with regards to SODIS as a recommended way to deal with cholera incidents and outbreaks.

Chapter 2

2 Materials and Methods

2.1 Bacterial Strain

V. cholerae polymerase chain reaction (PCR) confirmed *ctx* gene positive strains NCTC 5941 O1 serotype obtained from the National Collection of Type Cultures, NCTC 12945 O139 serotype obtained from the National Collection of Type Cultures and *ctx* gene negative 1009 Vaal river isolate (also referred to as the environmental strain) were used for this study (Table 1).

Table 1: Bacteria used for this Study

Bacteria	Strain	Serotype /Toxicity	Isolated From
<i>V. cholerae</i>	NCTC 5941	O1 / Toxigenic	Unknown
<i>V. cholerae</i>	NCTC 12945	O139 / Toxigenic	Unknown
<i>V. cholerae</i>	1009	Unknown / Non Toxigenic	Vaal river

2.2 Resuscitation of the Bacterial Strains

Luria broth (LB) (10g Tryptone per litre, 5g Yeast Extract per litre, 10g Sodium Chloride per litre) at pH 8.5 was prepared, autoclave sterilized at 121°C for 15 minutes and used for batch cultivation. Precultures for all the experiments were prepared from the appropriate cryo-vials (stored at -80°C) by spreading 3 beads from the stock onto appropriately labelled nutrient agar plates. After 18 hours of incubation at 37°C, two to five colonies of each strain were separately picked using a flame sterilized inoculation loop, streaked out onto new appropriate nutrient agar plates and incubated at 37°C. The following day one colony from each strain was picked using a flame sterilized inoculation loop, inoculated into the appropriate 50ml Erlenmeyer flask containing 14ml of LB at pH 8.5 and incubated at 37°C on a rotary shaker at 200 r.p.m for more than 15 hours when the stationary phase was reached. Due to the slow growth rate and in some cases lack of increase in biomass, the microbes were not batch cultivated in ground water, but instead LB stationary phase cells known to be resistant to ultra violet treatment were used (Joux et al., 1999; Qiu et al., 2004).

2.3 Determination of Growth Curves

2.3.1 Preparation of Growth Media

Two different kinds of media which included Luria Broth (LB) and ground water from a bore hole in Soshanguve, Pretoria, South Africa were used. The two media were chosen for the growth of *V. cholerae* based on their nutritional content and community significance. LB was chosen as a representative of a nutrient rich environment resembling that of the human gut or faecal material. Ground water was used as a representative of a nutrient poor environment resembling a more natural environment for *V. cholerae* and thus significant to the community in Soshanguve.

These media were each prepared at different pHs (pH 6.5, 7.5 and 8.5) and autoclaved at 121°C for 15 minutes then used for the determination of growth curves for all the *V. cholerae* strains used in this study (Table 1). These pHs were chosen based on the reports from the Department of Water Affairs (DWA) pertaining to the assessment of the quality of the natural water reservoirs within South Africa. pH 8.5 was used because the 90th percentile alkalinity of most water bodies was around that value while the medium pH on average was around pH 7.5. On the other hand the acidity for most of the water bodies was around pH 6.5.

2.3.1.1 Growth curve of *V. cholerae* in LB

Overnight cultures of *V. cholerae* strains O1, O139, 1009 grown in LB at 37°C pH 8.5 (optimal laboratory conditions) (ESR LTD, 2001) were diluted in a ratio of 1:100 in fresh LB at pH 6.5, 7.5, 8.5 separately and incubated at 37°C, 30°C, 20°C for 26 hours. At a predetermined time point a sample was withdrawn and the OD₆₀₀ was determined using a spectrophotometer with a 1cm path cuvette.

2.3.1.2 Growth Kinetics of *V. cholerae* in LB

In order to determine the growth rates, individual growth curves were processed in sequential sets of 3 data values. The data values consisted of x-y pairs of elapsed time and the natural log of optical density. In these experiments the data points processed were 1 through 3, 2 through 4, 3 through 5 e.t.c. Using the slope of the line generated by the data points, the growth rate (μ) for each set of x,y data points was determined. In addition to that the doubling time was also determined using the equation below where μ = growth rate and td= doubling time.

$$\mu = \ln 2 / td$$

2.3.2 Growth curve of *V. cholerae* in Ground Water

Overnight cultures of *V. cholerae* strains O1, O139 and 1009 were harvested by centrifugation from batch cultures (3000 rpm for 10 minutes), washed three times with filter sterilized (0.22 μ m pore) in house 1x phosphate buffer saline (PBS) (0.2g Potassium Chloride per litre, 8g Sodium Chloride per litre, 1.44g of di-Sodium orthophosphate per litre, and 0.24g Potassium di-Hydrogen Phosphate) at pH 7.5 and diluted in autoclave sterilized ground water from a borehole in Soshanguve in a ratio of 1:100 at pH 6.5, 7.5, 8.5 separately and incubated at 37°C, 30°C, 20°C for 4 to 5 days. Then at each determined time point a sample was withdrawn serially diluted, spread plated in nutrient agar, incubated overnight at 37°C and counted the following day. Colony forming unit counts were eventually used for the formation of the growth curves.

2.3.2.1 Modelling of *V. cholerae* survival in Ground water using the GInaFiT tool

The Geeraerd and Van Impe inactivation model fitting tool (GInaFiT) was used for analysing different configurations of pH and temperature for ground water. The following models were used; log linear regression, log linear +shoulder, log linear + tail, log linear + shoulder and tail, weibull, weibull + tail, weibull + tail fix, double Weibull, biphasic model and biphasic + shoulder model. All these models were run for each experiment and the root mean sum of the squared errors (RMSE) were compared. The RMSE is considered the most simple and informative measure of goodness of fit for linear and non-linear models. The model with the lowest RMSE was considered the best fit for the respective inactivation curve. If two models had the same or similar RMSE values the simplest (the least degrees of freedom) model was considered to fit best (Geeraerd et al., 2005).

2.4 Sample Preparation Prior and Enumeration after SUVR Exposures

Overnight cultures of *V. cholerae* serotypes O1, O139 and strain 1009 were harvested by centrifugation from batch cultures (3000 rpm for 10 minutes), washed three times with filter sterilized (0.22 μ m pore) in house 1x phosphate buffer saline (PBS) (0.2g Potassium Chloride per litre, 8g Sodium Chloride per litre, 1.44g of di-Sodium orthophosphate per litre, and 0.24g Potassium di-Hydrogen Phosphate) at pH 7.5 so as to strip them of any LB and diluted in autoclave sterilized ground water from a borehole in Soshanguve either pH 8.5 or 6.5 to an optical density at 600nm (OD₆₀₀) of approximately 0.01 corresponding to 7 or 8 Log colony

forming units per ml (Log CFU/ml) before SUVR exposure. Cultures exposed in LB on the other hand did not require any washing but they were also inoculated at the same OD as that of ground water. Fifteen ml of the bacterial suspension was exposed to SUVR on the unshaded roof top of building 21 at CSIR campus in Pretoria. The samples were exposed in transparent polystyrene Twenty five cm² unventilated tissue culture flasks, placed over a brown cardboard so as to prevent any reflection. The controls for the experiments were exposed to similar atmospheric conditions except for SUVR that was eliminated by enclosure using an opaque ventilated board box. During exposure, one flask for each of the ground water experiments, at each pH for each strain was withdrawn at a chosen time point and diluted in decimal steps (10^{-1} to 10^{-6}) with filter sterilized (0.22 μ m) 1x PBS then an optimized version of the Miles and Misera drop counting technique (that will be described shortly) was used for bacterial counts. Ten micro litres of the appropriate dilutions of the sample were dropped onto sterile agar plates in duplicate or quadruplicate. The plates were then incubated at 37°C and counted the following day. Only those plates that produced less than 50 colonies per drop were selected and counted. The count was divided by the number of drops, multiplied by 100 to convert to 1ml, and then divided by the dilution itself to give the number of CFU/ml. As for LB exposed samples only the OD_{600nm} reading was done in duplicate for each sample.

2.5 Solar Ultra Violet Radiation measurement

Two UV metres (Solar Light Co., Philadelphia, PA, USA) were installed on the unshaded roof top (latitude 25°44'50.40"S and longitude 28°16'50.50"E, at an elevation of 1.4km above sea level) of build 21 at the CSIR. One of the metres recorded radiance due to UVA while the other recorded radiance due to UVB. Both metres where connected to a PMA data logger at the pent house via an 80m cable. The data logger was set to record UV exposures of both UVA (wavelength range 320 – 400 nm) and UVB (wavelength rage 290 – 320 nm) radiance for each 10 minute period of the day and some other days for periods of 1hour. The UVB data was captured in μ W/cm² and then converted to W/m², while UVA data was recorded in W/m². Data was download every after 2 days (where 5min exposures where used) or 20 days (where 1hr exposures where used) using the solar light PMA organiser program (Solar Light Co., Philadelphia, PA, USA). In addition to the raw data the program produced graphs showing the daily patterns of UVA and UVB.

2.6 Cholera Toxin Determination using ELISA

Greiner bio-one, 96 well ELISA microplates were obtained through LASEC SA Centurion, South Africa. Purified cholera toxin rabbit polyclonal IgG horseradish peroxidase (HRP) conjugated antibody (catalogue number PA1-73189) against the beta subunit of the cholera toxin was obtained through BIOCOM Biotech from Thermo scientific, Rockford, IL, USA. Monosialoganglioside G_{M1} (Sigma, City, South Africa, G7641-1MG) from bovine brain was obtained as 1mg powder and was dissolved in 1ml of methanol to a final concentration of 1mg/ml (1,000 μ g/ml or 1,000,000ng/ml). The resultant ganglioside G_{M1} solution was stored at -20°C in small aliquots disabling repeated freeze thaw cycles and only diluted 1xPBS prepared in the laboratory just before use. PBS - Tween 20 also known as wash buffer was prepared by adding 0.05% tween 20 1x PBS. Blocking buffer was prepared by adding 1% Bovine Serum Albumin (BSA) to the wash buffer. Finally tetramethylbenzidine (TMB) substrate reagent (catalogue number 421101) obtained from BioLegend, San Diego, CA, USA through BIOCOM biotech was prepared and used according to the manufactures instructions.

2.6.1 Ganglioside G_{M1} Cholera Toxin Assay

All incubations during the assays were done at room temperature (23-25°C) and after each incubation period each microplate was emptied and washed 3 times with wash buffer. To each well in the plate, 100ng/ml of ganglioside G_{M1} 1xPBS was added and left overnight (c.a 15hours) before subsequent treatment with blocking buffer, sample, polyclonal rabbit HRP (conjugated anti-cholera toxin beta subunit antibody (1:200 dilution in blocking buffer) and TMB substrate. Incubation times were 1hour for the blocking buffer and antibody, and 1.5 hours for the samples. For colour development 100 μ l of TMB substrate was added to each well for 30 minutes followed by the addition of 100 μ l of 1M sulphuric acid (H_2SO_4) stop solution. Each plate was finally read at OD₄₅₀ in the BioTek Power Wave HT plate reader within 10 minutes of adding the stop solution. The assay for each sample was performed in duplicate.

2.7 Flow cytometric Analysis

2.7.1 Preparation of *V. cholerae* for Flow Cytometry

V. cholerae strain NCTC 5941 was grown in Luria broth to an OD of 1.191 and thereafter washed twice in 1xPBS through centrifugation at 10,000g for 5 minutes. The pellet was then resuspended in 1x PBS buffer and heat stressed in a dry bath for 4 hours at 90°C. Another sample of the same strain was grown in LB to an OD of 0.828 so as to obtain a late log phase culture. This was done because the microorganisms at this stage of growth are resilient. The culture was then washed in the same way as described above and then resuspended 1xPBS.

2.7.2 Flow-cytometric measurements

Flow cytometric measurements were done using an Easy-Cyte Plus flow cytometer (Guava Technologies, Billerica, MA) with an excitation of 488nm from a laser. Four fluorescent dyes were used alone or in different combinations: Sybr Green I (SGI) (S940 Sigma-Aldrich, St. Louis, USA), propidium iodide (PI) (Catalogue number 81845 Fluka Sigma-Aldrich, St. Louis, USA), carboxyfluorescein diacetate (cFDA) (C4916 Sigma-Aldrich, St. Louis, USA) and ethidium bromide (EB) (E1510 Sigma-Aldrich, St. Louis, USA). Heat stressed and late log phase cultures of *V. cholerae* prepared as explained above were divided into seven subsamples and immediately stained with a mixture of two fluorescent dyes (SGI / PI, SGI/EB and cFDA/PI) and single fluorescent dyes (SGI, cFDA, PI and EB). However, samples taken from the solar irradiation experiments were only stained with a cocktail of SGI and PI since the major objective was to assess the effect of solar exposure on the cytoplasmic integrity of the cells. All the samples were incubated in the dark at 37°C for 45 minutes before analysis. Prior to flow cytometric analysis all the microbial samples were diluted to 10^{-2} with filter (0.22µm pore) sterilised 1x PBS (in house) and the flow cytometer was set to acquire ten thousand events per sample. Stock solutions of the dyes were prepared as follows: PI and EB were prepared at 300µM using ultra-pure water and stored at 4°C, SGI was prepared in dimethylsulfoxide (DMSO) at 10x and cFDA was prepared in acetone at 0.00217µM and stored at -20°C. In flow cytometer optical filters were set up such that PI and EB were measured above 590nm while cFDA and SGI at 520nm.

2.7.3 Data analysis

Data was collected with the Guava CytoSoft Data Acquisition and Analysis Software (Guava software) (Version 3.6) and analysed with the same software or WinMDI (version 2.9) where necessary. The bacterial populations were analysed using histograms and necessary dot plots. Before analysis, detectors were adjusted and compensation setting was performed on a sample with unstained cells using the Guava software. The corresponding signal was set to the far left so as to reduce background autofluorescence as much as possible.

Chapter Three

3 Results

3.1 Growth Properties of *Vibrio cholerae*

Vibrio cholerae is a Gram negative facultative aerobic microorganism that exists naturally in aquatic environments. In nature this microorganism is exposed to ambiguous environmental and climatic factors such as nutrient availability, pH, temperature and SUVR among others. In turn these factors have paved a way for natural selection by influencing the way through which the microorganism survive and adapt within their natural dynamic habitats (David A. Relman, Alison Mack, & Forum on Microbial, 2009; Kassen & Bataillon, 2006; Wyss, 1956). Knowledge about the sensitivity of an organism towards any disinfection method such as SODIS is essential. Thus the main aim of this study was to evaluate the effects of SUVR treatment on the growth of *V. cholerae*. In order to achieve this aim, it was important to determine the growth properties of *V. cholerae* under varying media, pH and temperature conditions within the laboratory before SUVR exposure. The effect of pH on all 3 strains of *V. cholerae* under varying temperature conditions is reported below.

3.2 Effect of the pH of LB and Temperature on the Growth of *V. cholerae*

The nature of *V. cholerae*'s growth under varying pH conditions in LB was found to be dependent on the strain, duration of growth, method of culturing and temperature. All strains were grown for a maximum of 26 hours and during that period no single pH dominated the increase in biomass.

3.2.1 Growth of the O1 Serotype

Serotype O1 in LB pH 6.5 at 37°C for the first 9 hours produced the highest turnover in biomass with an OD₆₀₀ reading of 1.2 Absorbance units (Abu) while the biomass at pH 8.5 (1.06Abu) and pH 7.5 (1.17Abu) at the same temperature was lower as shown in Figure 2. Over the 26 hour period of incubation at 37°C the greatest biomass turnover (1.57Abu) was produced at pH 7.5 and the lowest biomass (1.36Abu) was at pH 6.5. Based on biomass formation, this serotype grew best in LB at pH 7.5 for a period of 26 hours at 37°C.

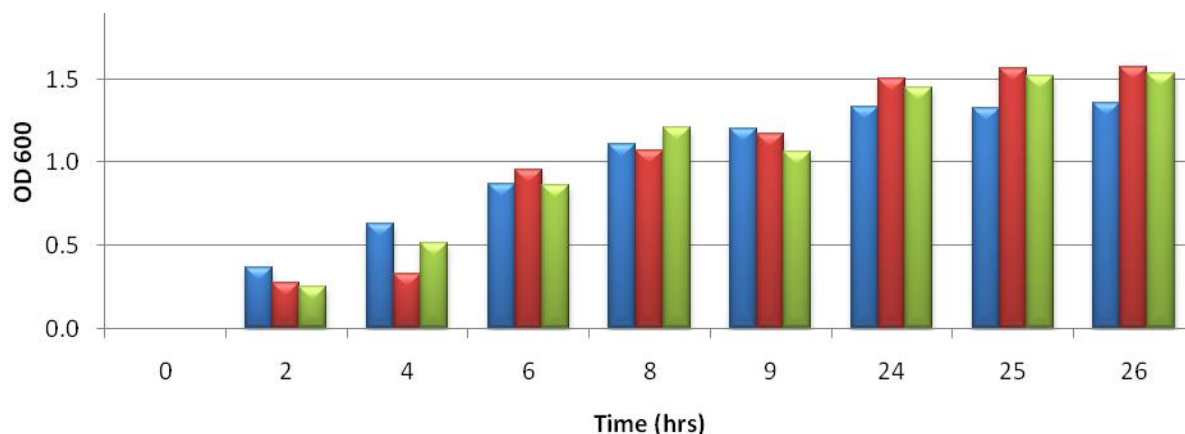


Figure 2: Relative increase in the biomass of *V. cholerae* serotype O1 grown at 37°C in LB. Three different pHs were used: pH 6.5 (blue bars), pH 7.5 (red bars) and pH 8.5 (green bars)

At a temperature of 30°C there was a high biomass turnover by the O1 serotype when grown at pH7.5. However at pH 8.5, the highest biomass turnover (1.78Abu) was observed from 4 hours right until the end of the 26 hour incubation period followed by growth at pH 7.5 as shown in Figure 3. Therefore LB at pH 8.5 resulted in the greatest biomass turnover for the duration of the incubation at 30°C.

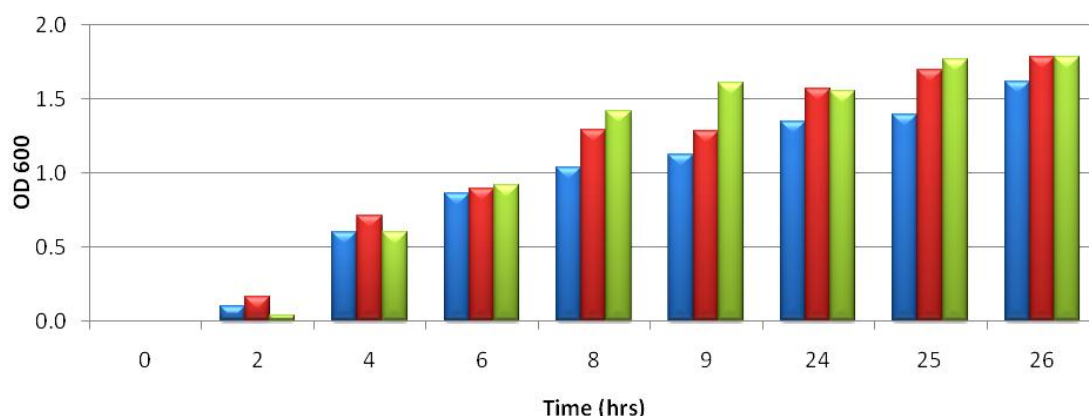


Figure 3: Relative increase in the biomass of *V. cholerae* serotype O1 grown at 30°C in LB. Three different pHs were used: pH 6.5 (blue bars), pH 7.5 (red bars) and pH 8.5 (green bars)

At 25°C and at pH 7.5 and pH 6.5 the greatest biomass turnover of 1.26Abu and 1.14Abu, respectively, was found to be in the first 9 hours (Figure 4). However, after 24 hours the greatest biomass turnover (1.91 Abs) was observed at pH 6.5 followed by pH 8.5 (1.77Abs) and lastly pH 7.5 (1.76 Abs). So pH 6.5 for the total duration of incubation at 25°C favoured the greatest increase in biomass (Figure 4).

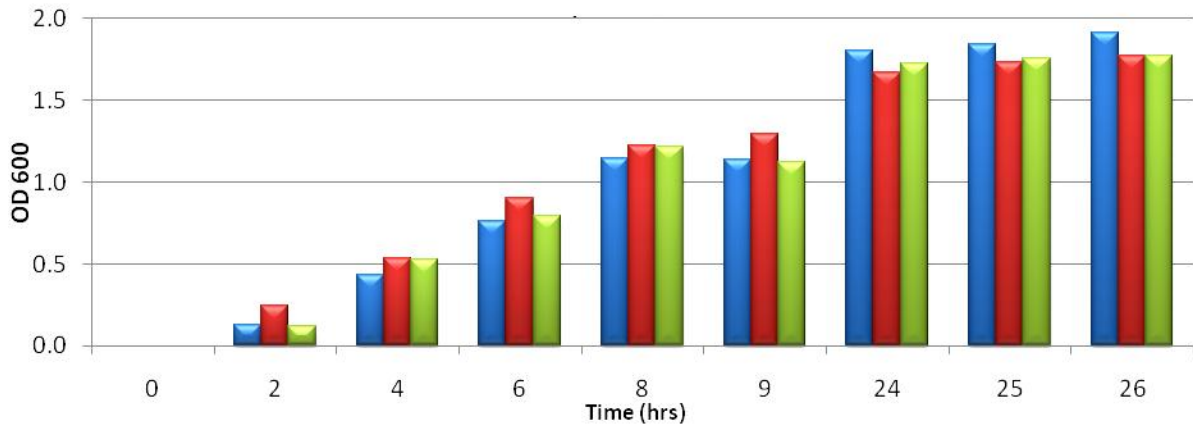


Figure 4: Relative increase in the biomass of *V. cholerae* serotype O1 grown at 25°C in LB. Three different pHs were used: pH 6.5 (blue bars), pH 7.5 (red bars) and pH 8.5 (green bars)

3.2.2 Growth of the O139 Serotype

Serotype O139 at 37°C for the first 24 hours had its greatest biomass turnover at pH 6.5 (1.25Abs). However, for the last 2 hours the biomass formation at pH 8.5 surpassed that at pH 6.5. The biomass turnover at pH 7.5 was the lowest at the end of the 26 hours incubation (1.11Abu). However on average, pH 6.5 from all the sampling points at this temperature resulted in the greatest biomass turnover followed by pH 8.5 and eventually that at pH 7.5 (Figure 5).

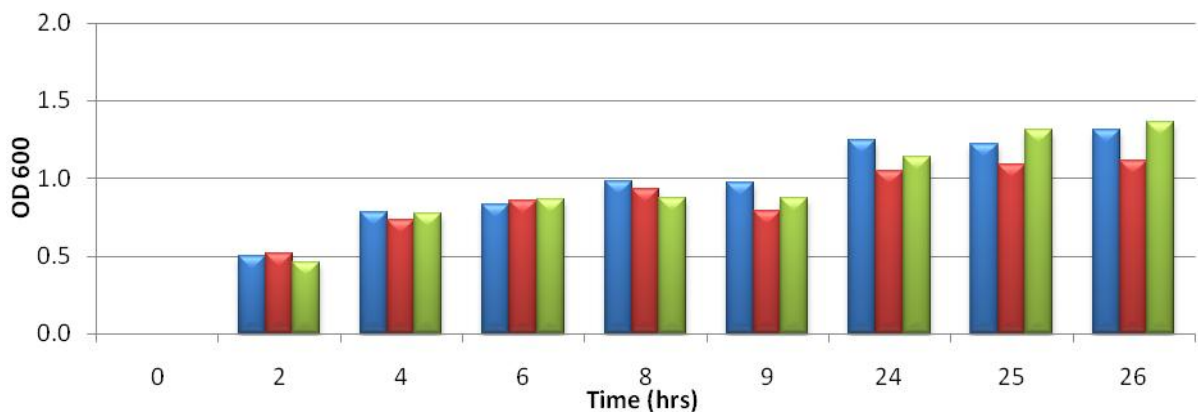


Figure 5: Relative increase in the biomass of *V. cholerae* serotype O139 grown at 37°C in LB. Three different pHs were used: pH 6.5 (blue bars), pH 7.5 (red bars) and pH 8.5 (green bars)

At 30°C LB at pH 8.5 showed the greatest increase in biomass of 1.56Abu for the majority of the sampling times followed by that at pH 6.5 and eventually the one at pH 7.5. However at

the end of the experiment pH 7.5 resulted in the greatest biomass turnover of 1.63Abu. So pH 8.5 favoured the greatest biomass increase on average of all the sampling times for the total duration of incubation at 30°C followed that at pH 7.5 and finally that at pH 6.5 (Figure 6).

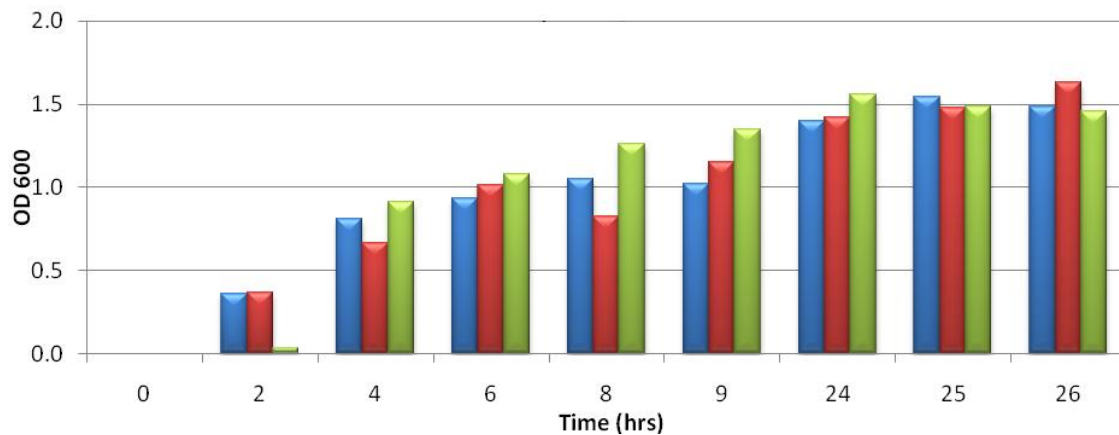


Figure 6: Relative increase in the biomass of *V. cholerae* serotype O139 grown at 30°C in LB. Three different pHs were used: pH 6.5 (blue bars), pH 7.5 (red bars) and pH 8.5 (green bars)

Growth in LB at pH 8.5 at 25°C resulted in the greatest biomass turnover consistently for the total period of incubation (Figure 7). However biomass formation at pH 6.5 and 7.5 closely followed each other with LB pH 7.5 resulting in a greater increase in biomass as compared to that at pH 6.5.

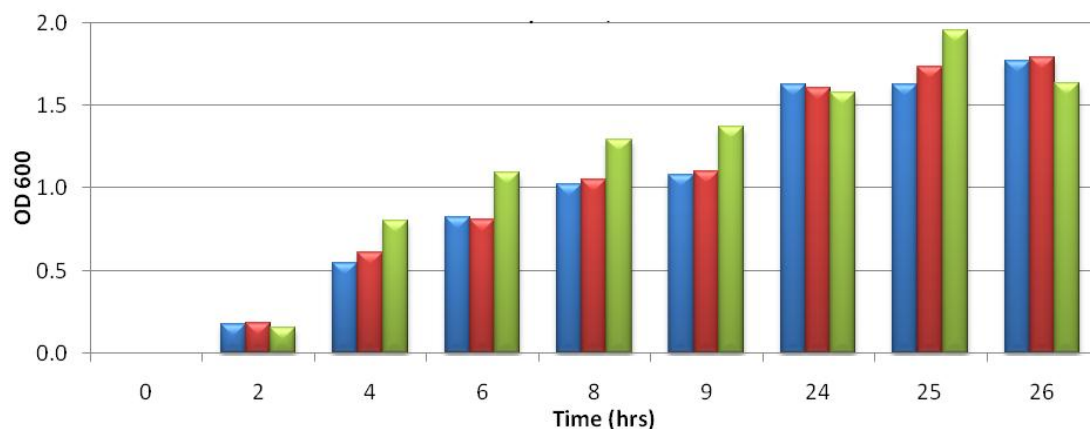


Figure 7: Relative increase in the biomass of *V. cholerae* serotype O139 grown at 25°C in LB. Three different pHs were used: pH 6.5 (blue bars), pH 7.5 (red bars) and pH 8.5 (green bars)

3.2.3 Growth of the 1009 strain

The growth of the 1009 strains in LB at pH 6.5 as well as pH 7.5 at 37°C throughout the duration of incubation resulted in similar biomass turnover; although initially lower, the biomass turnover at pH 8.5 towards the end of the incubation period surpassed that of both pH 6.5 and 7.5 (Figure 8). On average no one pH was better than the other even though growth in pH 8.5 resulted in the highest biomass yield of 1.36Abu.

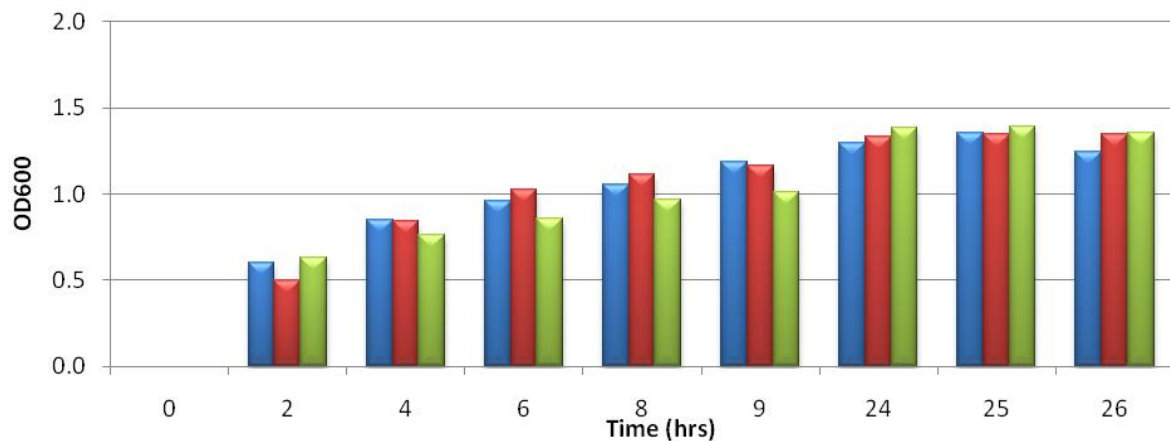


Figure 8: Relative increase in the biomass of *V. cholerae* strain 1009 grown at 37°C in LB. Three different pHs were used: pH 6.5 (blue bars), pH 7.5 (red bars) and pH 8.5 (green bars)

At 30°C pH 8.5 favoured the greatest increase in biomass (1.90Abu) followed by that at pH 7.5 (1.74Abu) and eventually at pH 6.5 (1.63Abu) (Figure 9). At this temperature the growth of the 1009 strain at pH 6.5 and pH 7.5 for the first 8 hours was similar however towards the end of the experiment LB at pH 8.5 favoured the greatest biomass turnover when compared to the other two pHs (pH 6.5 and 7.5). The result suggests that pH 8.5 provided the most favourable conditions for biomass turnover followed by pH 7.5 and 6.5 for the total duration of incubation.

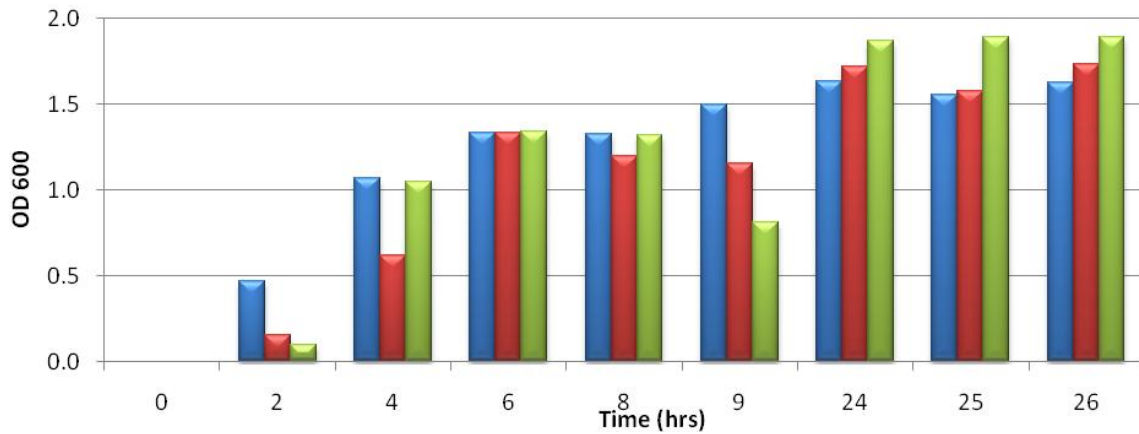


Figure 9: Relative increase in the biomass of *V. cholerae* strain 1009 grown at 30°C in LB. Three different pHs were used: pH 6.5 (blue bars), pH 7.5 (red bars) and pH 8.5 (green bars)

At 25°C, pH 6.5 provided the most favourable conditions for biomass yield (2.05Abu) compared to growth at pH 8.5 (1.97Abu) and 7.5 (1.60Abu). This is a clear indication that LB at pH 6.5 provided the best conditions for biomass turnover followed by LB at pH 8.5 and eventually that at pH 7.5 (Figure 10).

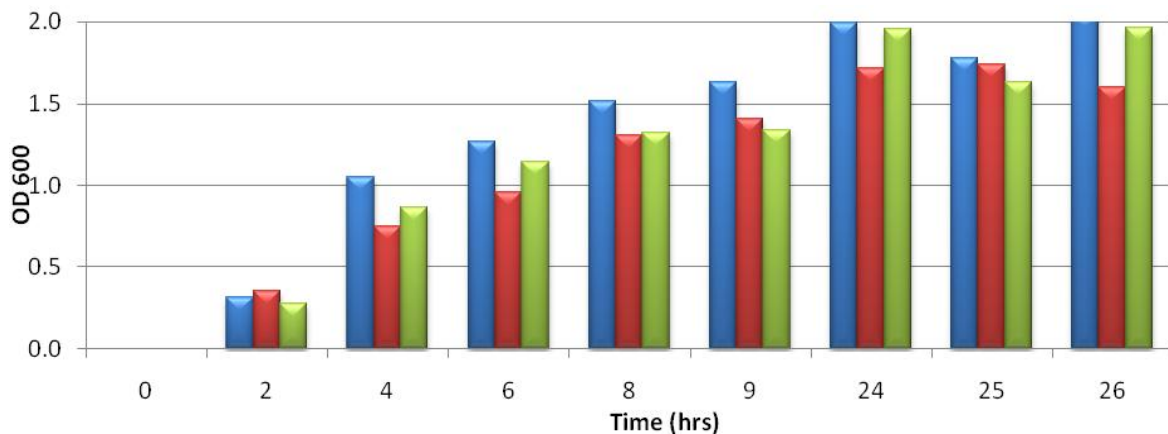


Figure 10: Relative increase in the biomass of *V. cholerae* strain 1009 grown at 25°C in LB. Three different pHs were used: pH 6.5 (blue bars), pH 7.5 (red bars) and pH 8.5 (green bars)

The nature of growth of all 3 strains of *V. cholerae* in LB at pH 8.5, 7.5 and 6.5 under varying incubation temperatures of 37°C, 30°C and 25°C was also simultaneously investigated. This was done to understand the effect that temperature had on the growth of all 3 strains of *V. cholerae* under the different pHs of LB.

The results show that low temperature favoured biomass increase for all the 3 strains of *V. cholerae* grown in LB at pH 6.5 (Figure 11). This observation was also true for the O139 strains at all the pHs unlike the O1 and 1009 strains. A closer examination of the results revealed that the increase in biomass with reduction in temperature was also true for pH's 7.5 and 8.5 for both the O1 and 1009 strains if comparing biomass turnover at incubation temperatures of 37°C and 30°C or 25°C (Figure 11). However it was important to note that both these strains had closely similar biomass peaks at 30°C and 25°C for pHs 7.5 and 8.5.

In addition to that the specific growth rate results show that the 30°C incubation provided conditions for the highest specific growth rate although its biomass turnover was not as high as that of the 25°C incubation for most for all the strains at pH 6.5.

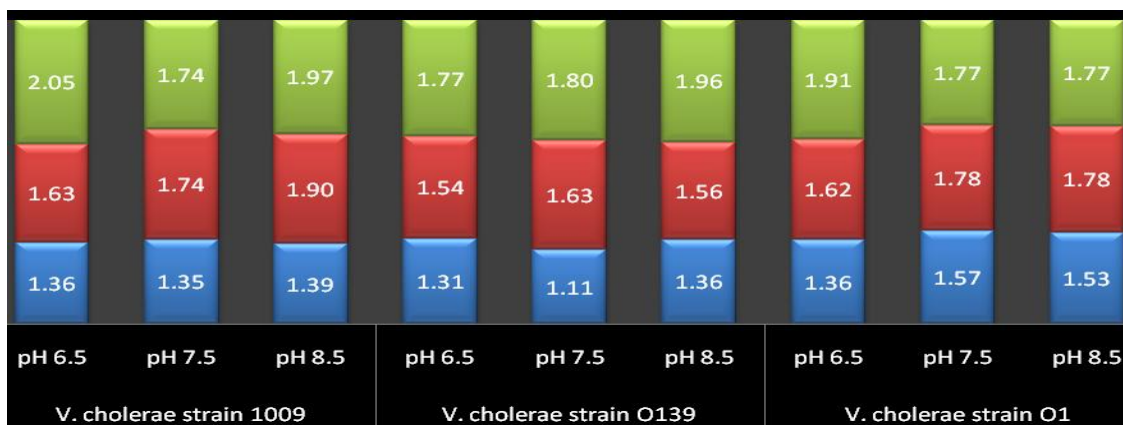


Figure 11: Stack chart showing the highest relative increase in the biomass of the 3 *V. cholerae* serotypes O1, O139 and strain 1009 grown in LB at pH 6.5, 7.5 and 8.5 and at 3 temperatures of incubation, 25°C (green), 30°C (red) and 37°C (blue)

The secretion of cholera toxin by the virulent strains of *V. cholerae* in LB at all pHs was investigated after 9 (late log phase) and 26 (Stationary phase) hours of incubation at all temperatures i.e. 37°C, 30°C and 25°C. The results (Figure 12) show that more cholera toxin was detected when both serotypes had been incubated in LB at pH 6.5. Nonetheless, both serotype evinced different behaviours. For instance, more cholera toxin was detected when the O1 serotype was incubated in LB (pH 7.5 and pH 8.5) at 30°C and 25°C which was not the case for LB at pH 6.5. The O139 serotype on the other hand released more cholera toxin, at 37°C and 30°C, regardless of the pH of the LB. A gradual increase in cholera toxin secretion was observed with decrease in pH by the O1 serotype.

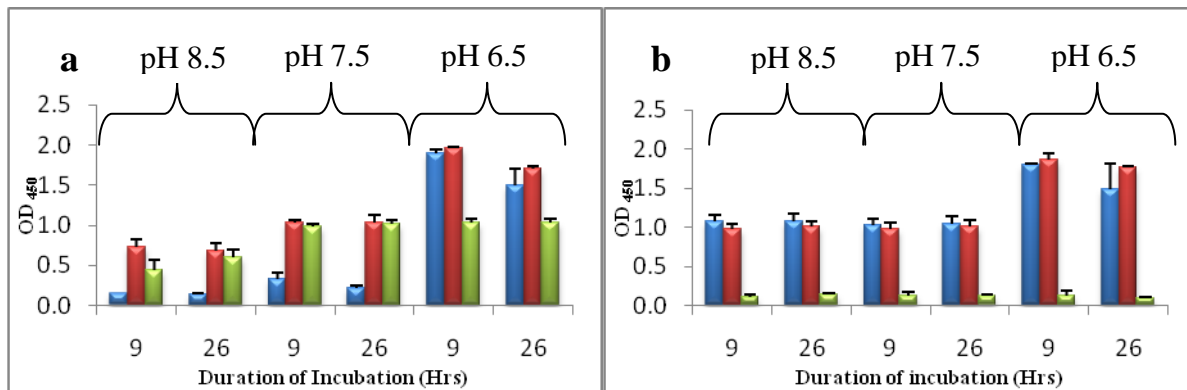


Figure 12: Cholera toxin secretion by the virulent *V. cholerae* serotypes O1(a) and O139 (b) when grown in LB under three different pH conditions for 9 and 26 hours at 37°C (blue bars), 30°C (maroon bars) and 25°C (green bars). Error bars indicate duplicate readings.

3.3 Effect of the pH of Ground Water and Temperature on the Growth of *V. cholerae*

The growth of each *V. cholerae* strain in ground water was investigated under three pHs (pH 6.5, 7.5 and 8.5) and three temperatures (25°C, 30°C and 37°C). All the strains were incubated for a maximum period of 7 days. These experiments were conducted to assess how the selected strains of *V. cholerae* would adapt to ground water a limited source of nutrients. These experiments were done to provide information on the adaptation and survival of these microorganisms in ground water. So in order to assess the adaptation and survival of these microbes in ground water it was necessary to use the GInaFiT Tool. All ten models in the GInaFiT Tool (described in the materials and methods Section 2.3.2.1), were used to analyse the nature of growth for each of the *V. cholerae* strains, and the model with the least RMSE value was taken as the best model describing the survival of the particular strain.

3.3.1 Ground Water at 25°C

All strains never showed any loss of culturability during the 25°C incubation for the duration of 7 days. Both the O1 serotype and 1009 strain showed an increase in colony forming units at pH 6.5 and at pH 8.5 and as a result GInaFiT reported a positive slope for all inactivation models since there was no inactivation. As a result no graph was generated by the GInaFiT tool since a positive slope was indicative of no reduction in colony forming units. Although there was a slight reduction in colony forming units at pH 7.5, there was no loss in

culturability. According to GInaFiT the suitable models describing the survival of both the O1 serotype and 1009 strain at pH 7.5 were the Geeraerd Log linear shoulder and tail (Figure 13) and Bigelow-Log linear (Figure 13), respectively.

On the other hand strain O139 maintained its colony forming units around the initial colony count which was Log 4.52 and Log 4.48 at pH 6.5 and pH 8.5, respectively. Unlike strains O1 and 1009, GInaFiT showed that the O139 strain mode of survival obeyed the Geeraerd Log linear tail and Bigelow-Log linear (Figure 13) models at pH 8.5 and 6.5, respectively. However, at pH 7.5 this strain showed a slight increase in colony forming units and as a result the GInaFiT tool was unable to model this kind of survival.

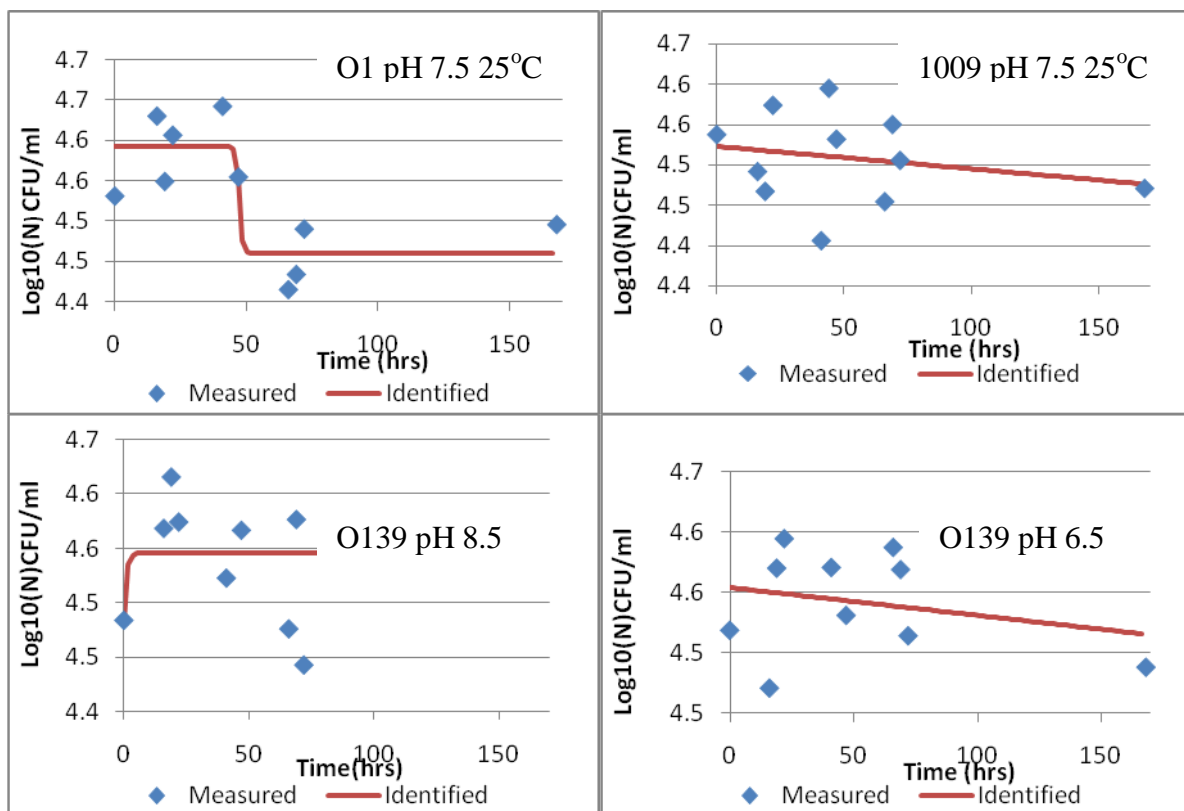


Figure 13: Inactivation curves of *V. cholerae* serotypes O1, O139 and strain 1009 incubated at 25°C under varying conditions of pH (as indicated in the graphs) for 7 days. Bacterial cells were harvested from LB batch cultures washed three times in 1X PBS and diluted in autoclaved ground water before incubation. Colony forming units were measured by the Miles and Misria drop technique. Measurements were done in triplicate. Lines represent the modelling results obtained with the GInaFiT Tool (Geeraerd et al., 2005). Graphs do not include strains whose CFU increased during the period of incubation (refer to results above).

3.3.2 Ground Water at 30°C

All *V. cholerae* strains used in this study were incubated at 30°C for 6 days. No increase in colony forming units was observed regardless of the strain at pH 6.5 and 8.5.

There was a slight loss in culturability by serotypes O1, O139 and strain 1009 when they were incubated in partially acidic ground water (pH 6.5) at 30°C. The *V. cholerae* strains behaved in a similar manner under these conditions. The O139 serotype showed the most sensitivity to ground water followed by the O1 and eventually the 1009 strain. During incubation at pH 6.5, all strains obeyed the Geeraerd Log linear shoulder tail model according to GInaFiT (Figure 14).

When these *V. cholerae* strains were incubated in ground water at pH 7.5 at 30°C, both the O1 and O139 serotypes displayed survival properties that were comparable to the ones shown at pH 6.5. According to GInaFiT both these serotypes obeyed the Geeraerd Log linear shoulder tail model (Figure 14). There was a slightly greater reduction in colony forming units at pH 7.5 than at pH 6.5. On the other hand the 1009 strain showed an increase in colony forming units and there was no model to describe the survival of this strain under these conditions.

V. cholerae serotypes O1, O139 and strain 1009 were also incubated in slightly alkaline (pH 8.5) ground water at 30°C for a maximum period of 6 days. During this period, none of the strains lost viability totally but each of the strains showed a slight decrease in colony forming units. The O1 serotype was most sensitive to these incubation conditions followed by the O139 serotype and finally the 1009 strain that proved to be the most resistant. According to the GInaFiT tool serotype O139 and strain 1009 obeyed the Geeraerd Log linear tail model of inactivation with a persistent residue population of 3.68 and 4.5 log CFU/ml, respectively (Figure 14b). On the other hand the O1 serotype obeyed the Corroller double weibull model (Figure 14a).

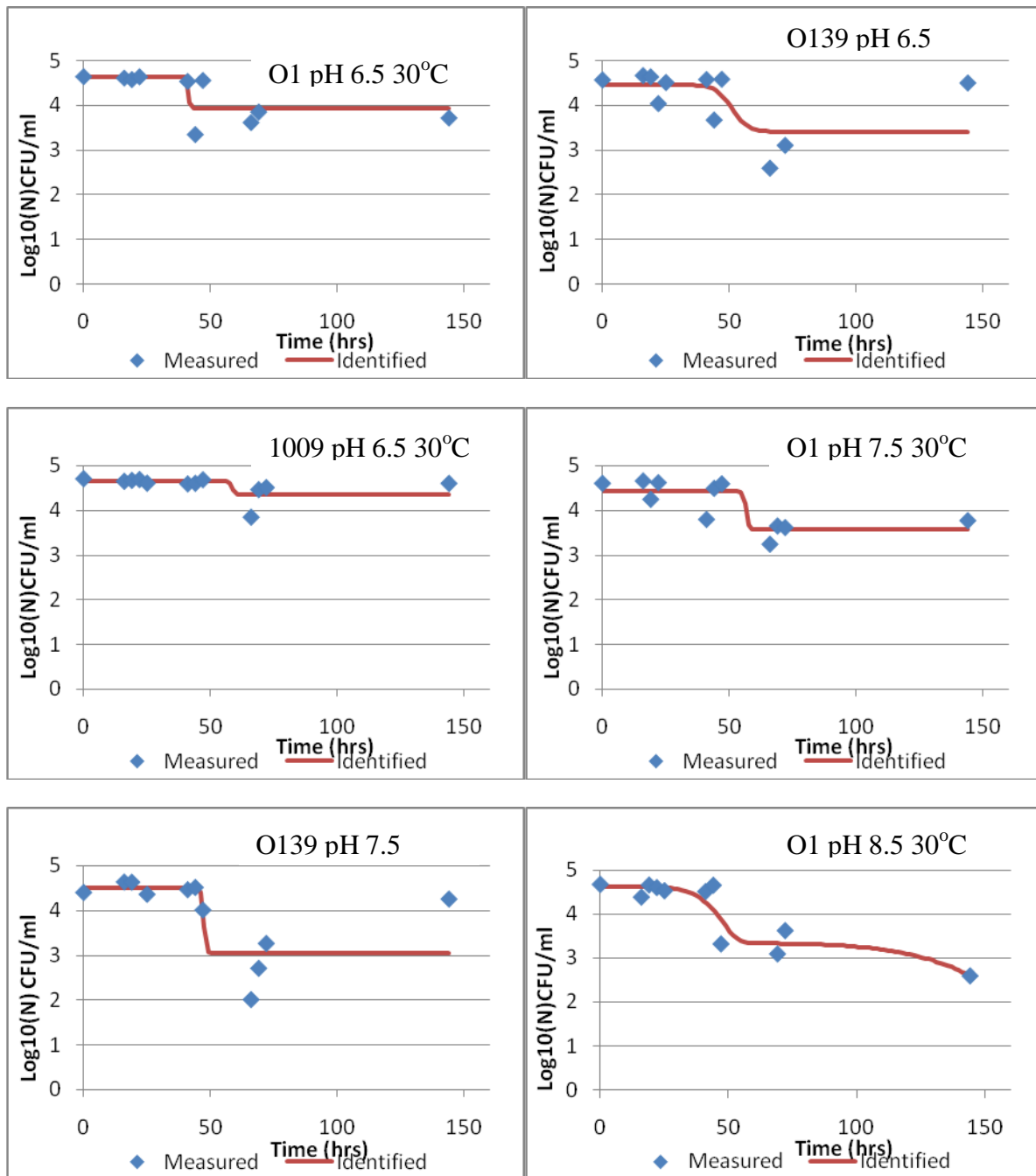


Figure 14 (a): Inactivation curves of *V. cholerae* serotypes O1, O139 and strain 1009 incubated at 30°C under varying conditions of pH (6.5, 7.5 and 8.5) for 6 days. Bacterial cells were harvested from LB batch cultures washed three times in 1X PBS and diluted in autoclaved ground water before incubation. Colony forming units were measured by the Miles and Misria drop technique. Measurements were done in triplicate. Lines represent the modelling results obtained with the GInaFiT Tool. Graphs do not include strains whose CFU increased during the period of incubation (refer to results above).

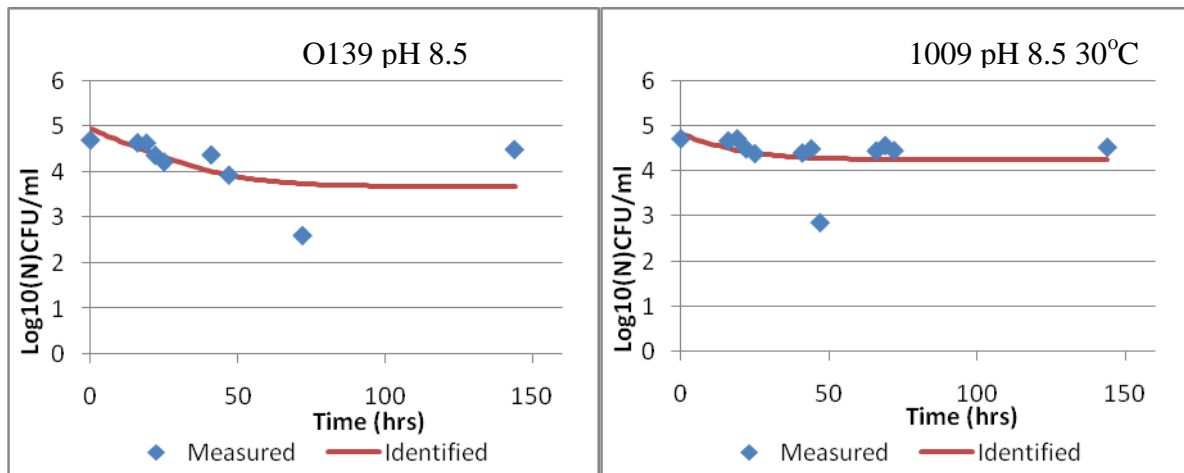


Figure 14 (b): Inactivation curves of *V. cholerae* serotypes O139 and strain 1009 incubated at 30°C pH 8.5 for 6 days. Bacterial cells were harvested from LB batch cultures washed three times in 1X PBS and diluted in autoclaved ground water before incubation. Colony forming units were measured by the Miles and Misria drop technique. Measurements were done in triplicate. Lines represent the modelling results obtained with the GInaFiT Tool. Graphs do not include strains whose CFU increased during the period of incubation (refer to results above).

3.3.3 Ground Water at 37°C

The nature of growth and survival of the 3 *V. cholerae* strains was investigated by culturing them in autoclaved ground water at pH 6.5, 7.5 and 8.5, at 37°C for a maximum period of 7 days.

Total inactivation without relapse was observed with serotypes O1 and O139 incubated at 37°C in slightly acidic (pH 6.5) autoclaved ground water. According to GInaFiT both the O1 and O139 obeyed different inactivation models (Figure 15). The O1 serotype obeyed the Cerf biphasic model of inactivation and according to which the serotype reached a 4D reduction time at 53.24 hours of incubation.

On the other hand the O139 serotype obeyed the Corroler double weibull model of inactivation and reached its 4D reduction at 57.6 hours of incubation. The 1009 strain was the least affected as it survived throughout the whole duration of incubation (7 days). During this period of incubation the strain did not increase in viability but reduced by at least 3 log CFU/ml. According to GInaFiT this strain obeyed the Bigelow Log linear model (Figure 15).

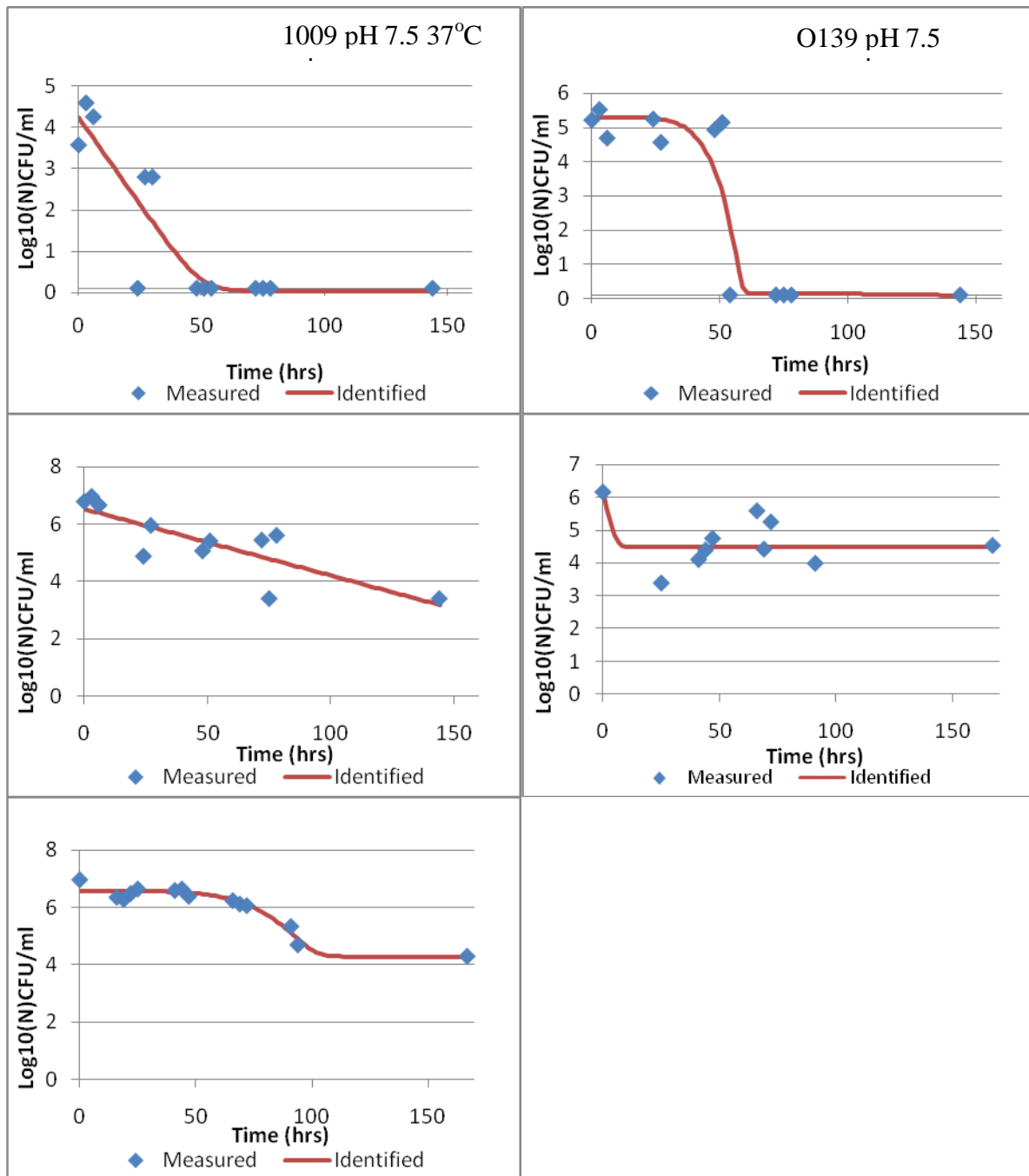


Figure 15: Inactivation curves of *V. cholerae* serotypes O1, O139 and strain 1009 incubated in autoclaved ground water at 37°C under varying conditions of pH (6.5, 7.5 and 8.5) for 6 days. Bacterial cells were harvested from LB batch cultures washed three times in 1X PBS and diluted in ground water before incubation. Colony forming units were measured by the Miles and Misria drop technique. Measurements were done in triplicate. Lines represent the modelling results obtained with the GInaFiT Tool. Graphs do not include strains whose CFU increased during the period of incubation (refer to results above)

When the *V. cholerae* strains were incubated at 37°C in autoclaved ground water at pH 7.5, serotype O139 and strain 1009 survived for the entire incubation. However, both strains showed a decrease in their colony forming units without total inactivation as 4.54 logs CFU/ml and 4.3 log CFU/ml remained at the end of the 7 day incubation for serotype O139 and strain 1009, respectively. According to GInaFiT the O139 serotype and 1009 strain obeyed the Geeraerd Log linear tail and Corroler double weibull models, respectively (Figure 15). On the other hand the O1 strain under the same conditions was unculturable and no attempts were made to culture it because pH 7.5 was not going to be used for SUVR.

The three *V. cholerae* strains were also incubated in slightly alkaline (pH 8.5) autoclaved ground water for a maximum period of 7 days. During this time, serotypes O1 and O139 were no longer culturable within 3 days of incubation. Strain 1009, however, showed a decrease in its Log CFU/ml counts but remained culturable throughout the entire incubation period. The results obtained for the nature of growth and survival of these *V. cholerae* strains were analysed by the GInaFiT tool. These results showed that the O1 and O139 strain obeyed the Geeraerd biphasic shoulder (Figure 19) and Corroler double weibull (Figure 20) models of inactivation, respectively. The O1 strain had a 4D reduction time of 69 hrs whereas the O139 strain had a 4D reduction time of 75 hrs. On the other hand the 1009 strain obeyed the Geeraerd Log linear shoulder tail model with a shoulder length of 62.93 hours and a residual viable population of 5.75 logs CFU/ml (Figure 21).

Cholera toxin secretion by the two virulent serotypes O1 and O139 in ground water at different pHs was investigated at the end of each incubation. The results show that there was less cholera toxin released when incubated in ground water at pH 6.5 by both serotypes. Interestingly enough there was a gradual increase in cholera toxin release with a decrease in pH especially by the O1 serotype. However, more cholera toxin was released by both serotypes when incubated at 37°C with the exception of those cultured in ground water at pH 6.5. It is also important to note that more cholera toxin was released in ground water at pH 7.5, followed that at pH 8.5 and eventually that at pH 6.5. The amount of cholera toxin secretion in ground water differed from that produced in LB with regards to pH and quantity (Figures 16a and 16b).

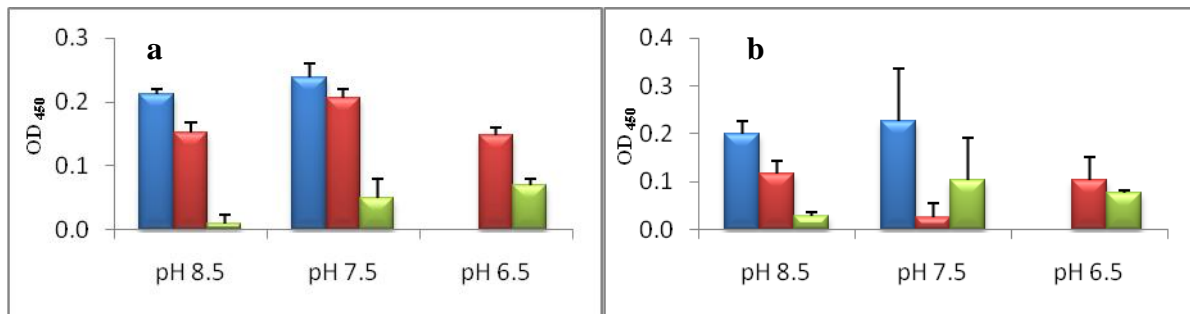


Figure 16: Cholera toxin secretion by the virulent *V. cholerae* serotypes O1(a) and O139 (b) at the end of 37°C (blue bars), 30°C (maroon bars) and 25°C (green bars) incubation in ground water under three different pH. Error bars indicate duplicate readings.

3.4 Optimal growth Conditions

3.4.1 Growth of *V. cholerae* in Luria Broth

The growth of all three strains of *V. cholerae* under optimal growth conditions (37°C and pH 8.5) for 26 hours in LB was plotted on a graph of time against OD 600 (Figure 17). The growth of all strains began with a log phase of varying durations depending on the strain. Strain 1009 had the shortest log phase of about 2 hours while the log phase of serotypes O139 and O1 lasted for 4 and 6 hours, respectively. The initial log phase was followed by a slower growth phase which also varied according to the strain; strain 1009 displayed a longer slowing down phase of 22 hours compared to that of the O1 serotype that lasted for 16 hours. The O139 serotype on the other hand showed a brief 2 hours slow down phase followed by what appeared to be a stationary phase for 3 hours. This stationary phase did not appear for any of the other strains. This was followed by a slow growth phase for 15 hours. Strain 1009 reached its stationary phase after 24 hours. However, strains O139 and O1 appeared to have a

slight increase in growth rate for an hour and growth seemed to level off at the 26th hour.

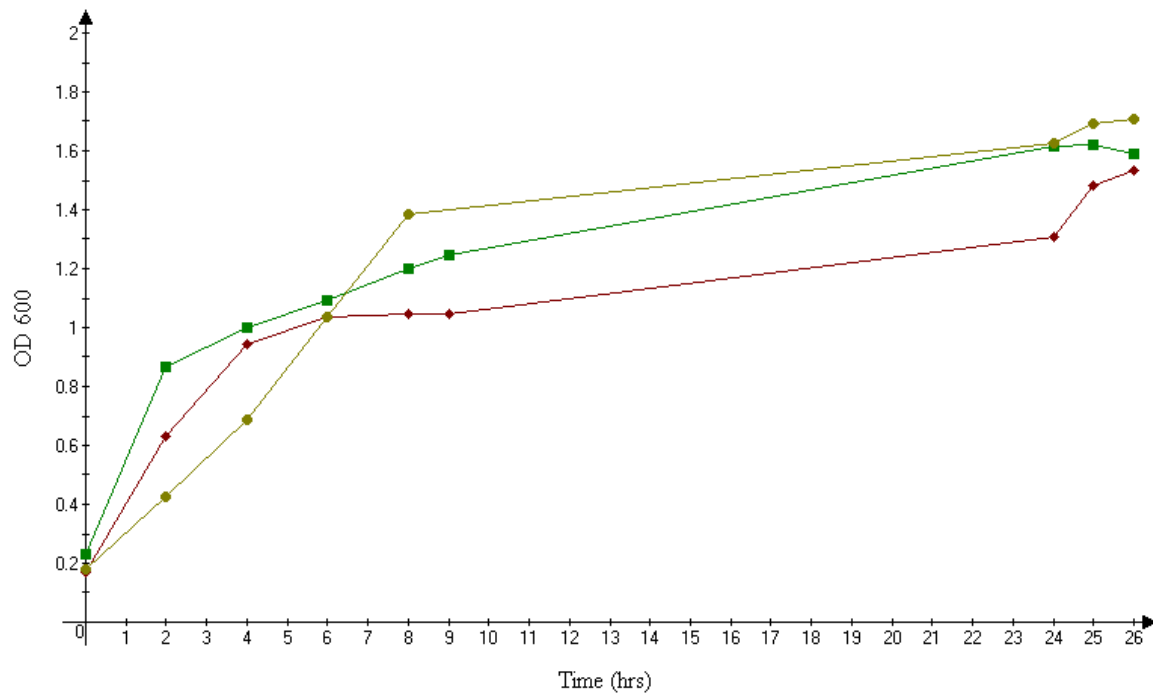


Figure 17: Growth curves of the *V. cholerae* serotypes O1 (yellow), O139 (maroon) and strain 1009 (green) in Luria Broth at 37°C, pH 8.5 for a period of 26 hours.

3.4.1.1 Growth Rate and Relative Increase in Biomass of *V. cholerae* in LB

The O139 serotype began with the highest growth rate when compared to serotype O1 and strain 1009 (Table 2). However, within a short period of time, the O139 serotype had undergone a steep decline in growth rate, which remained constantly low for the rest of the 24 hours. On the other hand, the 1009 strain followed a growth rate pattern similar to that of the O139 serotype but with a slightly higher growth rate as shown in Table 1. The O1 serotype unlike the O139 and 1009 did not have a steep decline in growth rate but rather a gradual decrease in its growth rate that roughly levelled off after 17 hours.

The nature of growth for all the three strains of *V. cholerae* depicted by the growth rates and doubling times is responsible for the increase in biomass. The histogram in Figure 15 shows the relative increase in biomass for each of the strains.

Table 2: Growth rates and doubling times of LB grown *V. cholerae* at 37°C pH 8.5

Time (hrs)	<i>V. cholerae</i> 1009		<i>V. cholerae</i> O139		<i>V. cholerae</i> O1	
	Growth rate (μ)	Doubling time (h-1)	Growth rate (μ)	Doubling time (h-1)	Growth rate (μ)	Doubling time (h-1)
0.5	0.36	1.90	0.43	1.63	0.34	2.05
5	0.06	12.04	0.12	5.68	0.22	3.10
7	0.04	15.84	0.02	30.09	0.17	4.01
9	0.04	15.84	0.02	30.09	0.07	10.03
17	0.02	42.99	0.01	50.15	0.01	60.18
20	0.02	42.99	0.02	37.61	0.02	37.61
26	-0.01	-100.30	0.08	8.85	0.02	30.09

Figure 18 shows that the O1 serotype had the greatest relative turnover in biomass of 1.532 Abu followed by the 1009 strain and eventually the O139 serotype with 1.39 and 1.36Abu, respectively. The relative increase in biomass is reflective of the nature of the growth rates and doubling times for the strains.

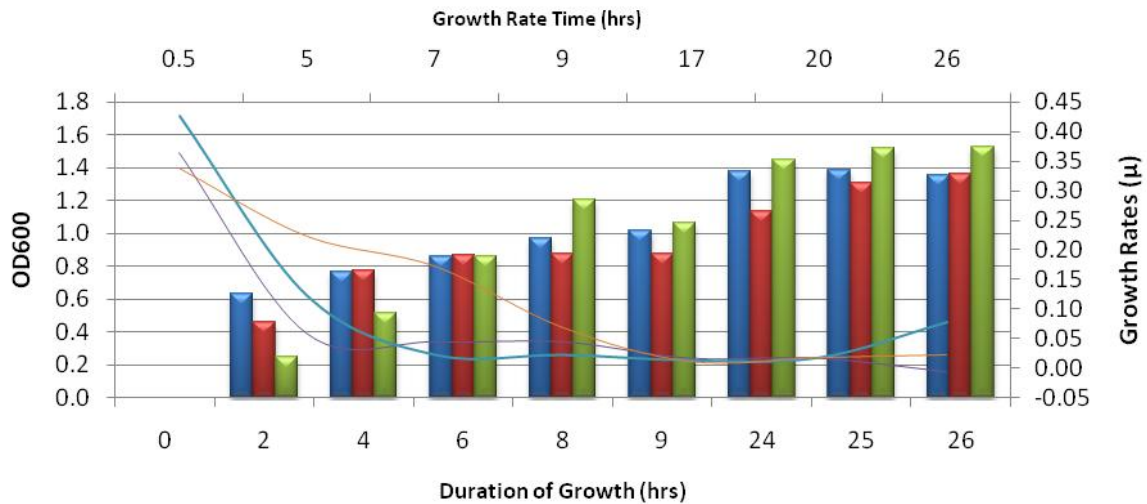


Figure 18: Bar and line graph showing the relative increase in biomass and relative growth rates respectively, of *V. cholerae* strain 1009 (blue bars and purple line), and serotypes O139 (maroon bars and blue line) and O1 (green bars and orange line) grown in LB broth under optimal growth conditions i.e. pH 8.5 and temperature 37°C.

3.4.2 Growth of *V. cholerae* in Ground water

The nature of survival of *V. cholerae* in ground water under optimal growth conditions of temperature and pH (defined as pH 8.5 and 37°C) was analysed using the GInaFiT modelling tool. Table 3 below shows the best models describing the survival for each strain of *V. cholerae* grown in ground water under optimal conditions.

Table 3 : Showing the GInaFiT modelling of *V. cholerae* Strain Grown in Ground Water

Strain	Fitting model	Parameters		
		$k_{max} [hr^{-1}]$	SI [hrs]	Log 10(Nres) [cfu/ml]
O1	Geeraerd Biphasic and Shoulder	3.15	65.87	-
O139	Corroler Double Weibull	-	-	-
1009	Geeraerd Log linear Shoulder and Tail	0.85	62.93	5.74

The information in Table 3 and Figures 19, 20 and 21 showed that each *V. cholerae* strain had a different model describing its survival in ground water under optimal growth conditions. The survival of serotypes O1, O139 and strain 1009 in ground water was best described by the Geeraerd Biphasic and Shoulder (Figure 19), Corroler Double weibull (Figure 20) and Geeraerd log linear + shoulder (Figure 21) models, respectively.

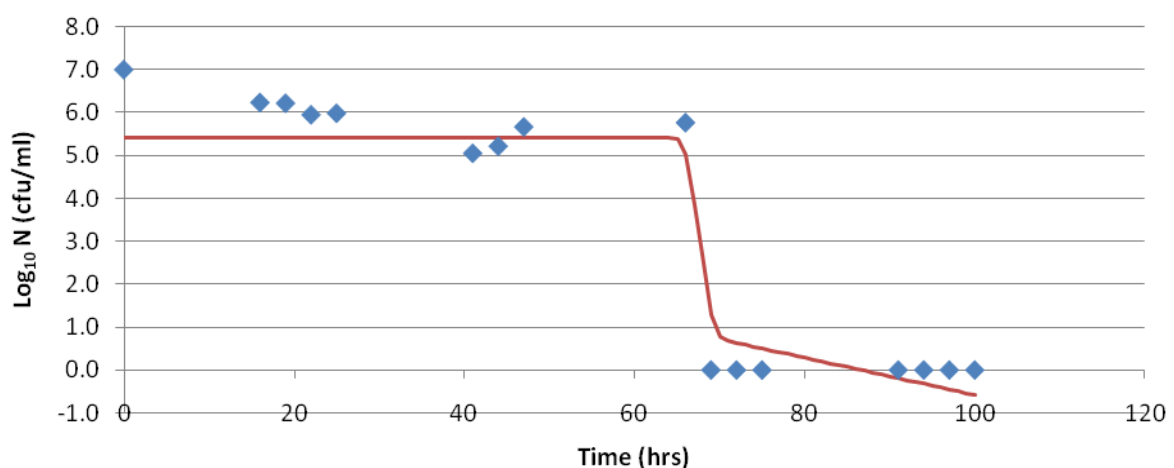


Figure 19: The best GInaFiT model describing the survival of *V. cholerae* serotype O1 in autoclaved ground water for a period of 80 hours at 37°C at pH8.5.

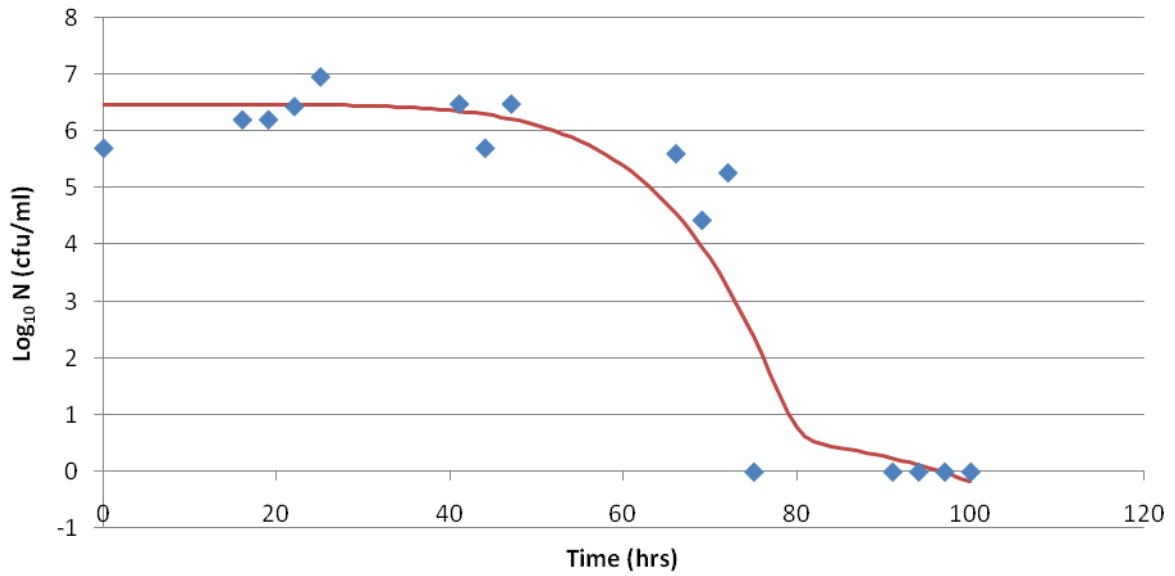


Figure 20: The best GInaFiT model describing the survival of *V. cholerae* serotype O139 in autoclaved ground water for a period of 80 hours at 37°C at pH8.5.

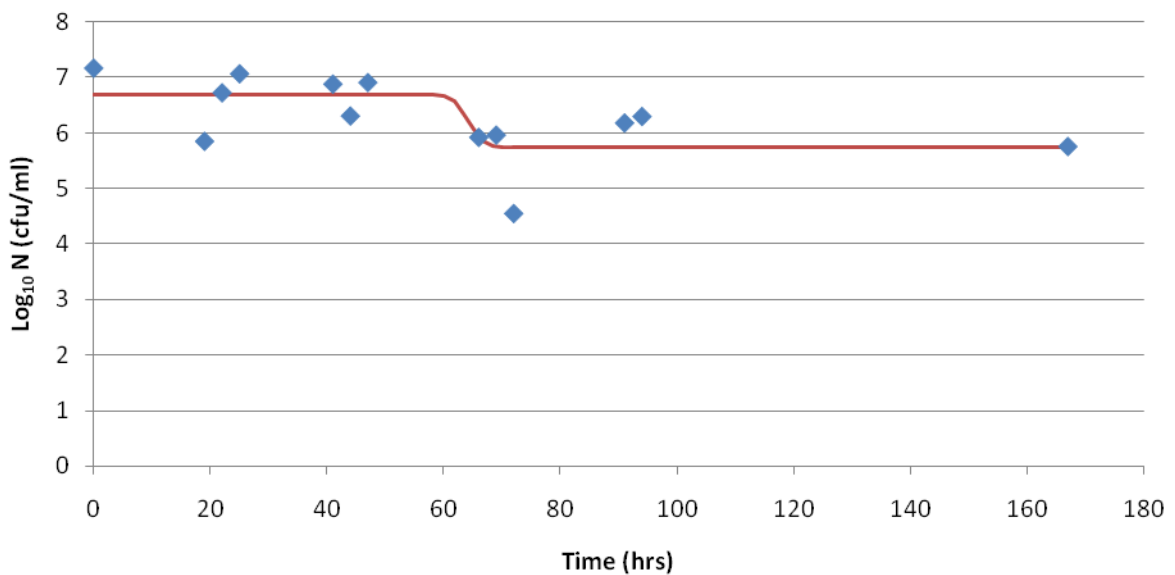


Figure 21: The best GInaFiT model describing the survival of *V. cholerae* strain 1009 in autoclaved ground water for a period of 80 hours at 37°C under alkaline conditions pH8.5.

After it was shown that the *V. cholerae* strains used in this study could grow in both media under all the different conditions, solar exposures were initiated.

3.5 Solar Ultraviolet Radiation

The amount of solar UVA and UVB radiation was captured by UV meters installed on the unshaded rooftop of the Natural Resources and Environment (NRE) Unit of CSIR and downloaded from the data logger via a computer. The temperature data was acquired from a weather station located in Meyers Park (less than 6km from NRE-CSIR) via the internet (Unknown, 2010b).

The temperature and solar UVA and UVB radiation data discussed in this study was captured between the 19th of May 2009 and the 16 of August 2010. The maximum UVA and UVB irradiance as well as the temperature for each day was obtained. This data was grouped according to the four seasons experienced in South Africa i.e. spring (August to mid-October), summer (mid-October to mid-February), autumn (mid-February to April) and lastly winter (May to July) (Unknown, 2010a). The average irradiance due to UVA and UVB as well as the temperature was then calculated for each season (Table 4).

Table 4: Mean and standard deviations of UVA, UVB and temperature for the different seasons for the period between 19 May 2009 and 31 July 2010

Seasons	Year	N ¹	Maximum		Maximum Temp (°C) & σ
			UVA (W/m ²) & σ	UVB (W/m ²) & σ	
Winter	2009	63	24.67 ± 3.86	0.08 ± 0.02	16.62 ± 2.67
Spring	2009	78	30.92 ± 5.15	0.10 ± 0.02	21.90 ± 4.95
Summer	2009/2010	57	45.79 ± 10.89	0.14 ± 0.04	27.04 ± 5.23
Autumn	2010	24	36.94 ± 6.78	0.09 ± 0.03	25.46 ± 2.98
Winter	2010	71	23.02 ± 4.41	0.05 ± 0.01	18.36 ± 3.07

¹ Number of data points analyzed during the entire period

3.6 SUVR and Temperature Pattern

Solar UVA, UVB irradiance and the temperature, displayed similar trend characterised by the increase and decrease of the parameters for the days analysed during the one year period. The period from 19 May 2009 to the end of July 2009 corresponded to the winter season in South Africa. During this period the maximum average UVA, UVB irradiance and temperature was 24.67W/m², 0.076W/m² and 16.62°C, respectively. In spring (August 2009 until mid-October 2009) on the average maximum UVA, UVB irradiance and temperature increased to

30.92W/m², 0.0988W/m² and 21.89°C, respectively. In summer (mid-October 2009 until mid-February 2010) the average maximum UVA, UVB solar irradiance and temperature was 45.787W/m², 0.144W/m² and 27.08°C, respectively. In autumn (mid-February 2010 to April 2010) the maximum UVA, UVB irradiance and temperature on averaged was 36.93W/m², 0.094W/m² and 25°C, respectively. In the second winter (May 2010 to July 2010) the mean maximum solar UVA, UVB irradiance and temperature was 23W/m², 0.0515W/m² and 18.36°C, respectively.

In summary, winter was characterized by low levels of solar irradiance due to UVA and UVB as well as lower temperatures. These parameters gradually increased in spring, reached their maximum levels in summer and gradually decreased in autumn and reached their minimal levels again in winter (Figure 22).

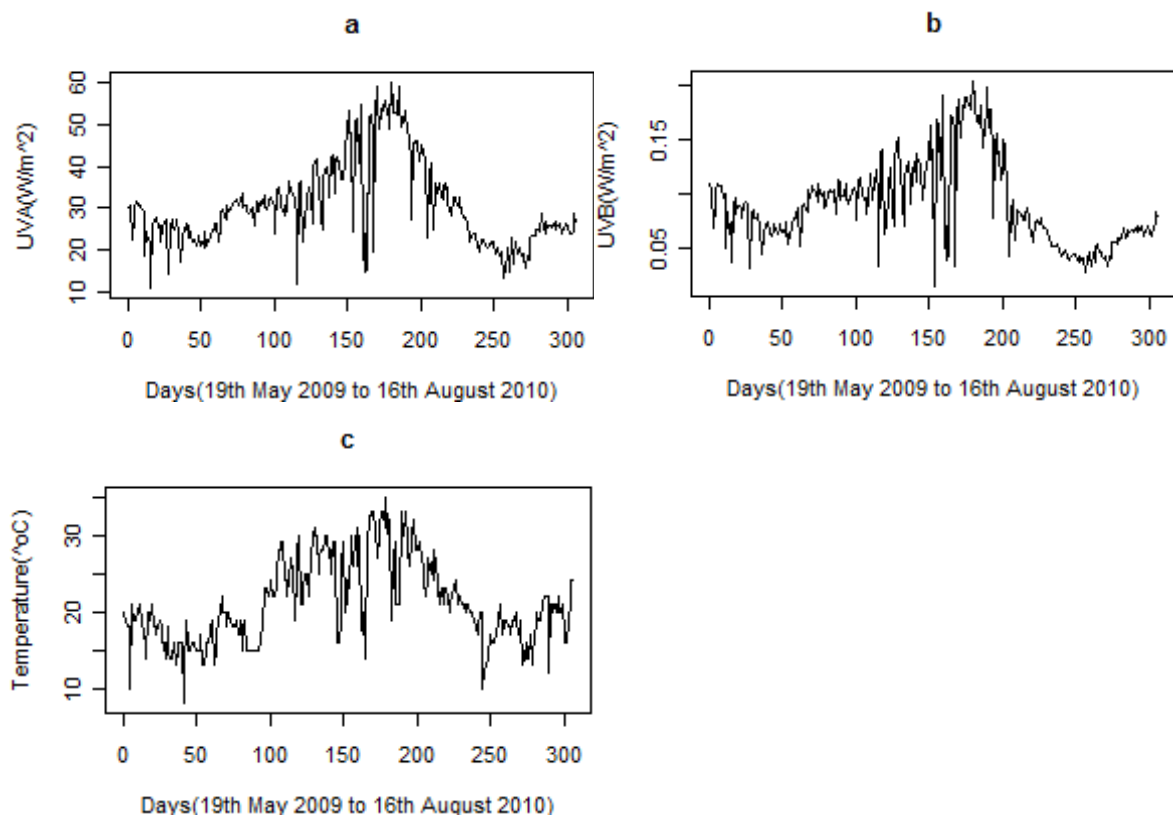


Figure 22: Daily maximum levels of UVA (a), UVB (b) solar irradiance (W/m²) and temperature (c) (°C) for the period between the 19th of May 2009 and 16th of August 2010

3.7 Exposure of *V. cholerae* to SUVR

V. cholerae was exposed to SUVR in ground water and LB twice during summer and autumn or thrice during spring and winter. The ground water was obtained from a bore hole in Soshanguve and analysed for its chemical content (Table 5) whereas LB was prepared in the laboratory. The *V. cholerae* strains were treated according to the media where they were to be exposed (refer to chapter 2). They were then exposed to solar radiation in transparent polystyrene 25cm² unventilated tissue culture flasks. One flask as well as one control for each strain at each pH were removed after 3, 7, 13 and 24 hours of exposure and processed accordingly.

Table 5: The physiochemical properties of ground water

Physiochemical Property (Units)	Value
Alkalinity (mg/L CaCO ₃)	25
Ammonia nitrogen (mg/L N)	<0.1
Calcium (mg/L Ca)	29
Chloride (mg/L Cl)	70
COD (mg/L COD)	<10
Elect Conductivity (mS/m [25°C])	56.9
Iron (mg/L Fe)	<0.06
Magnesium (mg/L Mg)	16
pH (pH units [25°C])	6.1
Sodium (mg/L Na)	43
Total Hardness (mg/L CaCO ₃)	137
Turbidity (NTU)	0.1

The effect of solar radiation of the three *V. cholerae* strains exposed in ground water at pH 8.5 and pH 6.5 was measured as growth inactivation and expressed as a function of Log (CFU_i^{-ml}/CFU_o^{-ml}) where CFU_i^{-ml} stands for the Colony Forming Units (CFU) counts per millilitre at a given sampling time point while CFU_o^{-ml} stands for the initial CFU counts per millilitre. This provided a better representation of the culturability status of the microorganisms after solar exposure. On the other hand the effect of solar exposure of the

three *V. cholerae* strains in LB was measured as the increase in biomass formation and determined by OD₆₀₀ after each time point.

Detection of cholera toxin by ELISA was performed on all the solar and non-solar exposed samples of the virulent strains of *V. cholerae* used in this study i.e. serotypes O1 and O139. The results have been reported as a function of the difference between solar exposed and non-solar exposed where cholera toxin produced by the non-solar exposed samples was subtracted from that produced when the samples were solar exposed. The resultant value was thus indicative of the actual effect of SUVR on the release of the cholera toxin. It should however be noted that the cholera toxin detection by ELISA was not performed as a means of determining or indicating increased virulence but only as a means of assessing the effect of SUVR on the release of cholera toxin and for that reason the samples were run without sonication or centrifugation.

The effect of SUVR on the cytoplasmic integrity of the microorganisms was also investigated with a flow cytometer using fluorescent dyes.

3.7.1 SUVR Exposures during Spring

The effect of SUVR on the culturability of the *V. cholerae* strains was investigated while following a natural temperature profile during spring. Non-solar exposed samples with the same temperature conditions were used as the controls for each strain. The effect of SUVR on the culturability of *V. cholerae* toxigenic and environmental strains after exposure in the media at pH 8.5 and 6.5 was assessed on three different days during spring; 25th of August 2009, 15th of September 2009 and 29th of September 2009 for ground water and two different days during spring; 1st of September 2009 and the 22nd of September 2009 (Table 6) for LB.

Table 6: SUVR, atmospheric conditions and temperature profiles for the days of solar exposure during spring

Date	Solar Conditions	Max UVA (W/m ²)	Max UVB (W/m ²)	Min-Max Temp (°C)
25-Aug-09 ²	Sunny	30.5	0.1024	8 – 36
1-Sept-09 ¹	Sunny	31.3	0.0981	14 – 36
15-Sept-09 ²	Sunny	29.21	0.0941	17 – 32
22-Sept-09 ¹	Sunny	33.6	0.108	13 – 34
29-Sept-09 ²	Cloudy	21.8	0.0627	11 – 25

1 represents days on which exposures were done in LB

2 represents days on which exposures were done in ground water

3.7.1.1 Ground water

Washed bacterial cells of *V. cholerae* toxigenic strains and environmental strain 1009 were suspended in ground water to a final OD₆₀₀ of 0.01 (~7.5 Log CFU ± 0.5). The effect of SUVR on the culturability of exposed *V. cholerae* toxigenic and environmental strains was determined 3hrs after exposure in ground water at both pH 8.5 and 6.5 on all the days of exposure during spring season. The culturability of these microorganisms declined on the 3 days with the exception of strain 1009 in the 25th of August 2009 at pH 8.5 (Figure 23a). The two *V. cholerae* virulent strains showed greater sensitivity to SUVR while the environmental strain showed the least sensitivity to SUVR (Figure 23). Throughout the 24hrs of exposures during spring, strain 1009 remained culturable almost at all-time points and at both pHs of ground water with the exception of the experiment performed on the 15th of September 2009. It did however lose its culturability after 7 hrs or 13 hrs of solar radiation even though regrowth was observed (Figure 23c and 23d).

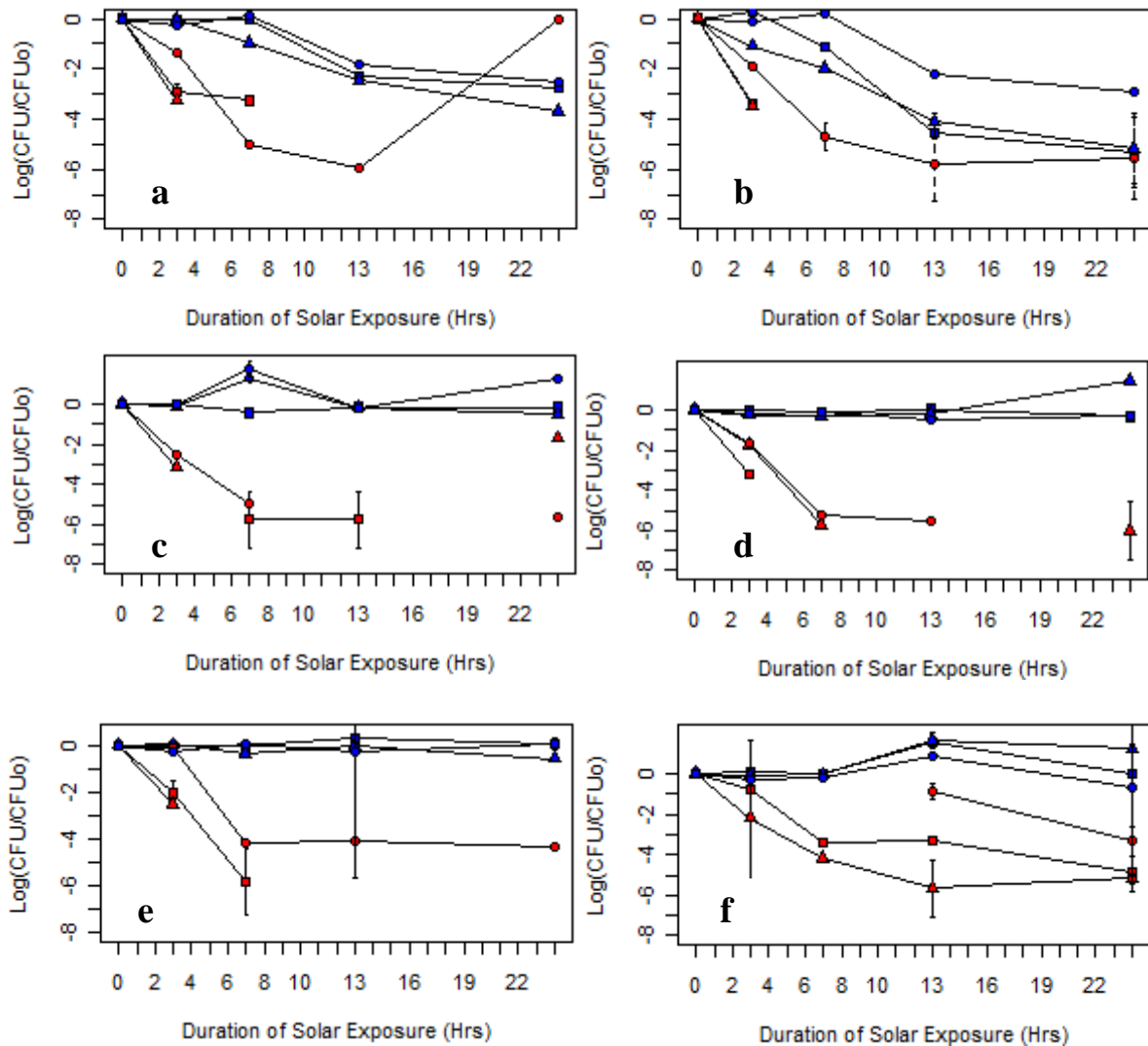


Figure 23: Inactivation kinetics of solar exposed *V. cholerae* serotypes O1 (red squares), O139 (red triangles) and strain 1009 (red circles) and non-exposed *V. cholerae* serotypes O1 (blue squares), O139 (blue triangles) and strains 1009 (blue circles) in ground water on the 25th of August 2009 at pH 8.5 (a) and pH 6.5(b), the 15th of September 2009 at pH 8.5 (c) and pH 6.5(d) and on the 29th of September 2009 at pH 8.5 (e) and pH 6.5 (f). Error bars indicate the standard deviation from duplicate measurements. Absence of the symbols indicates non culturability.

The toxigenic strain behaved in a similar mode in that they lost culturability at some stage of exposure and relapsed. For instance the O1 serotype was not culturable after 3hrs of solar exposure as indicated by the experiment conducted on the 15th of September (Figure 23c) however after 7hrs of exposure on that very day, this strain regained culturability which it maintained for the next 6 hrs but was lost only after 24hrs of exposure (Figure 23c).

The effect of SUVR during spring on the release or secretion of cholera toxin was also investigated. The results obtained from the CT- ELISA on the virulent *V. cholerae* strains suggest that cholera toxin is produced in spite of the culturability status of the microorganism (Figure 23c, 23f and Figure 24a for serotype O1 and Figure 23c and 23f and Figure 24c for serotype O139). Both the O1 and O139 serotypes showed a greater ability to secrete the cholera toxin in ground water at pH 8.5 as opposed to that at pH 6.5.

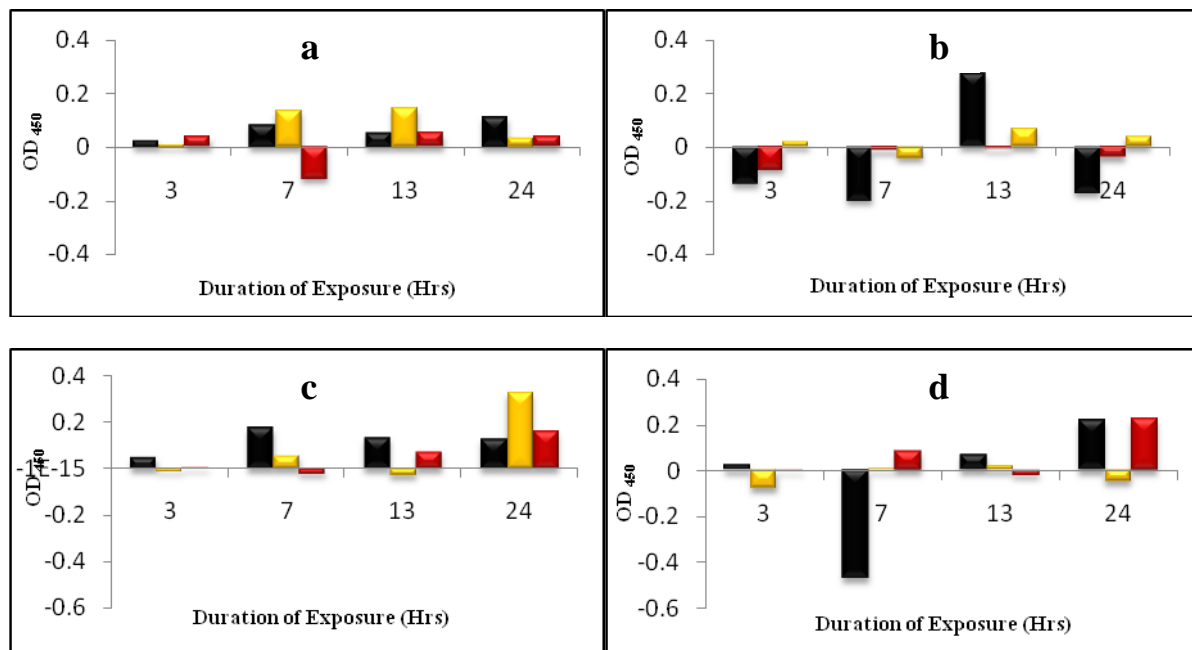


Figure 24: The effect of SUVR on the release of cholera toxin expressed as the difference between the solar exposed and non-solar exposed *V. cholerae* strain O1 in ground water at pH 8.5 (a) and pH 6.5 (b) and *V. cholerae* strain O139 in ground water at pH 8.5 (c) and pH 6.5 (d). During spring on the 25th of August 2009 ■ the 15th of September ■ and the 29th of September 2009 ■.

3.7.1.2 LB

Bacterial cells of *V. cholerae* toxigenic and environmental strains were suspended in full strength LB broth to a final OD₆₀₀ of 0.01 and exposed to SUVR at two pHs i.e. pH 6.5 and 8.5 on two different days. The O1 solar exposed samples did not show any increase in biomass on both days they were exposed. However serotype O139 and strain 1009 showed an increase in biomass formation and in some instances surpassed their controls (Figure 25a, 25b and 25c).

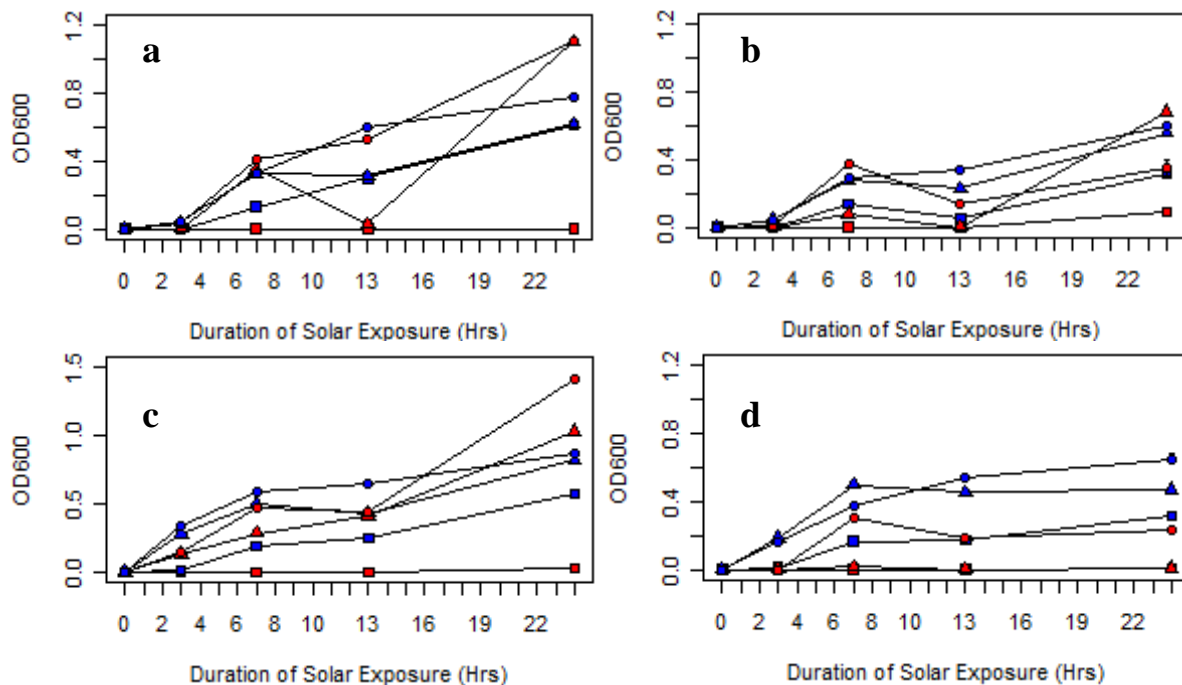


Figure 25: Representative growth curves of solar exposed *V. cholerae* serotypes O1 (red squares), O139 (red triangles) and strain 1009 (red circles) and non-exposed *V. cholerae* serotypes O1 (blue squares), O139 (blue triangles) and strain 1009 (blue circles) in LB on the 1st of September 2009 at pH 8.5 (a) and pH 6.5(b), the 22nd of September 2009 at pH 8.5 (c) and pH 6.5 (d). Error bars indicate the standard deviation from duplicate measurements.

Cholera toxin release by the *V. cholerae* toxigenic strains due to SUVR in LB at pH 8.5 and pH 6.5 was investigated. The results show that although both virulent strains were capable of releasing toxin the influence of SUVR on cholera toxin production was strain dependent. Cholera toxin secreted by serotype O1 was not necessarily due to SUVR exposure. In Figure 26a and 26b the negative value bars indicate that more cholera toxin was released by the non-solar exposed samples of the O1 serotype at both pH 8.5 and pH 6.5 and on both days of exposure. Serotype O139 on the other hand produced more cholera toxin when exposed to solar radiation during spring. Furthermore the effect of SUVR was greater at pH 6.5 than at pH 8.5 (Figure 26c and 26d). So even though there was greater secretion of cholera toxin it was not necessarily connected to an increase in biomass by serotype O139 at pH 6.5 (Figure 25d).

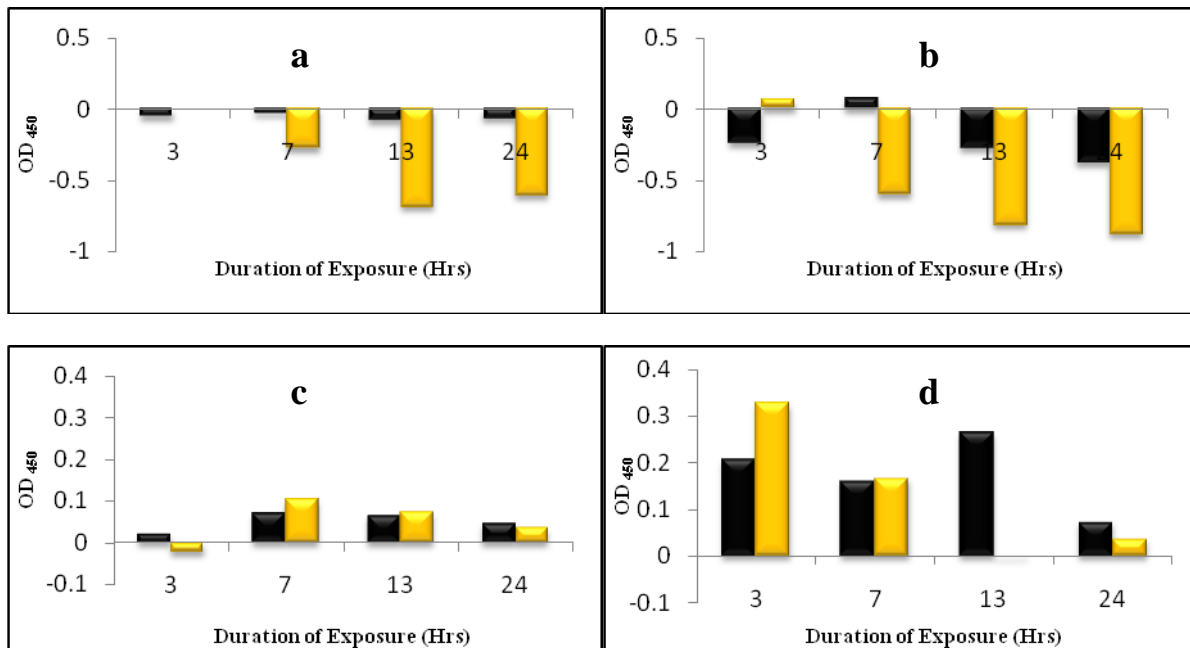


Figure 26: The effect of SUVR on the secretion of cholera toxin expressed as the difference between the solar exposed and non-solar exposed *V. cholerae* serotype O1 in LB at pH 8.5 (a) and pH 6.5 (b) and *V. cholerae* serotype O139 in LB at pH 8.5 (c) and pH 6.5 (d) during spring on the 1st of September 2009■ and the 22nd of September 2009□

3.7.2 SUVR Exposures during Summer

The effect of SUVR on the culturability of the *V. cholerae* strains was investigated while following a natural temperature profile during summer. Non solar exposed samples but under the same temperature conditions were used as the controls for each strain. The effect of SUVR on the culturability of *V. cholerae* toxigenic (serotypes O1 and O139) and environmental strains (1009) after exposure in media at pH 8.5 and 6.5 was assessed on two different days during summer i.e. the 24th of November 2009 and the 2nd of February 2010 (Table 7) for ground water and two different days i.e. the 17th of November 2009 and the 9th of February 2010 for full strength LB (see Table 7 for the days solar conditions).

Table 7: SUVR, atmospheric conditions and temperature profiles for the days of solar exposure during summer

Date	Solar Conditions	Max UVA (W/m ²)	Max UVB (W/m ²)	Min-Max Temp (°C)
17-Nov-09 ¹	Cloudy	20.41	0.059	10 – 17
24-Nov-09 ²	Sunny	52.3	0.17	21 – 35
02-Feb-10 ²	Sunny	54.9	0.177	25 – 37
09-Feb-10 ¹	Sunny	53.4	0.177	23 – 36

1 represents days on which exposures were done in LB

2 represents days on which exposures were done in ground water

3.7.2.1 Ground water

Washed bacterial cells of *V. cholerae* toxigenic strains O1, O139 and environmental strain 1009 were suspended in ground water to a final OD₆₀₀ of 0.01 (~7.5 Log CFU ± 0.5). Then the effect of SUVR on the culturability of the *V. cholerae* strains was investigated. During summer the duration of exposure to SUVR required for each strain of *V. cholerae* to suffer the loss of culturability differed from one strain to the other. It took however on average about 7 hrs of solar exposure to render the three *V. cholerae* strains non culturable without relapse. On the 24th of November serotype O1 only needed 3hrs of solar exposure to become non culturable while the other two serotypes, O139 and 1009, were no longer culturable after 7hrs exposure (Figure 27).

On the 2nd of February 2010 both serotype O139 and strain 1009 were no longer culturable after 3hrs of solar exposure in ground water at pH 8.5 but this was not the case for ground water at pH 6.5 (Fig27c and 27d). These results seem to suggest that during summer on a clear day it would take 7hrs of solar exposure to render approximately 7 Log CFU/ml non culturable without relapse.

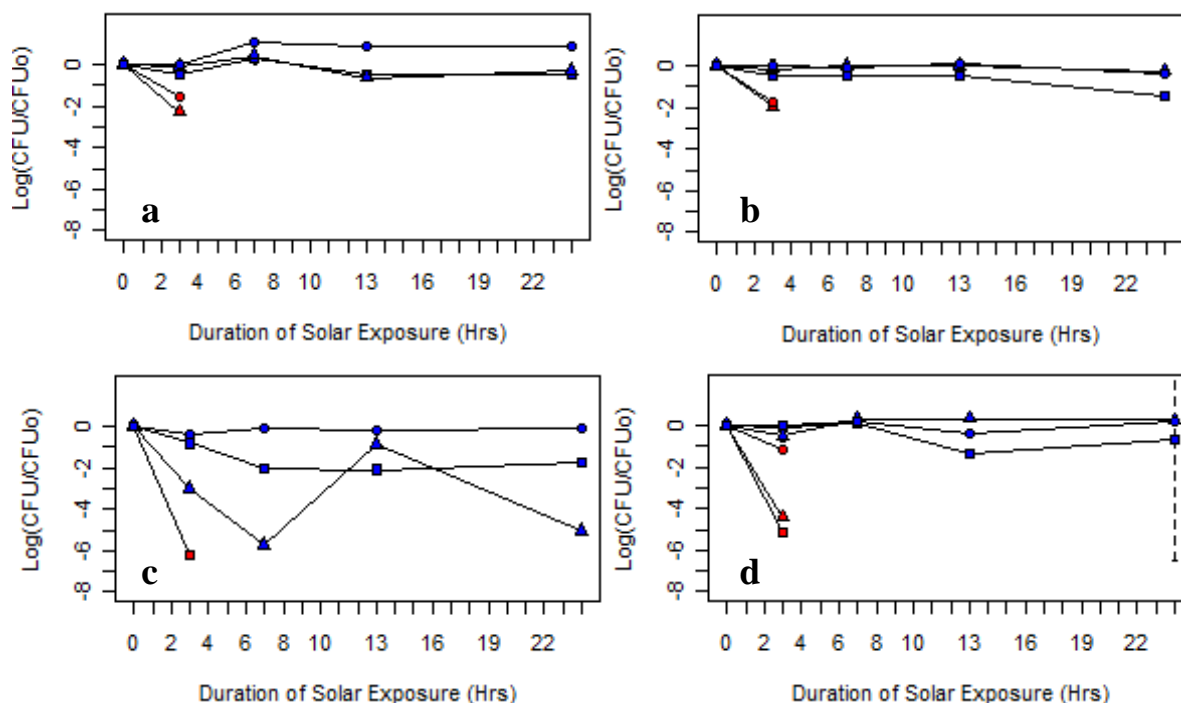


Figure 27: Inactivation kinetics of solar exposed O1 (red squares), O139 (red triangles) and 1009 (red circles) and non-exposed O1 (blue squares), O139 (blue triangles) and 1009 (blue circles) *V. cholerae* strains in ground water during summer on the 24th of November 2009 at pH 8.5 (a) and pH 6.5(b), the 2nd of February 2010 at pH 8.5 (c) and pH 6.5(d). Error bars indicate the standard deviation from duplicate measurements. Absence of the symbols indicates non culturability.

The effect of SUVR during summer on the release of the cholera toxin by the two virulent strains was investigated. Results from the cholera toxin ELISA indicate that there was still greater secretion of cholera toxin even after culturability had been lost (Figures 28 and 27). Upon solar exposure serotype O1 secreted more cholera toxin at pH 8.5 as opposed to serotype O139 under the same conditions (Figure 28a and 28c) However by the end of the 24hrs exposure there was more toxin produced and released by the non-solar exposed samples as indicated by the negative value bars for serotype O139 in Figure 28.

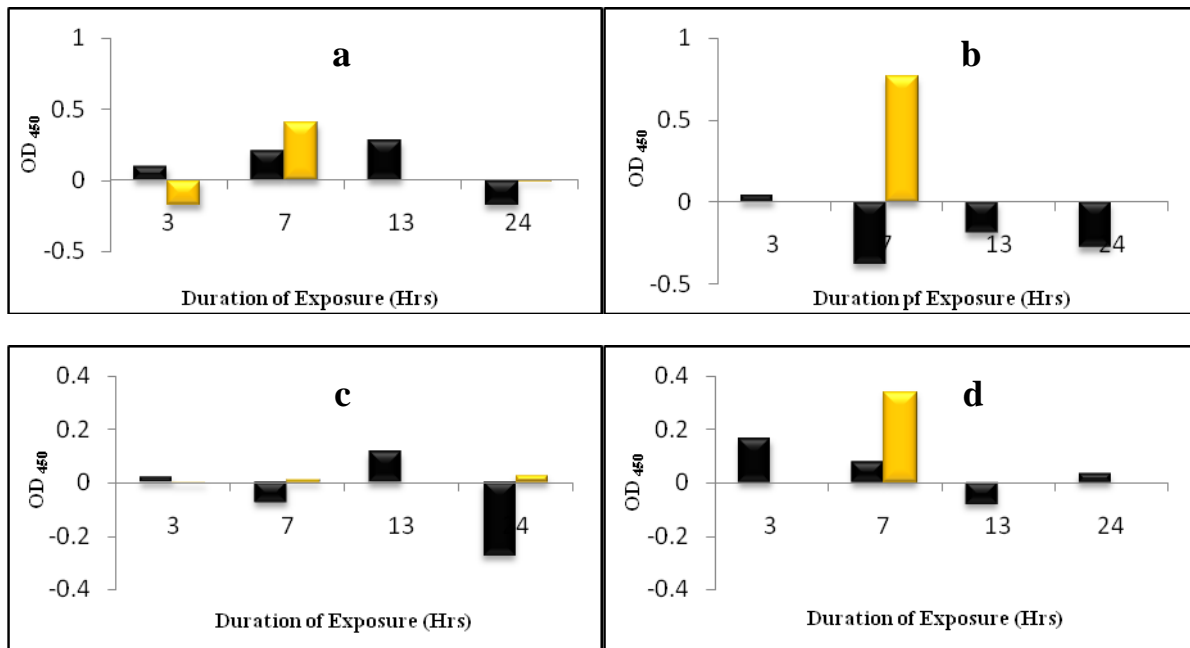


Figure 28: The effect of SUVR on the production and release of cholera toxin when expressed as the difference between the solar exposed and non-solar exposed *V. cholerae* serotype O1 in ground water at pH 8.5 (a) and pH 6.5 (b) as well as the O139 serotype in ground water at pH 8.5 (c) and pH 6.5 (d) during summer on the 24th of November 2009 ■, the 2nd of February 2010 ■

3.7.2.2 LB

Bacterial cells of *V. cholerae* toxigenic (serotypes O1, O139) and environmental (1009) strains were suspended in LB broth to a final OD₆₀₀ of 0.01. Then the effect of SUVR on the biomass formation of the *V. cholerae* strains was investigated. The days during which the experiments were carried out were representative of the extreme weather patterns that were experienced during summer (Table 7). During the 17th of November 2009 there was hardly any increase in biomass form all the solar exposed samples as indicated by the growth curves in Figures 29a and 29b. In addition on both occasions serotype O1 controls were as sensitive as the experimental samples.

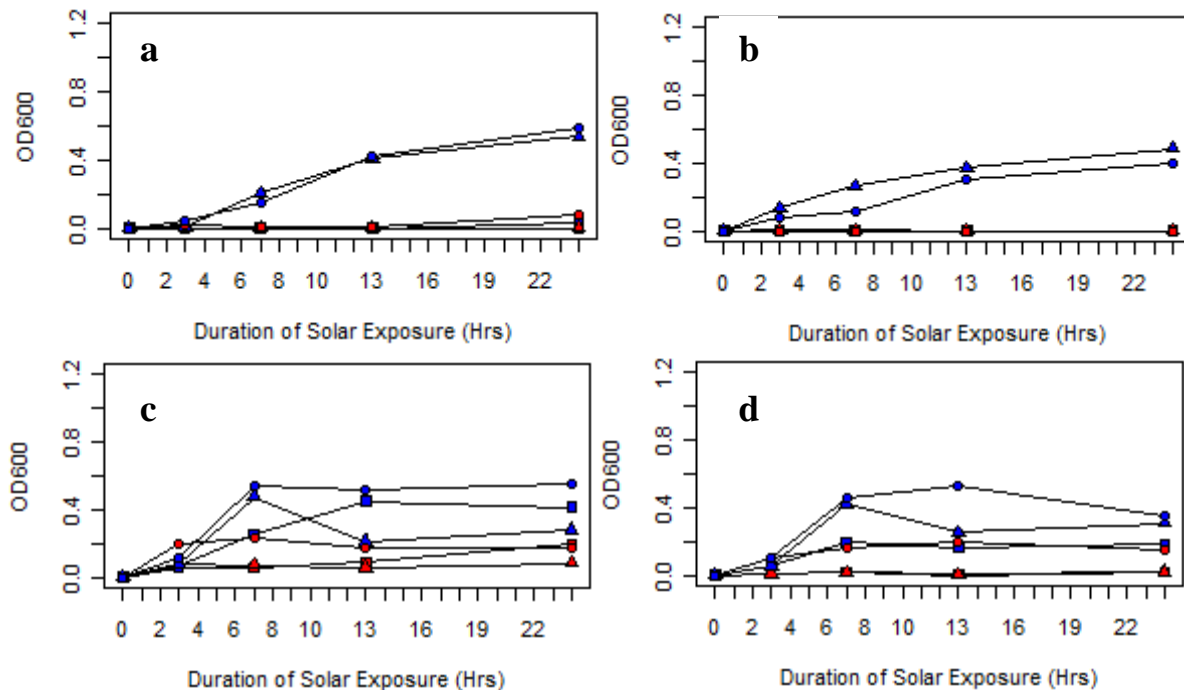


Figure 29: Representative growth curves of solar exposed O1 (red squares), O139 (red triangles) and 1009 (red circles) and non-exposed O1 (blue squares), O139 (blue triangles) and 1009 (blue circles) *V. cholerae* strains in LB on the 17th of November 2009 at pH 8.5 (a) and pH 6.5(b), the 9th of February 2010. Error bars indicate the standard deviation from duplicate measurements.

Then on the 9th of February 2010 there was a slight increase in the biomass formation as indicated by the growth curves in Figures 29c and 29d. However the solar conditions experienced during the 9th of February 2010 resulted in biomass increase by the environmental strain when compared to the virulent strains (Figures 29c and 29d). So SUVR during both days in summer inhibited the full potential of biomass increase by all the strains i.e. in comparison with the respective controls.

Cholera toxin secretion by the virulent strains of *V. cholerae* was also investigated. Results from the cholera toxin ELISA indicate that, cholera toxin was secreted by both strains and during both days of exposure with the exception of the O1 serotype during the 9th of February 2010 in LB at pH 8.5. However it can be suggested that release of cholera toxin especially in the case of O139 serotype was slightly influenced by SUVR as indicated by the negative effect represented by the negative value bars in Figure 30.

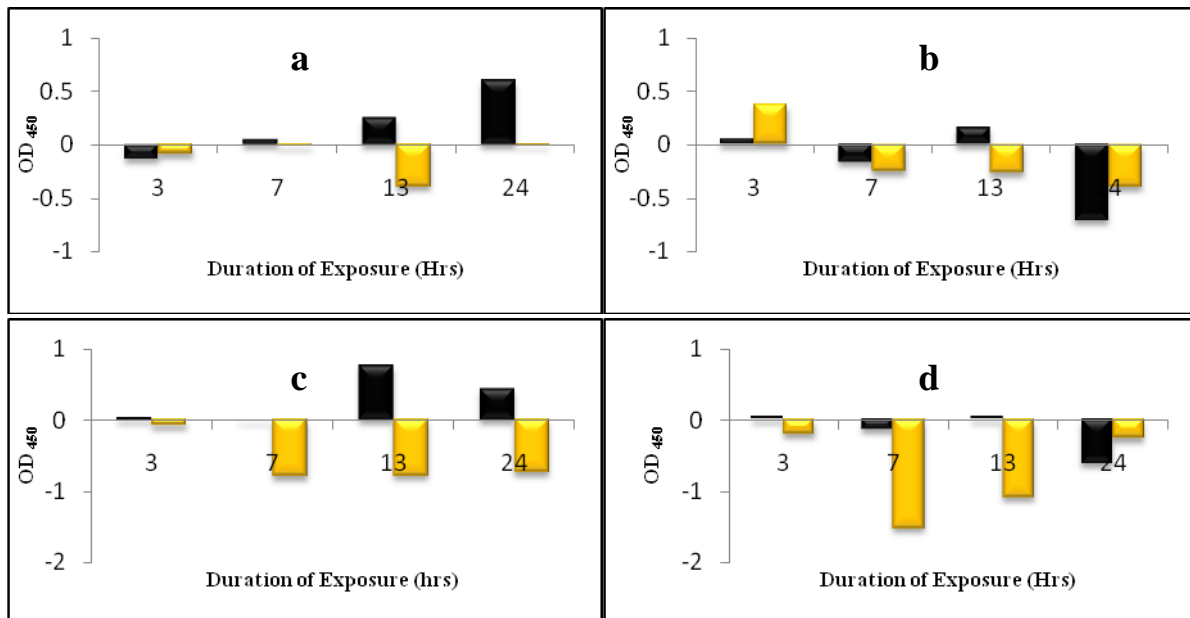


Figure 30: The effect of SUVR on the release of cholera toxin when expressed as the difference between the solar exposed and non-solar exposed *V. cholerae* strain O1 in LB at pH 8.5 (a) and pH 6.5 (b) as well as the O139 strain in LB at pH 8.5 (c) and pH 6.5 (d) during summer on the 17th of November 2009 ■ and the 9th of February 2010 ■

The O1 serotype and to a lesser extent the O139 serotype was greatly affected by SUVR when exposed in LB at pH 8.5 under the solar conditions experienced on the 17th of November 2009 (black bars in Fig 30a and 30c). However it should be noted that the increase in CT production and secretion was usually after daylight i.e. after 13 and 24 hours exposure.

3.7.3 SUVR Exposures during Autumn

The effect of SUVR on the culturability of the *V. cholerae* strains was investigated while following a natural temperature profile during autumn. Non solar exposed samples but under the same temperature conditions were used as the controls for each strain. The effect of SUVR on the culturability of *V. cholerae* toxigenic (serotypes O1 and O139) and environmental strains (1009) after exposure in media at pH 8.5 and 6.5 was assessed on two different days during autumn i.e. the 16th of March 2010 and the 13th of April 2010 for ground water and two different days i.e. the 8th of March 2010 and the 20th of April 2010 for full strength LB (see Table 8 for the days solar conditions).

Table 8: SUVR, atmospheric conditions and temperature profiles for the days of solar exposure during autumn

Date	Solar Conditions	Max UVA (W/m ²)	Max UVB (W/m ²)	Min-Max Temp (°C)
08-Mar-10 ¹	Sunny	-	-	23 – 37
16-Mar-10 ²	Sunny	-	-	16 – 30
13-April-10 ²	-	33.14	0.076	18 – 34
20-April-10 ¹	-	36.1	0.081	10 – 33

¹ represents days on which exposures were done in LB

² represents days on which exposures were done in ground water

Blank spaces indicate unavailable data points

3.7.3.1 Ground water

Washed bacterial cells of *V. cholerae* toxigenic (serotypes O1, O139) and environmental strains (1009) were suspended in ground water to a final OD600 of 0.01 (~7.5 Log CFU ± 0.5). Then the effect of SUVR on the culturability of the *V. cholerae* strains was investigated while following a natural temperature profile in autumn. During this season exposures on two separate days were carried out and the effects of SUVR were not any different from those observed during summer. A total loss in culturability was observed by the virulent strains right after 3hrs of solar exposure save for the O1 strains exposed in ground water at pH 8.5 during the 16th of March 2010 (Figure 31).

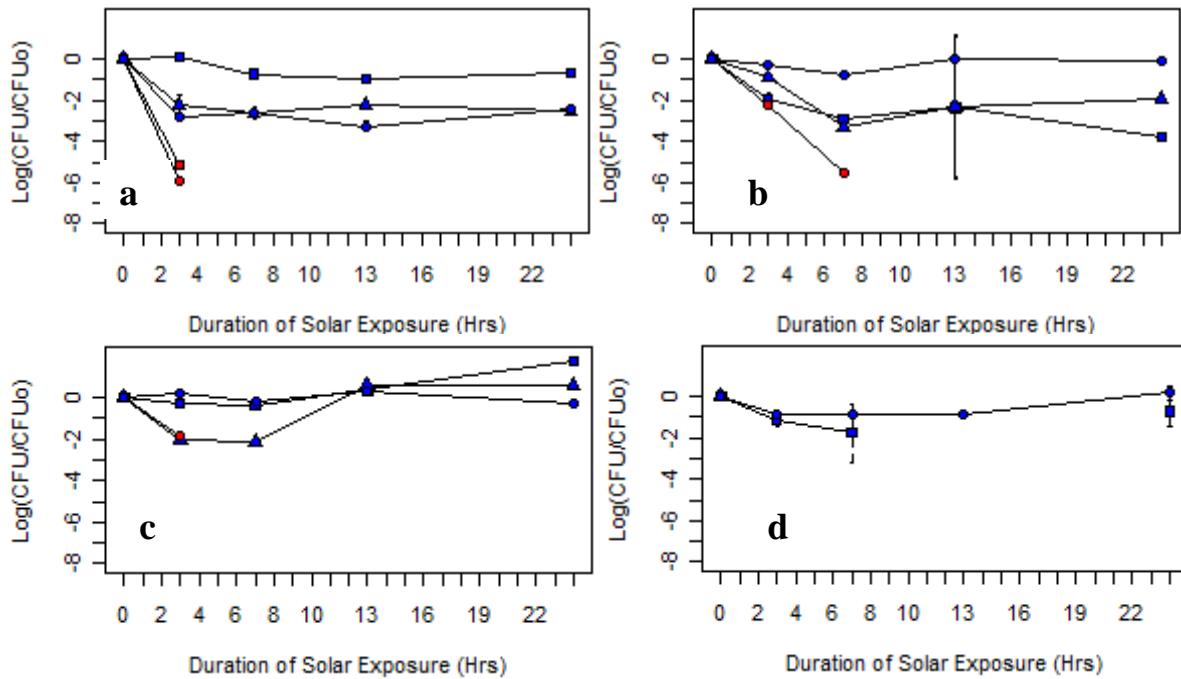


Figure 31: Inactivation kinetics of solar exposed O1 (red squares), O139 (red triangles) and 1009 (red circles) and non-exposed O1 (blue squares), O139 (blue triangles) and 1009 (blue circles) *V. cholerae* strains in ground water during autumn on the 16th of March 2010 at pH 8.5 (a) and pH 6.5(b), the 13th of April 2010 at pH 8.5 (c) and pH 6.5(d). Error bars indicate the standard deviation from duplicate measurements. Absence of symbols indicates non culturability.

Cholera toxin secretion by the two virulent strains of *V. cholerae* was accessed using the cholera toxin ELISA assay and the effect of SUVR deduced by subtraction of cholera toxin reading by the non-solar exposed samples from that of the solar exposed samples. This way the bars shown in Figure 32 are indicative of the effect of SUVR since that was the only variable. So during autumn the culturability profile of these strains was similar to that observed during summer. However serotype O1 secreted more cholera toxin (Figure 32a and 32b). The O139 serotype on the other hand did produce cholera toxin but it was not as much as that produced by its controls (the negative effect represented by the negative value bars in Figure 32c and 32d)

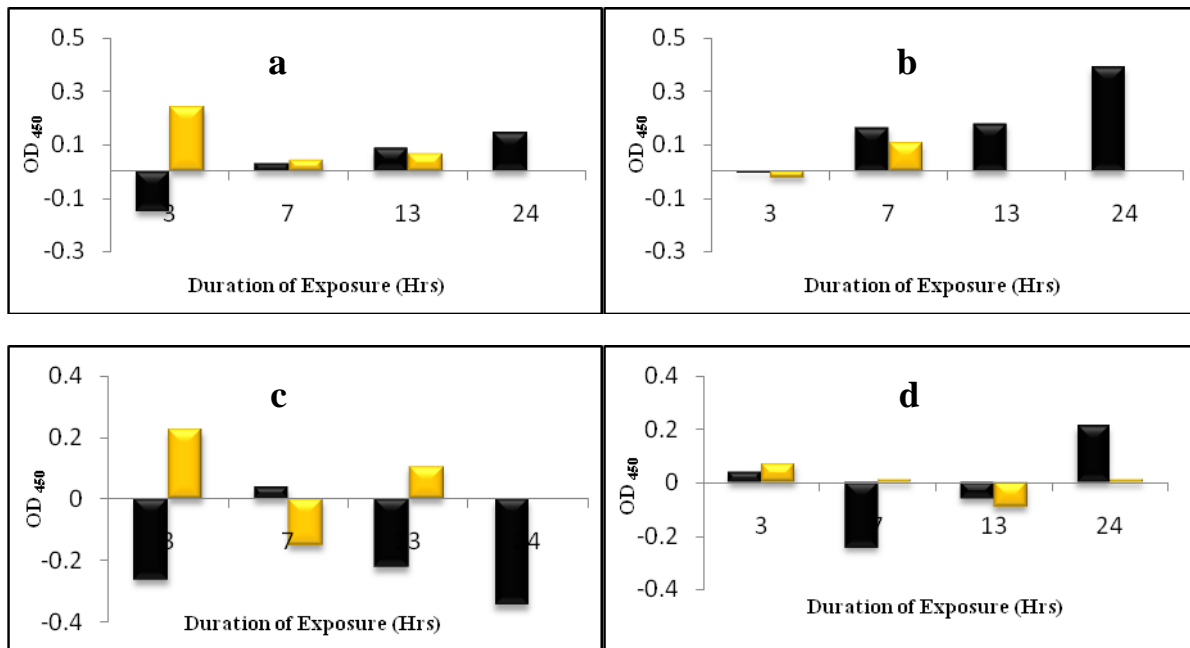


Figure 32: The effect of SUVR on the production and release of cholera toxin when expressed as the difference between the solar exposed and non-solar exposed *V. cholerae* strain O1 in ground water at pH 8.5 (a) and pH 6.5 (b) as well as the O139 strain in ground water at pH 8.5 (c) and pH 6.5 (d) during summer on the 16th of March 2010 ■, the 13th of April 2010 ■

3.7.3.2 LB

Bacterial cells of *V. cholerae* toxigenic strains O1, O139 and environmental strain 1009 were suspended in LB broth to a final OD₆₀₀ of 0.01. Then the effect of SUVR on the biomass formation of the *V. cholerae* strains was investigated while following a natural temperature profile in autumn. Results from the exposures suggest that the microorganisms behaved differently on both days. During the exposure on the 8th of March 2010 there was hardly any increase in biomass by all the solar exposed samples at both pH 8.5 and 6.5 (Fig 33a and 33b). However during the second exposure only LB at pH 6.5 seemed to inhibit the increase in biomass formation as shown by the growth curves in Figure 13d. pH 8.5 however seemed to provide right conditions for the increase in biomass by all the 3 strains (Figure 33c).

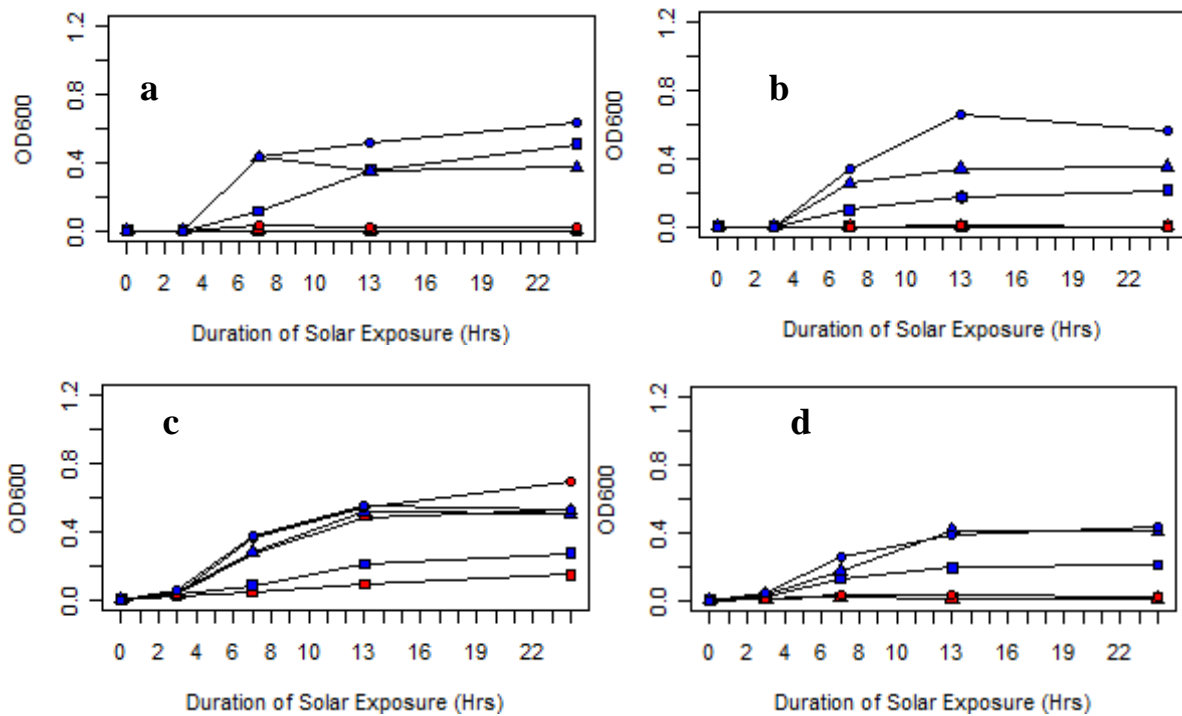


Figure 33: Representative growth curves of solar exposed O1 (red squares), O139 (red triangles) and 1009 (red circles) and non-exposed O1 (blue squares), O139 (blue triangles) and 1009 (blue circles) *V. cholerae* strains in LB on the 8th of March 2009 at pH 8.5 (a) and pH 6.5(b), the 20th of April 2010. Error bars indicate the standard deviation from duplicate measurements.

Cholera toxin secretion by the *V. cholerae* virulent strains during the two days of exposure in autumn was investigated for each sampling time point. The results obtained from this analysis show that there was cholerae toxin release by both strains at both pHs of LB for the exposure conducted on the 8th of March 2010 even though there was hardly any increase in biomass by any of the strains (Figure 33a and 33b). SUVR had a greater effect on the release of cholera toxin by the O1 serotype on that day when compared to the O139 serotype (Figure 34a and 34c). The O139 serotype on the other hand even though it secreted cholera toxin when exposed to SUVR, it was not as much as that secreted by the non-exposed control hence the negative value bars in Figure 34c and 34d. Results from the cholera toxin ELISA done on samples exposed to SUVR on 20th of April 2010 show that there was no cholera toxin detected after exposing the O1 serotype (absence of yellow bars in Figure 34a). The O139 serotype however produced cholera toxin but not at all the sampling time points (yellow bars in Figure 34c and 34d).

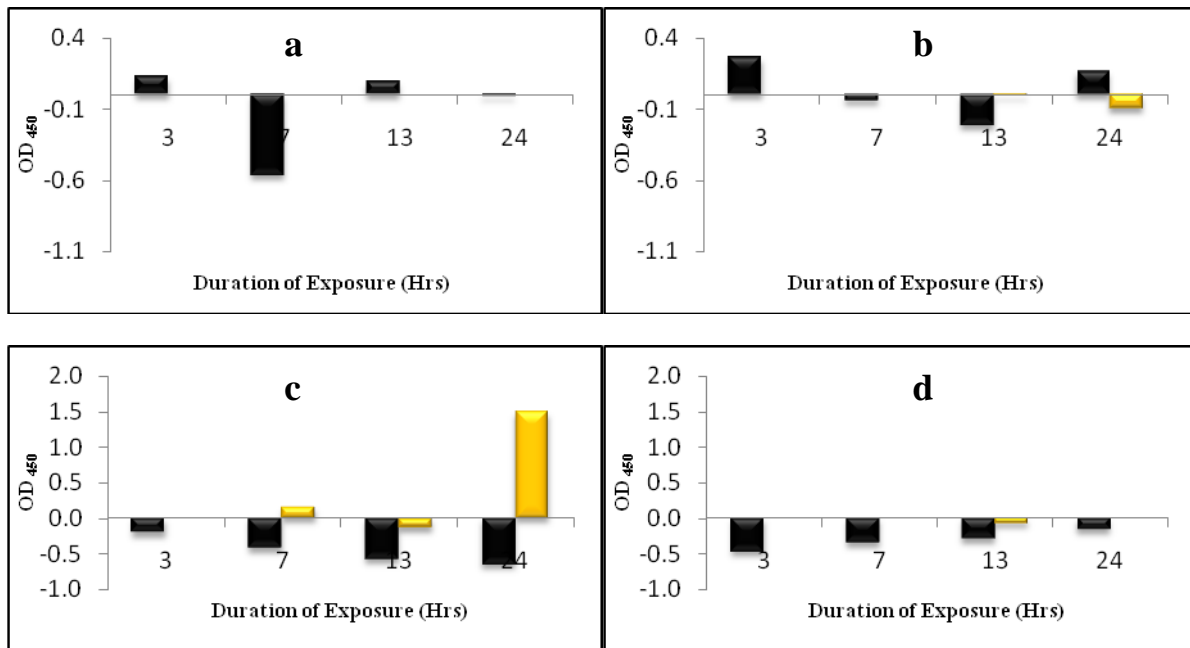


Figure 34: The effect of SUVR on release of cholera toxin when expressed as the difference between the solar exposed and non-solar exposed *V. cholerae* O1 serotype in ground water at pH 8.5 (a) and pH 6.5 (b) as well as the O139 serotype in LB at pH 8.5 (c) and pH 6.5 (d) during autumn on the 8th of March 2010 ■ and the 20th of April 2010 ■

3.7.4 SUVR Exposures during Winter

The effect of SUVR on the culturability of the *V. cholerae* strains was investigated while following a natural temperature profile during winter. Non solar exposed samples but under the same temperature conditions were used as the controls for each strain. The effect of SUVR on the culturability of *V. cholerae* toxigenic (serotypes O1 and O139) and environmental strains (1009) after exposure in media at pH 8.5 and 6.5 was assessed on three different days during winter i.e. the 18th of May 2010, 8th of June 2010 and the 20th of July 2010 for ground water and three different days i.e. the 11th of May 2010, 16th of June 2010 and on 13th of July 2010 for full strength LB (see table 9 for the days solar conditions).

Table 9: SUVR, atmospheric conditions and temperature profiles for the days of solar exposure during winter

Date	Solar Conditions	Max UVA (W/m ²)	Max UVB (W/m ²)	Min-Max Temp (°C)
11-May-10 ¹	Sunny	32.71	0.077	9 – 27
18-May-10 ²	Sunny	27.51	0.066	7 – 30
08-June-10 ²	Partially Sunny	23.81	0.053	7 – 26
16-June-10 ¹	Partially Sunny	21.43	0.040	-1 – 13
13-July-10 ¹	Partially Sunny	15.94	0.033	2 – 18
20-July-10 ²	Partially Sunny	25.10	0.059	3 – 24

¹ represents days on which exposures were done in LB

² represents days on which exposures were done in ground water

3.7.4.1 Ground water

Washed bacterial cells of *V. cholerae* toxigenic (serotypes O1, O139) and environmental (1009) strains were suspended in ground water to a final OD600 of 0.01 (~7.5 Log CFU ± 0.5). Then the effect of SUVR on the culturability of the *V. cholerae* strains was investigated while following a natural temperature profile during winter. During winter experiments were performed on the three afro mentioned days (see Table 9 for the conditions). On these days the virulent *V. cholerae* strains were no longer culturable after 7hrs of solar radiation (Figure 35) regardless of the pH of the ground water they were exposed in. The environmental strain on the other hand was the least affect by SUVR as it remained culturable throughout the period of exposure with the exception of the experiment carried out on the 18th of May 2010 (Figure 35); however a relapse (regrowth) in its culturability was observed (Figure 35d and 35f). During this season the virulent strains were very susceptible to solar exposure, while the environmental strain was the least sensitive.

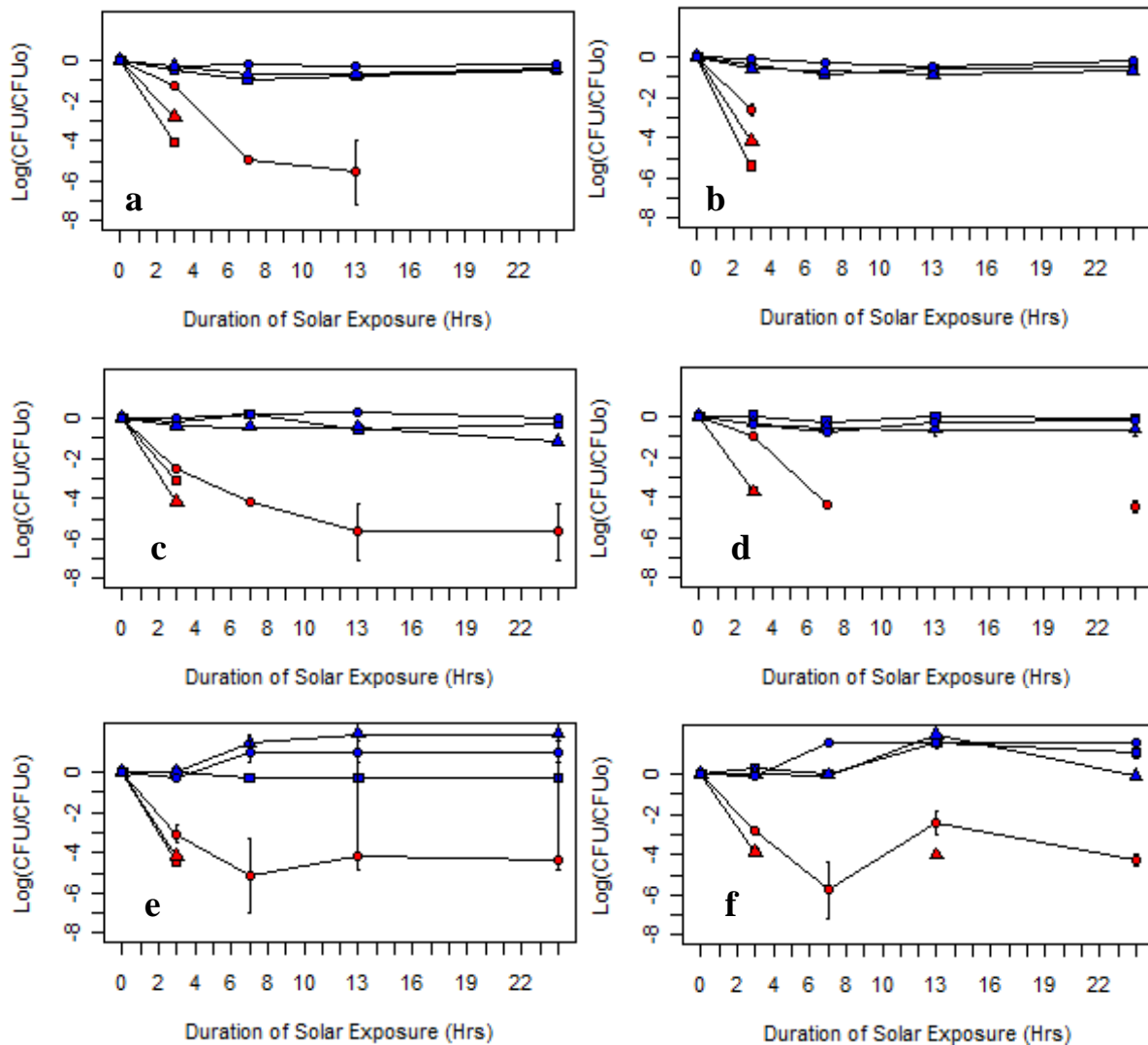


Figure 35: Inactivation kinetics of solar exposed O1 (red squares), O139 (red triangles) and 1009 (red circles) and non-exposed O1 (blue squares), O139 (blue triangles) and 1009 (blue circles) *V. cholerae* strains in ground water on the 18th of May 2010 at pH 8.5 (a) and pH 6.5(b), the 8th of June 2010 at pH 8.5 (c) and pH 6.5(d) and on the 20th of July 2010 at pH 8.5 (e) and pH 6.5 (f). Error bars indicate the standard deviation from duplicate measurements. Absence of symbols indicates lack of culturability.

Cholera toxin ELISA of all the sampling times of the virulent strains of *V. cholerae* that were solar exposed indicate that although both strains released cholera toxin it was at the lowest levels in comparison to other seasons. The O139 serotype released more cholera toxin compared to the O1 serotype. Furthermore more cholera toxin was released at pH 6.5 than at pH 8.5 by the O139 serotype. So this season highlights an important fact that lack of culturability does not necessarily mean the inability to secrete cholera toxin since even though

the solar exposed virulent strains were not culturable after 7hrs of exposure (Figure 36) they released more cholera toxin than their controls (non-solar exposed samples).

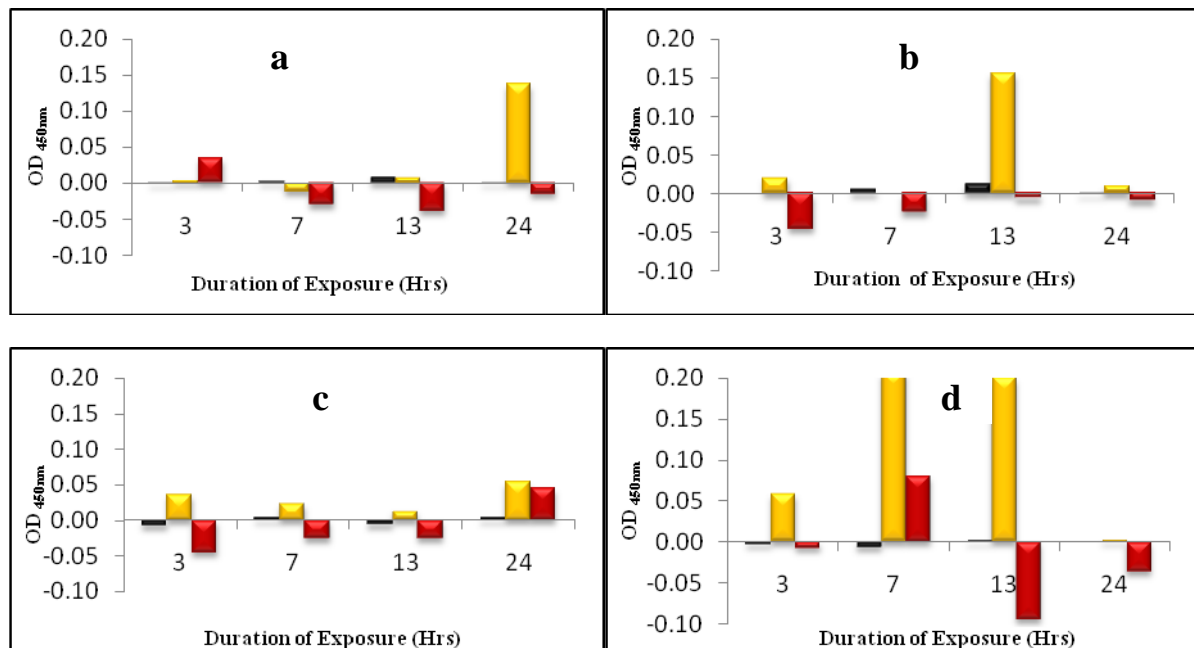


Figure 36: The effect of SUVR on the release of cholera toxin when expressed as the difference between the solar exposed and non-solar exposed *V. cholerae* strain O1 in ground water at pH 8.5 (a) and pH 6.5 (b) as well as the O139 strain in ground water at pH 8.5 (c) and pH 6.5 (d). During spring on the 18th of May 2010 ■ , the 8th of June 2010 ■ and the 20th of July 2010 ■

3.7.4.2 LB

Bacterial cells of *V. cholerae* toxigenic strains O1, O139 and environmental strain 1009 were suspended in LB broth to a final OD₆₀₀ of 0.01. Then the effect of SUVR on the biomass formation of the *V. cholerae* strains was investigated while following a natural temperature profile during winter. In this season SUVR was at its lowest and so was the temperature with the exception of the month of May 2010 since the winter was setting in. So during this season three experiments were conducted on the three separate days mentioned above. All the *V. cholerae* strains i.e. both the virulent and environmental strains except for the exposure done on the 11th of May 2010 in LB at pH8.5 behaved in a very similar manner (Figure 37).

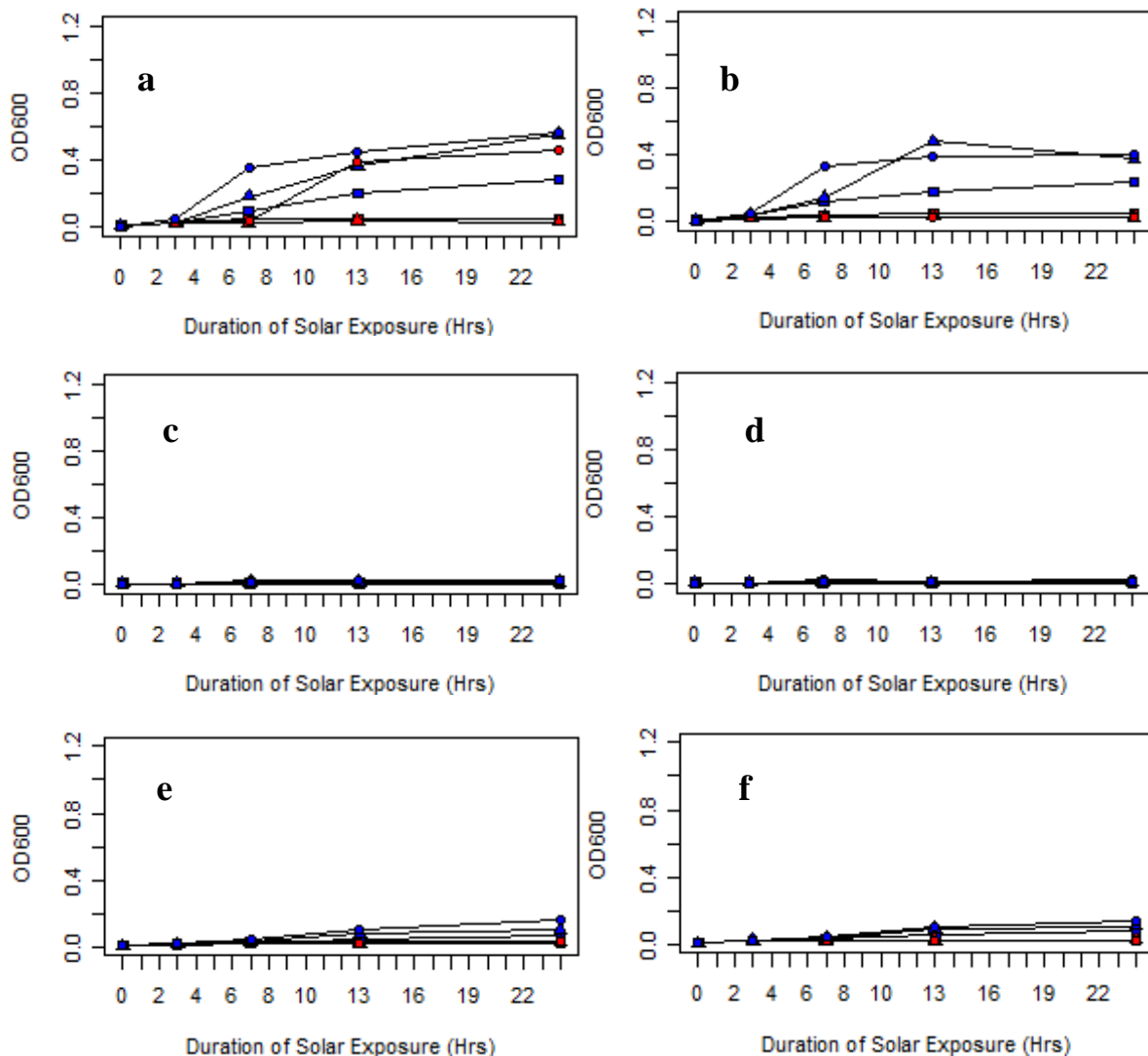


Figure 37: Inactivation kinetics of solar exposed O1 (red squares), O139 (red triangles) and 1009 (red circles) and non-exposed O1 (blue squares), O139 (blue triangles) and 1009 (blue circles) *V. cholerae* strains in LB on the 11th of May 2010 at pH 8.5 (a) and pH 6.5(b), the 16th of June 2010 at pH 8.5 (c) and pH 6.5(d) and on the 13th of July 2010 at pH 8.5 (e) and pH 6.5 (f). Error bars indicate the standard deviation from duplicate measurements.

There was hardly any noticeable increase in biomass by any of these strains at all pHs save for the 1009 strain exposed on the 11th of May 2010 in LB at pH 8.5. The environmental strain on that day showed a drastic increase in the biomass. It is however also important to note that on two occasions the controls behaved in a similar mode as their experimental (Figure 37c and 37f)

Cholera toxin release by each of the virulent strains of *V. cholerae* (i.e. serotypes O1 and O139) at each sampling time point was assessed by the cholera toxin ELISA. The results suggest that cholerae toxin release differed from one strain to the other, especially in the case of solar exposure in LB at pH 8.5 (Figure 38a and 38c). In addition there was hardly any cholera toxin detected from the majority of the samples exposed on the 16th of June 2010 in LB at pH 8.5 by both strains (yellow bars in Figure 38a and 38c).

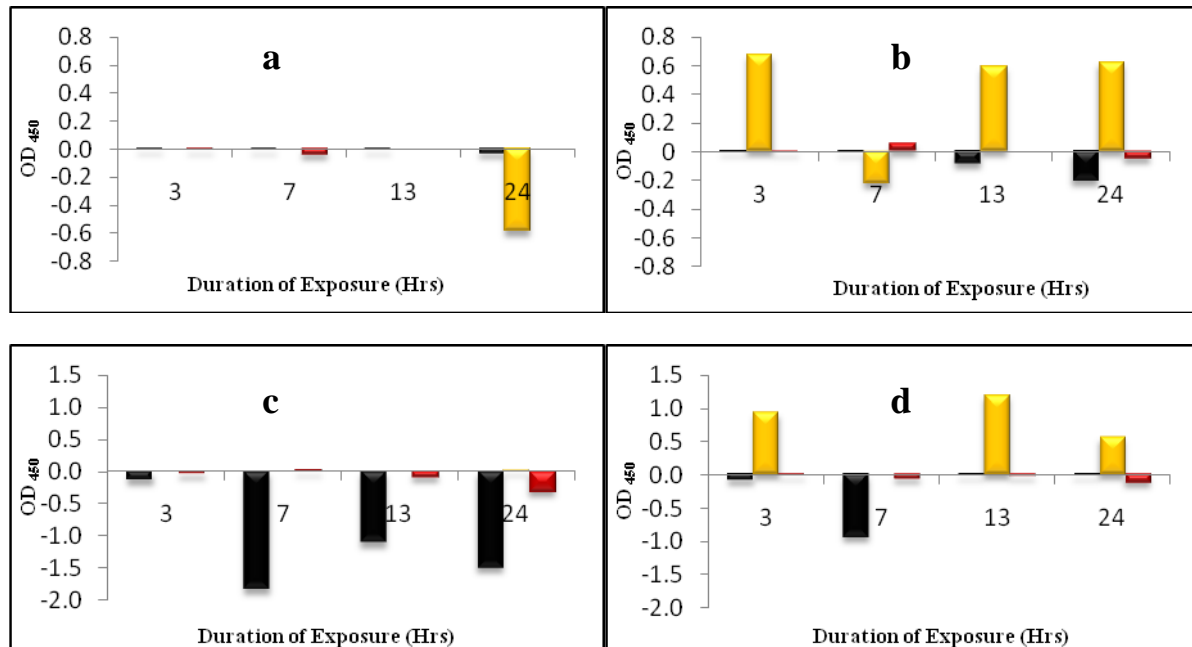


Figure 38: The effect of SUVR on the release of cholera toxin when expressed as the difference between the solar exposed and non-solar exposed *V. cholerae* strain O1 in LB at pH 8.5 (a) and pH 6.5 (b) as well as the O139 strain in LB at pH 8.5 (c) and pH 6.5 (d). During spring on the 11th of May 2010 ■, the 16th of June 2010 ■ and the 13th of July 2010 ■

However at the same pH on the other days of exposure, there was more cholera toxin released by the non-solar exposed samples as indicated by the negative value bars (black and red bars in Figure 38a and 38c). The O139 serotype released more cholerae toxin than the O1 serotype but it was not due to SUVR exposure. On the other hand at pH 6.5 most especially during the exposure done on the 16th of June 2010 (yellow bars in Figure 38b and 38d) SUVR had a positive effect on the release of cholera toxin. Even though there was no detectable increase in biomass as indicated by the growth curves from the exposure of that day at pH 6.5 (Figure

37 d), increased levels of cholera toxin production due to SUVR were observed from both strains.

The effects of SUVR were further assessed with a flow cytometer using fluorescent dyes. The effect of SUVR on the cytoplasmic integrity of the samples exposed during one of the season of exposure i.e. summer was assessed using a flow cytometer. Since the use of a flow cytometer was a new technique acquired while working on the study the optimization of several fluorescent stains was done and is described below.

3.8 Flow Cytometric Analysis

3.8.1 Optimization of flow cytometry for *Vibrio cholerae*.

Flow cytometric analysis depicting the staining characteristics of culturable late log phase and heat stressed *V. cholerae* after incubation with a single or a combination of fluorescent dyes was evaluated. For the optimization of flow cytometry only the toxigenic *V. cholerae* serotype O1 was used.

3.8.1.1 Staining properties of the fluorescent dyes

Before analysing the samples containing any fluorescent dyes, the flow cytometer was calibrated using unstained samples of the late log phase (refer to materials and methods for preparation of these cells) and heat stressed bacterial cells (Figure 39). This was done to determine the region that would characterise the ability or inability for the stain to enter the cell and / or to be retained by the *V. cholerae* cells. Calibration of the flow cytometer was done through the adjustment of the voltage for the green fluorescence ($525\pm 30\text{nm}$) and red fluorescence ($680\pm 30\text{nm}$) so as to have the background within the M1 marker indicated on the histograms (M1 in Figure 39).

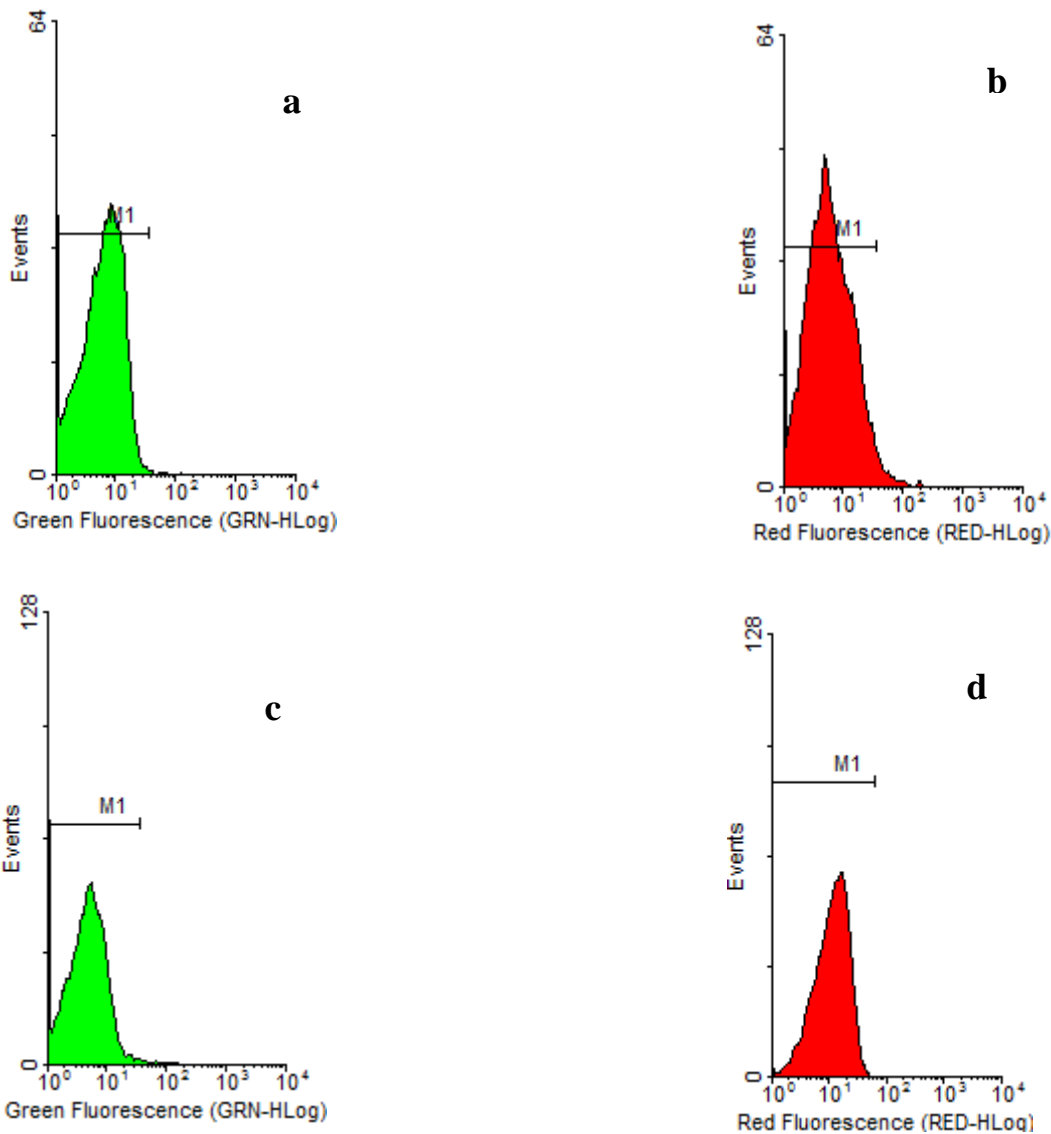


Figure 39: Flow cytometry histograms of compensated settings for unstained late log phase (a and b) and heat stressed (c and d) *V. cholerae* cells after reducing autofluorescence through the adjustment of the voltage for Green (GRN) and Red (RED) fluorescence detectors. M1 indicates autofluorescence due to green or red as indicated by their respective colours.

3.8.1.2 Staining Characteristics of the Single Dyes

3.8.1.2.1 Sybr Green I Staining

Sybr Green I is a green fluorescent stain known to stain both live and dead gram positive and gram negative bacterial cells (Falcioni et al., 2008). When the late log phase and heat stressed *V. cholerae* cells were stained with SGI there was an increase in green fluorescence as indicated by the shift of the peak from the region indicated by M1 to M2 region (Figure 40).

However there was a greater fluorescence signal due to late log cultures as compared to heat stressed cultures as indicated by both the histograms and dot plots in Figure 40. The great increase in fluorescence intensity by the late log culture could imply that bacterial cells had high nucleic acid content as compared to the lower fluorescence intensity indicative of low nucleic acid content (Gasol, Zweifel, Peters, Fuhrman, & Hagstrom, 1999).

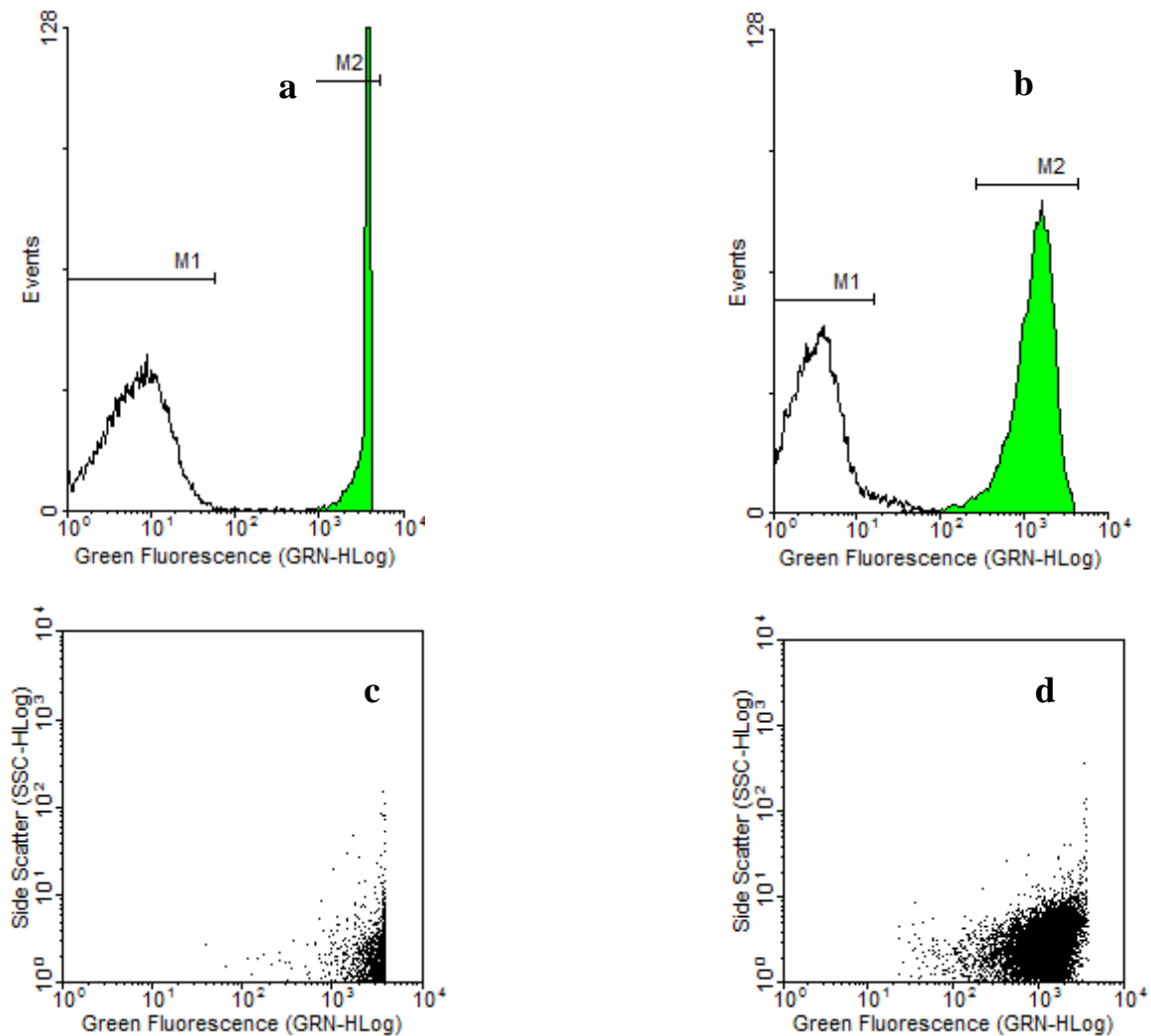


Figure 40: Flow cytometry histogram and dot plots (GRN versus SSC plot) showing the fluorescence intensity of a late log phase *V. cholerae* culture histogram (a) dot plot (c) as well as a heat stressed *V. cholerae* culture histogram (b) and Dot plots (d) incubated in SGI at 37°C for 45 minutes.

3.8.1.2.2 Carboxyfluorescein diacetate Treatment

Carboxyfluorescein diacetate (cFDA) is a compound that emits green fluorescence once cleaved by an esterase (Czechowska et al., 2008; Nebe-von-Caron et al., 2000). When late log phase *V. cholerae* cells were treated with cFDA, there was a great increase in the GRN

fluorescence intensity due to the cleavage of cFDA as indicated by the shift of the fluorescence peak (green curve) from region M1 to M2 (Figure 41a). The increase in fluorescence intensity was also observed by a gated dot plot against non-fluorescent events (Figure 41c). On the other hand, heat stressed *V. cholerae* cells showed no shift in the GRN fluorescence meaning that the population had lost esterase enzymatic activity (Figure 41b and d).

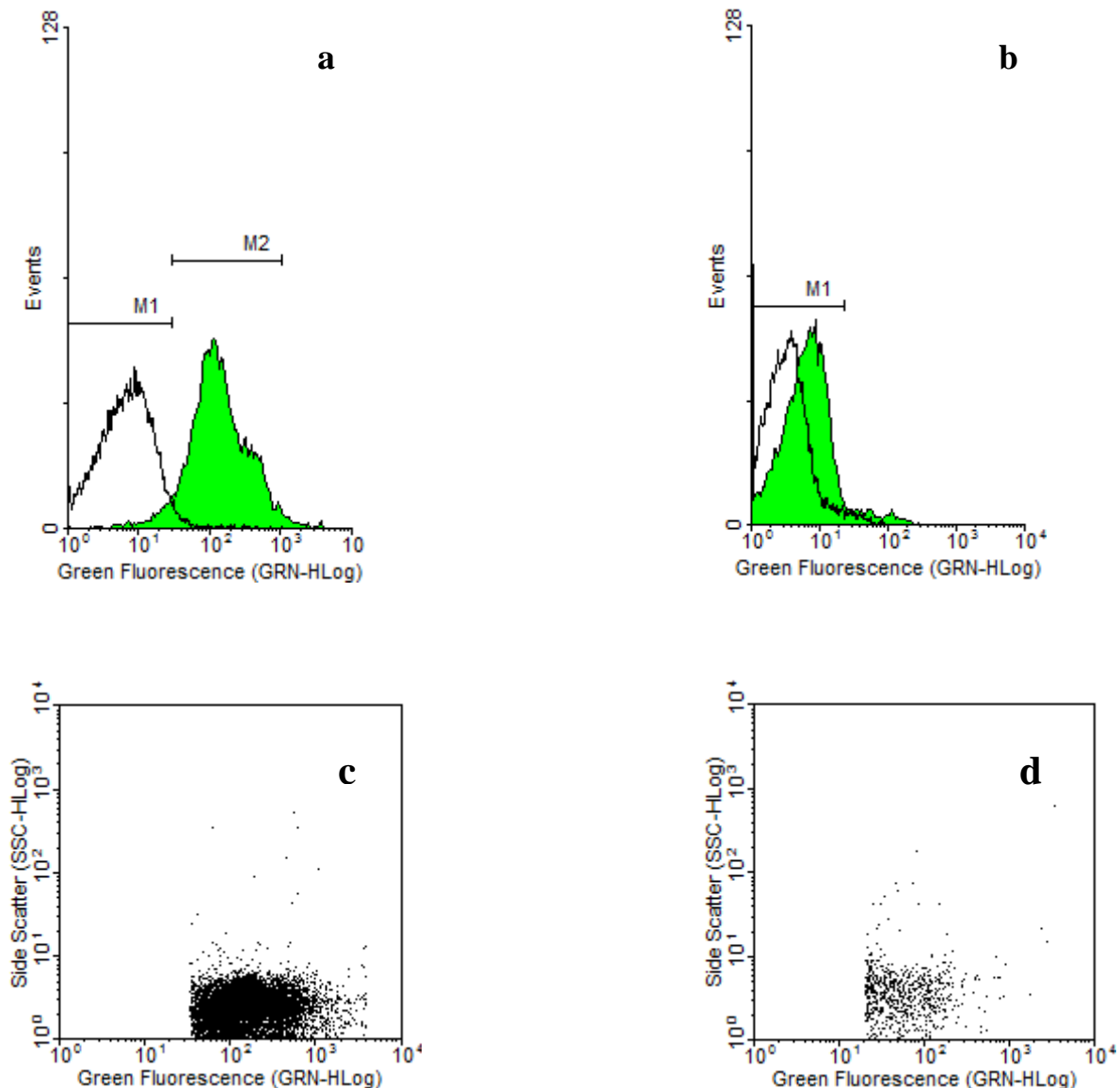


Figure 41: Flow cytometric histograms and gated dot plots (GRN versus SSC plot) showing the fluorescence intensity of a late log phase *V. cholerae* culture histogram (a) dot plot (c) and a heat stressed *V. cholerae* culture histogram (b) and Dot plots (d) incubated in cFDA at 37°C for 45 minutes.

3.8.1.2.3 Propidium Iodide Staining

Propidium iodide is a fluorescent dye that intercalates with double stranded DNA and only enters permeabilised cytoplasmic membranes (Berney et al., 2007; Walberg, Gaustad, & Steen, 1999). When the late log phase *V. cholerae* culture was stained with PI, there was no increase in the red fluorescence intensity as indicated by the lack of shift (red curve) from region M1 characteristic of the unstained cells (white curve) in the histogram (Figure 42). This was also shown by the dot plots in Figure 42c and 42f. The dot plot in Figure 42c shows the RED fluorescence intensity due to an unstained late log phase *V. cholerae* culture with a region marked R1 indicating PI negative events.

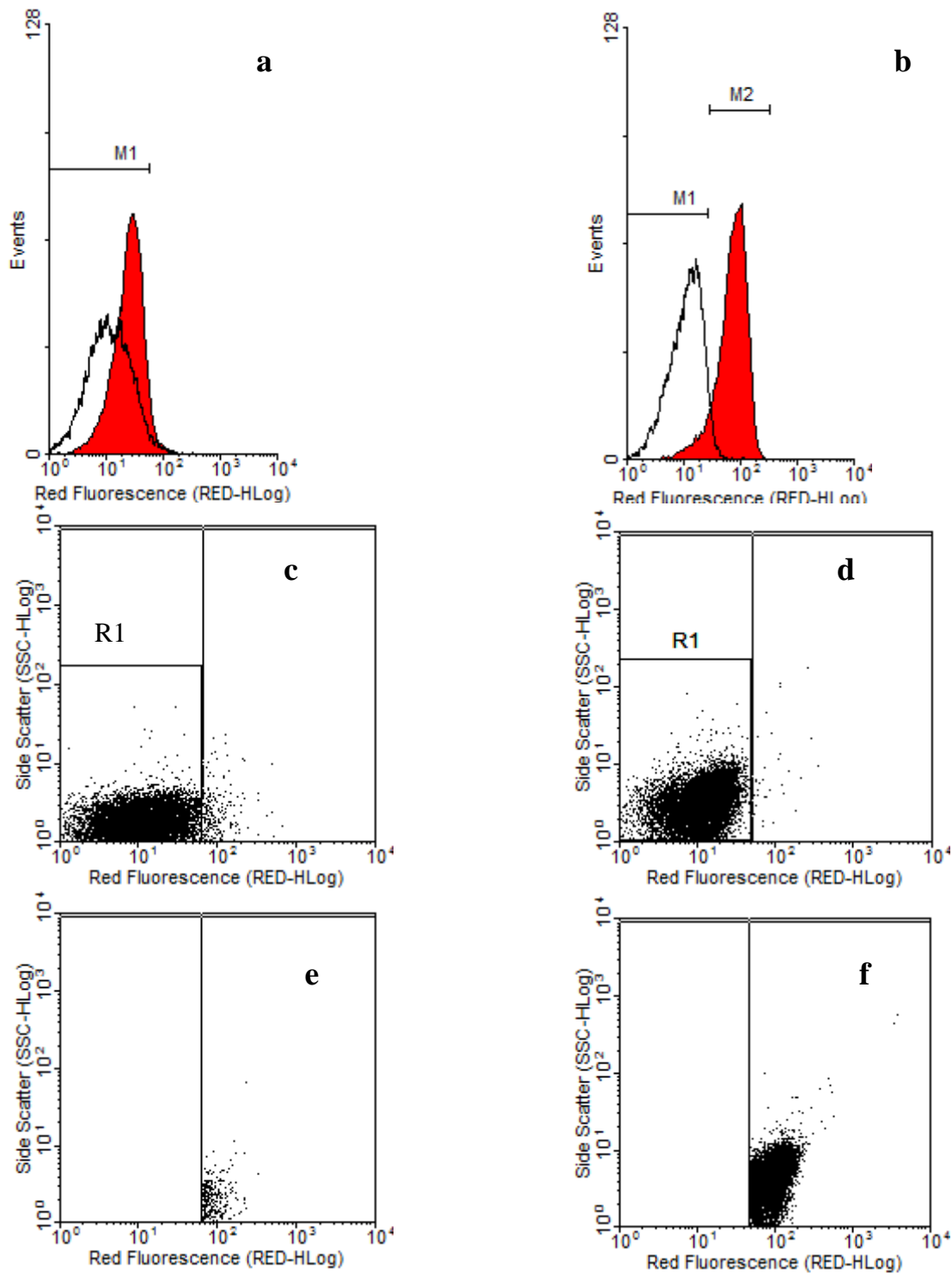


Figure 42: Flow cytometric histograms and gated dot plots (RED versus SSC plot) on the R1 region showing the fluorescence intensity of a late log phase *V. cholerae* culture histogram (a) dot plots (c and e) and a heat stressed *V. cholerae* culture histogram (b) and Dot plots (d and f) stained with PI for 45 minutes at 37°C.

R1 was used to gate all PI positive events as shown in Figure 4E. Both the histogram and dot plot in Figures 42a and 42e indicate lack of PI staining by the late log phase *V. cholerae*

culture. On the other hand the heat stressed *V. cholerae* cells behaved differently from the late log phase cells. After staining the heat stressed cells with PI there was an increase in RED fluorescence as indicated by the shift of the fluorescence peak from region M1 to the right as indicated by the red curve in region M2 in the histogram in Figure 42b. The same effect can be seen from the dot plots in Figure 42d and 42f. The dot plot Figure 42d shows the R1 region which is characteristic of an unstained sample of heat stressed cells. However after staining with PI there was an increase in fluorescence by approximately 77% (Figure 42f). The results from PI staining of the late log phase *V. cholerae* cells mean that the cytoplasmic membrane of the majority of the bacterial cells was still intact and therefore there was no entry point for PI resulting in no increase in the red fluorescence. However there was a breach in the cytoplasmic membrane of the heat stressed *V. cholerae* and as a result PI was able to gain entry into the cells hence the shift of the peaks from region M1 characterized by non-stained cells into region M2 characterized by PI positive cell population.

3.8.1.2.4 Ethidium Bromide Staining

Ethidium Bromide (EB) is a nucleic acid binding stain that is small enough to travel across an intact cytoplasmic membrane but is actively pumped out of the cell via a non-specific proton antiport transport system in active cells (Midgley, 1987; Walberg et al., 1999). Both the late log phase and heat stressed *V. cholerae* cells stained positive for EB as indicated in Figure 43 by the histograms and respective dot plots. There was a greater fluorescent signal from the late log phase culture (Figure 43a and 43c) when compared to that from the heat stressed culture (Figure 43b and 43d). These results seem to suggest that the efflux pumping system for bacterial cells in both samples was already faulty. Although the difference in fluorescence intensity is still unclear, it is possible that the RNA content and the DNA in the late log phase culture was still intact resulting in a greater fluorescence signal.

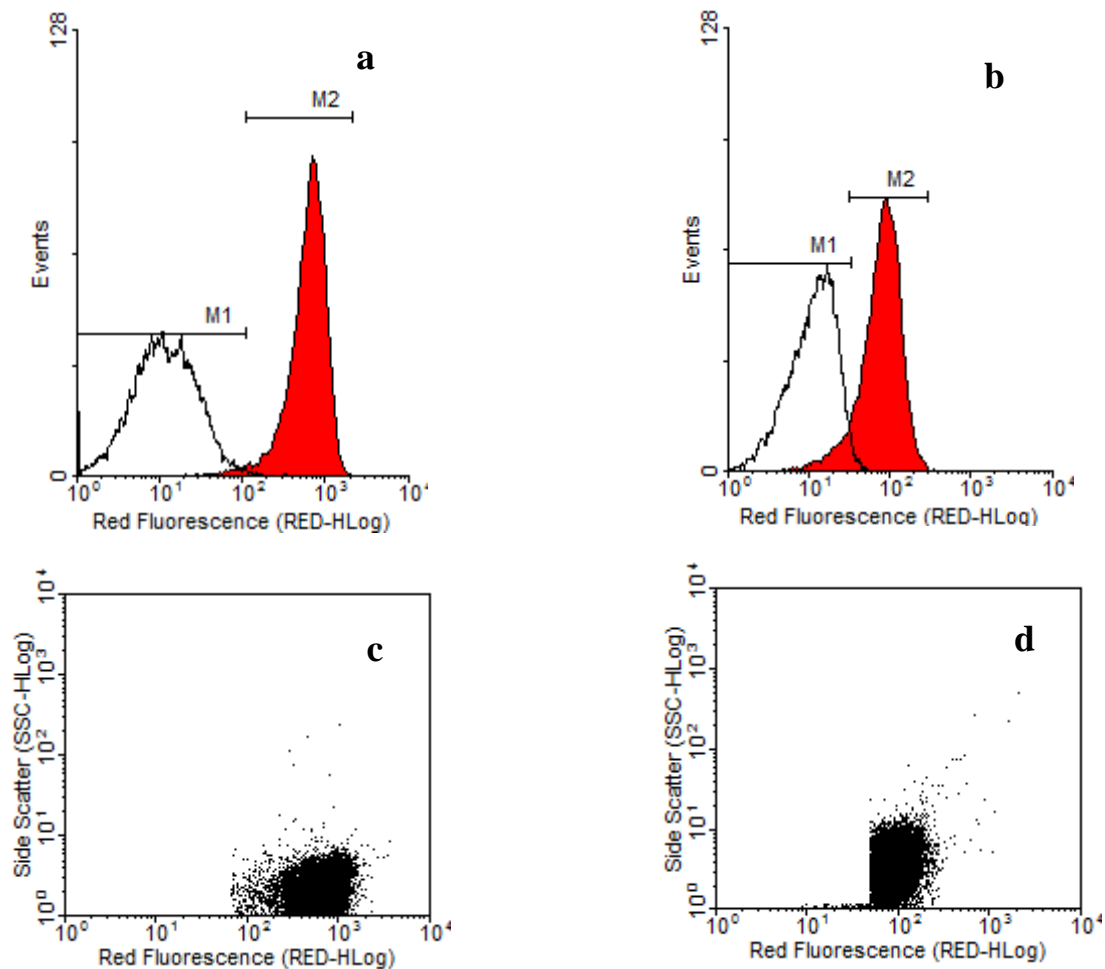


Figure 43: Flow cytometry histograms as well as gated dot plots (RED versus SSC plot) for the fluorescence intensity of a late log phase *V. cholerae* culture histogram (a) dot plot (c) and a heat stressed *V. cholerae* culture histogram (b) and Dot plots (d) incubated in EB at 37°C for 45min.

3.8.1.3 Staining Characteristics of Dye Mixtures

3.8.1.3.1 Sybr Green and Propidium Iodide

When a mixture of fluorescent dyes containing PI and SGI is used to stain bacterial cells, a quenching effect on the green fluorescence intensity, due to SGI, is observed as soon as the red fluorescence, due to PI, enters the cell enabling the identification of bacterial cells with partially damaged cell walls (Barbesti et al., 2000; Berney et al., 2007).

After staining the late log phase *V. cholerae* culture with a mixture of the SGI and PI fluorescent dyes, there was no distinct increase in either the green or red fluorescence intensity as indicated by the histogram in Figure 44a. However a closer examination of Figure 44a revealed a great reduction in the green fluorescence intensity when compared to the

Figure 40a of the same sample but without PI. This result was better instanced by the dot plot in Figure 45c where the majority of the events were localized in the region marked R2 (negative for PI) and a minority of them was seen in the region marked R1(positive for PI).

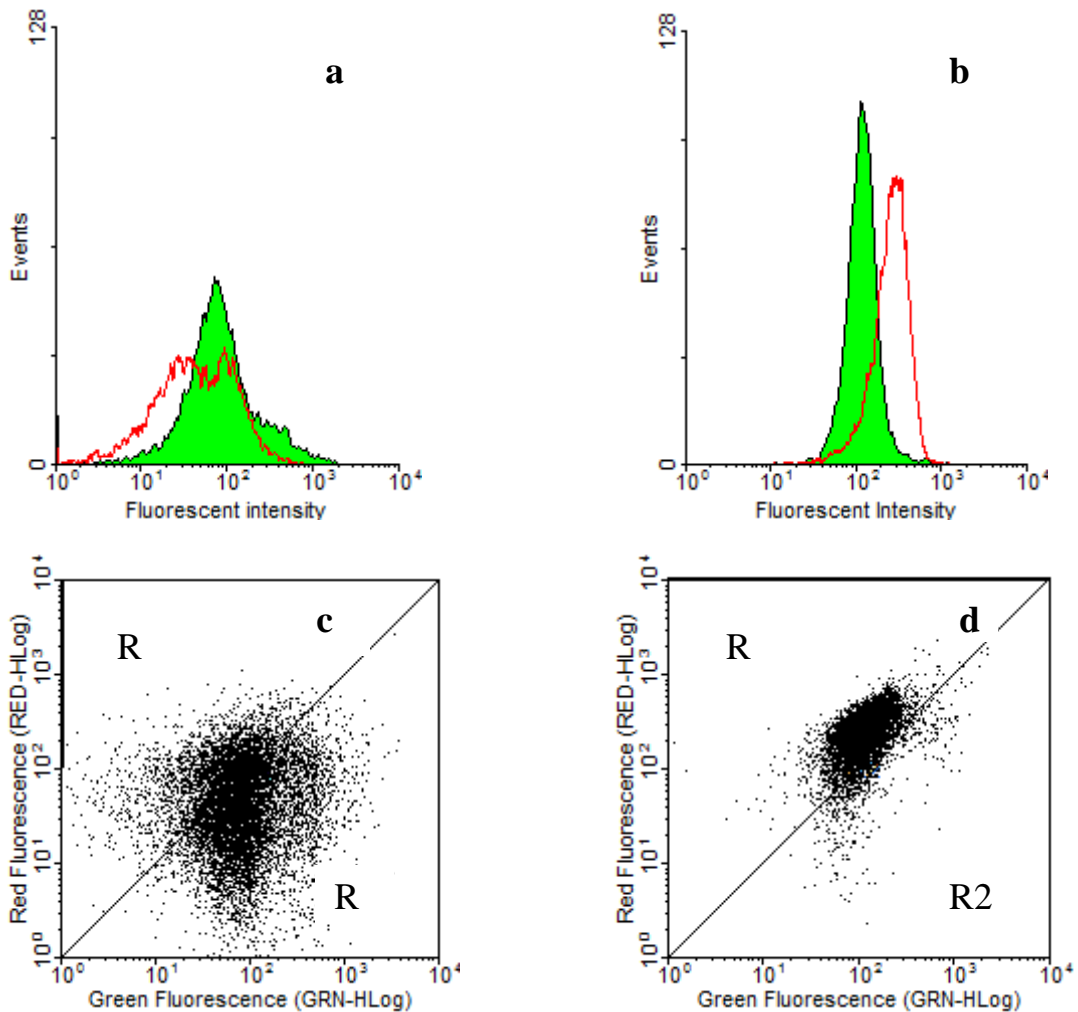


Figure 44: Flow cytometry histograms and dot plots (GR R1 vs RED plot) showing the fluorescence intensity of a late log phase *V. cholerae* culture histogram (a) dot plot (c) as well as a heat stressed culture histogram (b) and dot plots (d) incubated in SGI and PI at 37°C for 45minutes.

When the heat stressed *V. cholerae* cells were stained with a mixture consisting of SGI and PI, there was almost a log reduction in the fluorescent intensity due to SGI as indicated by the green curve in the histogram in Figure 44b when compared to the histogram in Figure 40b that is characteristic of just SGI staining. The reduction in the fluorescence intensity due to

SGI was simply due to the presence of PI. The presence of PI led to an increase in the red fluorescent intensity as indicated by the shift of the red curve towards the right as shown in Figure 44b. This result is however better illustrated by the dot plot in Figure 44d where there is an almost total shift of the fluorescent events from the region marked R2 (negative for PI) to R1 (PI positive). So the entry of PI into the heat stressed *V. cholerae* culture had a quenching effect on SGI.

Generally reduction in fluorescence due to SGI is indicative of a quenching effect and the increase in PI fluorescence was due to the gain of energy by PI from the quenching SGI (Berney et al., 2007).

3.8.1.3.2 Sybr Green I and Ethidium Bromide

When a mixture containing EB and SGI is used to stain bacterial cells, a quenching effect on the green fluorescence intensity, due to SGI, is observed as soon as the red fluorescence, due to EB, enters the cell thus enabling the identification of cells with a faulty ion pump mechanism (Midgley, 1987; Walberg et al., 1999).

Once the late log phase *V. cholerae* culture was stained with a SGI and EB mixture there was high fluorescence green intensity (green curve in Figure 45b) due to SGI when compared to the red fluorescence intensity due to EB (red curve in Figure 45b). The dot plot in Figure 45d is indicative of a similar situation as majority of the events are within R2 region. This was probably due to the fact that majority of the bacteria had intact cell walls. In addition to that they were also capable of pumping EB out and as result limited its internalization hence preventing the quenching of the green fluorescence intensity and increase in red fluorescence. However the overlap between green and red fluorescence cannot be ignored as it was indicative of dual staining that is symbolic of cells losing their capability to pump items out of the cells. When the heat stressed *V. cholerae* culture was stained with a SGI and EB mixture there was an increase in the fluorescence intensity due to EB as it is indicated by the shift of the red curve from the left to the right (Figure 45a) and concentration of majority of the events within the region marked R1 in the dot plot (Figure 45c).

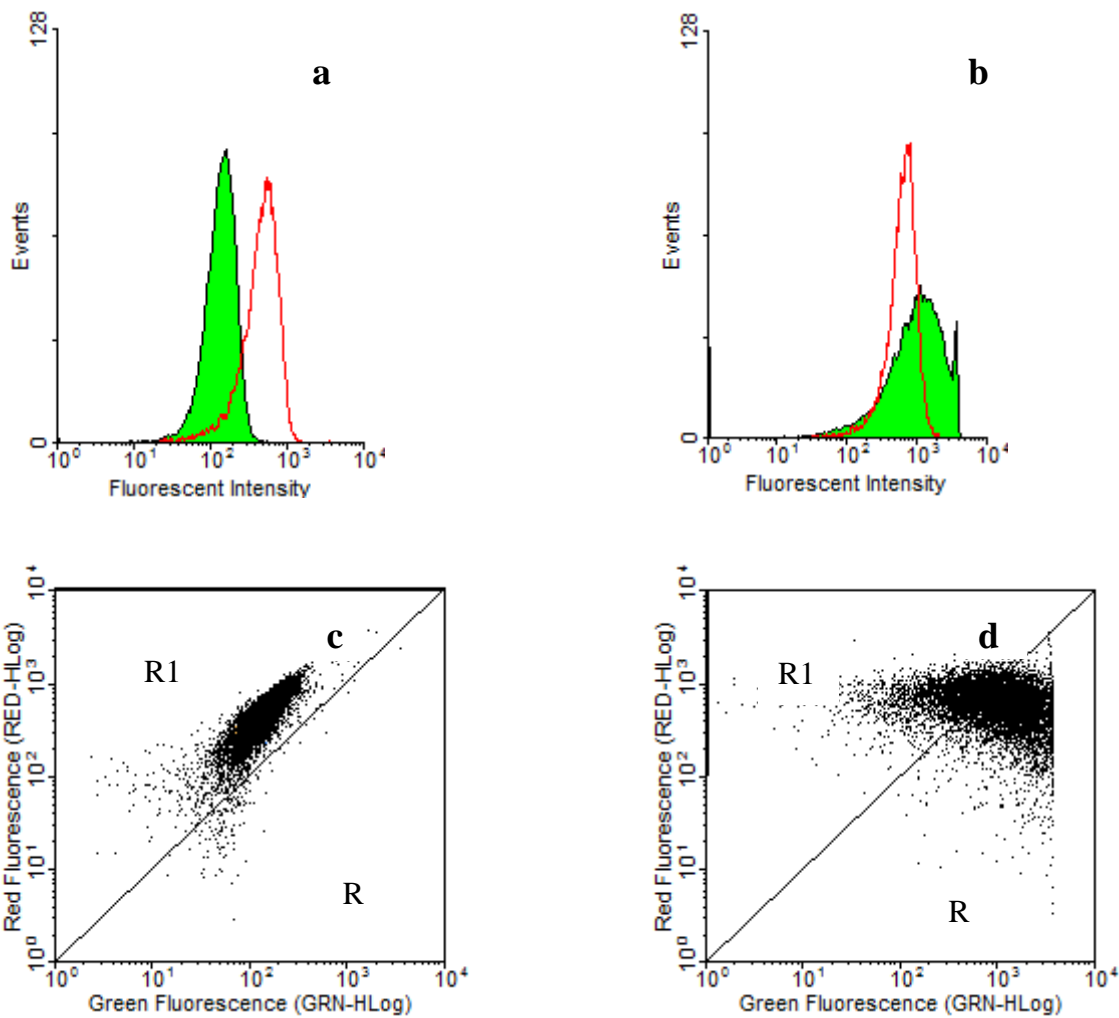


Figure 45: Flow cytometry histograms and dot plots (GRN versus RED plot) showing the fluorescence intensity of a late log phase *V. cholerae* culture histogram (b), dot plot (d) and a heat stressed *V. cholerae* culture histogram (a) and Dot plots (c) incubated in SGI and EB at 37oC for 45 minutes.

3.8.1.3.3 Carboxyfluorescein diacetate and Propidium Iodide

When a mixture containing cFDA and PI is used to stain bacterial cells, a quenching effect on the green fluorescence intensity due to formation of carboxyfluorescein from the cleavage of cFDA is observed as soon as the red fluorescence due to PI enters the cell thus enabling the identification of metabolically active bacterial cells from non-viable/ non-metabolic bacterial cells (Czechowska et al., 2008; Nebe-von-Caron et al., 2000).

When late log phase *V. cholerae* cells where stained with a cFDA and PI mixture the majority of the cells stained positive for cFDA as indicated by the increase in fluorescence intensity in the dot plot of SSC vs. GRN (Figure 46f).

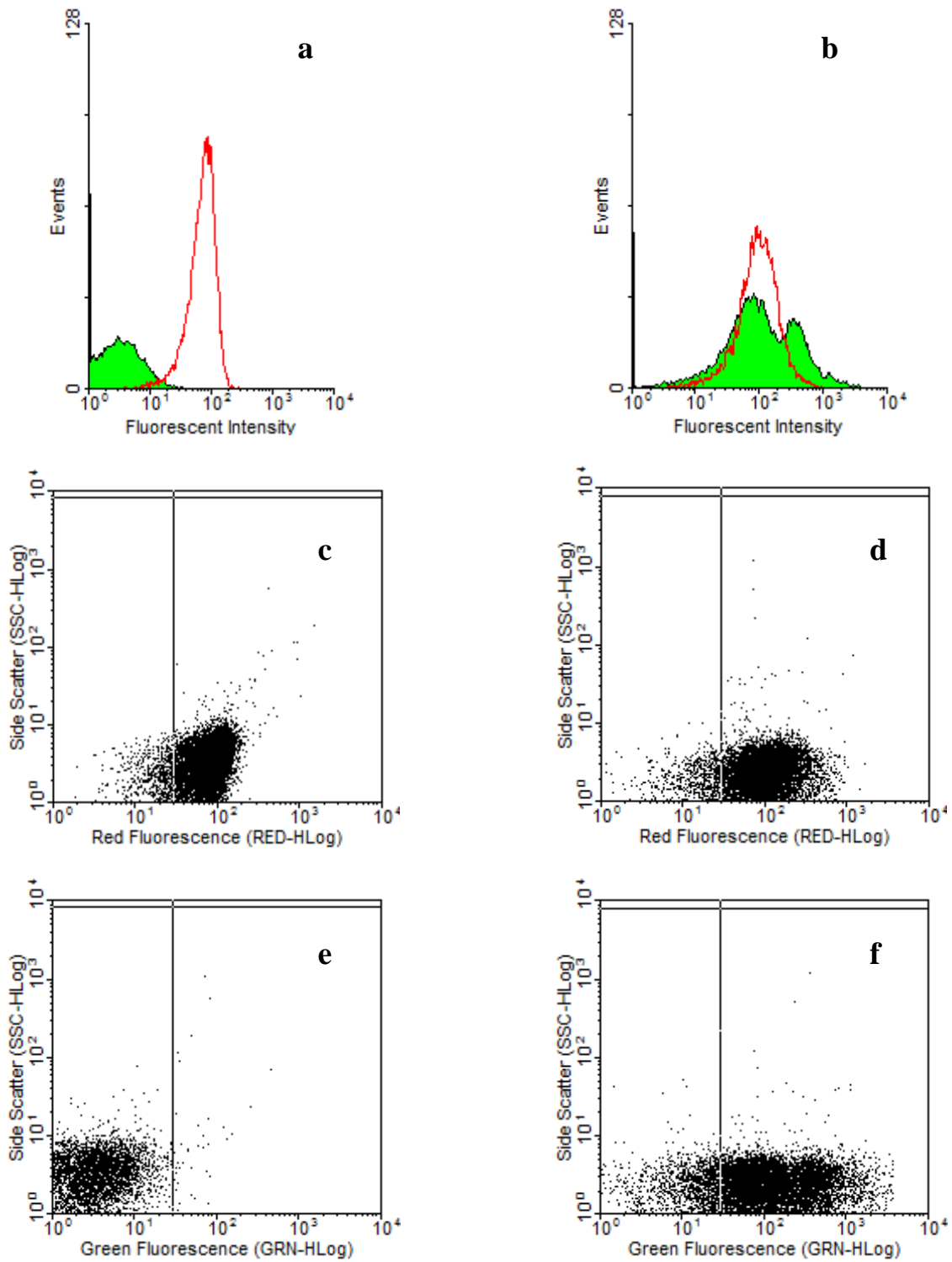


Figure 46: Flow cytometry histograms and dot plots (GRN vs. SSC / RED vs. SSC) showing the fluorescence intensity of heat stressed (a, c and e) and late log samples (b, d and f) of *V. cholerae* dual stained with cFDA and PI for 45minutes at 37°C.

However the majority of the samples were also positive for PI as shown by the red curve in the histogram in Figure 46b and dot plot in Figure 46d. So these cells were still metabolically

active even though their cell membranes were partially damaged. On the other hand there was no GRN fluorescence from the heat stressed *V. cholerae* culture (Figure 46e) but the red fluorescence intensity, due to PI, was high (Figure 46a and 46c). These results show that the heat stressed cells had lost the esterase activity and therefore were not metabolically active.

3.9 Flow cytometric analysis of solar radiated samples

The effect of SUVR on the membrane integrity of *V. cholerae* toxigenic strains (serotypes O1 and O139) and non-toxigenic strain 1009 was assessed using flow cytometry after solar exposure for 3, 7, 13 and 24 hours, in ground water and Luria Broth at pH 6.5 and 8.5. A mixture of fluorescent dyes SGI and PI was used to determine the effect of SUVR on the membrane integrity of the *V. cholerae* cells. SUVR is known to provide conditions suitable for the formation of dangerous chemical radicals such as the peroxides that damage the cytoplasmic membrane (Navntoft et al., 2008). So to understand how SUVR affects the cytoplasmic membrane it was necessary to use SGI and PI.

Solar exposed *V. cholerae* cultures were stained with the above mixture of fluorescent dyes and were analysed based on histograms showing green fluorescence intensity only. This criterion was used because green fluorescence intensity histograms provide more information on the physiological state of the cell than the red fluorescence. Another reason for using this criterion was that the red fluorescence intensity histograms could only account for PI positive events while the rest of the events (PI negative) would have been registered as background regardless of the physiological state of the cell. These reasons highlight one of SGI's most important features, the capability to infiltrate both damaged and intact cells. Therefore using a histogram displaying green fluorescent intensity (due to SGI) it was possible to observe the quenching effect (due to fluorescence resonance energy transfer) typical of the presence/entry of PI.

Three regions were identified on the histograms and were referred to as M1, M2 and M3. All results of solar exposed cultures were based on these regions. M1 was a representation of red fluorescence background signal due to unstained cells, cellular debris or waste. This region was identified during calibration of the flow cytometer. M2 on the other hand was indicative of quenching due to cells with a compromised cytoplasmic membrane. M3 was indicative of all the events that were PI negative but SGI positive and hence intact cytoplasmic membranes.

3.9.1 Flow cytometric analysis of solar exposed *V. cholerae* in ground water

The above mentioned *V. cholerae* strains were exposed to SUVR in ground water at pH 8.5 and 6.5 on the 24th of November 2009. On this day the maximum temperature and UVA recorded at the place of exposure was 35°C and 52W/m² respectively.

Before solar exposure, at time zero hours, the majority of the *V. cholerae* cells for the three strains, at both pHs, stained with SGI and PI fluorescent dyes were mainly grouped within the M2 region followed by the M3 region and lastly with the least cells the M1 region (Figure 49 and 50). Cells within the M2 region showed properties characteristic of partially damaged cell membrane which could have been the result of the centrifugation step of the overnight culture prior to exposure (Figure 47 and 48).

Soon after exposure to sunlight (solar radiation), the uptake of PI by all the *V. cholerae* strains started regardless of the pH of the ground water. The PI positive cells showed a decrease in the green fluorescence intensity (quenching effect) due to SGI and an increase in red fluorescence intensity due to PI uptake (Figures 47, and 48). On the flow cytometer this effect differed from one strain to another although in some instances strains showed similar properties and staining patterns (Figures 49 and 50).

After three hours of solar exposure, there was an increase in the percentage of cells with exhibiting the quenching effect that is characteristic of a compromised cytoplasmic membrane as indicated by the events within the M2 region. There seemed to be a slightly higher percentage of events within the M2 region for ground water at pH 6.5 (Figures 48 and 50) compared to that at pH 8.5 (Figures 47 and 49) regardless of the strain. The increase in the percentage of events within the M2 region coincided with the decrease in the percentage of intact cells (M3) (Figures 49 and 50). The pH 6.5 ground water exposed cultures for all the strains showed a greater percentage loss of intact cells when compared to those exposed in ground water at pH 8.5 for this time point (Figures 47a and 48a). The percentage of background events (M1) after solar exposure of the O1 serotype at both pHs' virtually remained the same. However strains O139 and 1009 showed a slight increase in unstained events in ground water at pH 6.5 whereas at pH 8.5 O139 serotype showed a slight decrease while strain 1009 showed an increase (Figures 47a and 48a). On the other hand all non-solar exposed samples at the same time point showed a remarkable increase in the percentage of intact (M3) *V. cholerae* cells regardless of the strain and pH, although the O1 serotype had the lowest percentage at both pHs (Figures 47b and 48b). A slightly higher percentage of

intact cells were however found for all the non-solar exposed ground water cultures at pH 6.5 than at pH 8.5. Furthermore there seemed to be a persistence in the percentage of partially damaged cells in the non-solar exposed samples however when plated there was above 6 log colony forming units (Figure 27).

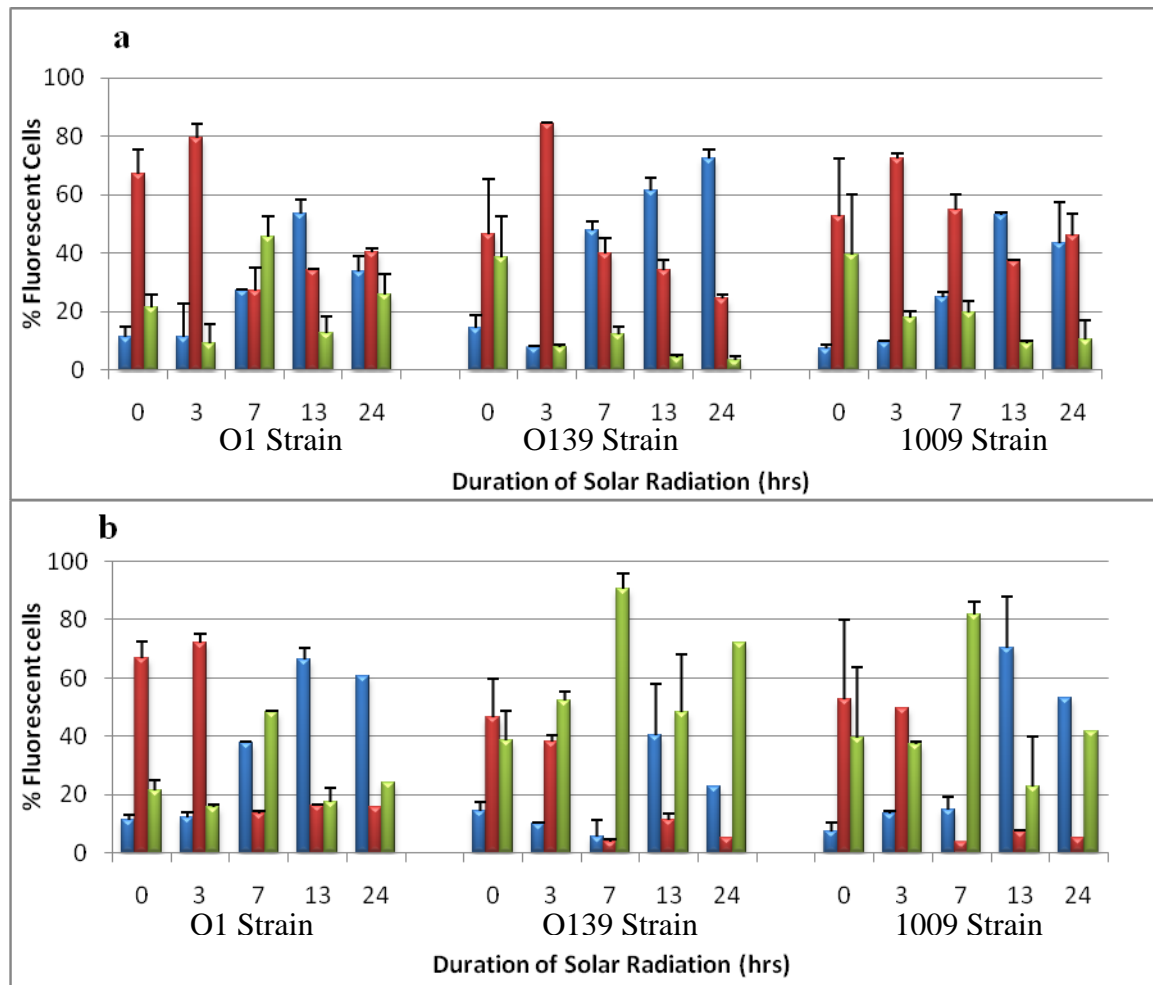


Figure 47: Flow cytometric analysis of green fluorescence histograms after staining 0, 3, 7, 13 and 24hr solar radiated (a) and non-radiated (b) cultures of *V. cholerae* strains O1, O139 and 1009 in ground water at pH 8.5 with a mixture of fluorescent dyes containing SGI and PI. The Red bars indicate percentage of events within the M1 region, the blue bars indicate percentage of events within the M2 region and the green bars indicate the percentage of events within the M3 region. Error bars represent standard deviations of duplicate measurements.

Seven hours after solar exposure, there was an increase in the percentage of both unstained (M1) and intact (M3) events and a decrease in events showing signs of quenching (M2) by all the strains regardless of the pH of the water when compared to the previous sample (three

hours solar exposure). However the staining properties (as explained below and also illustrated in Figures 49 and 50) were different for each strain at each pH of ground water. The O1 strain after seven hours of solar exposure had the highest percentage of intact cells (M1) in ground water at pH 8.5 when compared to the other strains regardless of the pH and to itself in ground water at pH 6.5 (Figures 47a and 48a). Even though strains O139 and 1009 showed an increase in the percentage of intact cells (M3) after seven hours of solar exposure (compared to the three hours solar exposure), this feature was not prominent as it had the lowest percentage of the total events analysed at both pH 8.5 and 6.5. In fact it accounted for the lowest percentage for both these strains at all pHs as well as the O1 strain in ground water at pH 6.5 (Figures 47a and 48a).

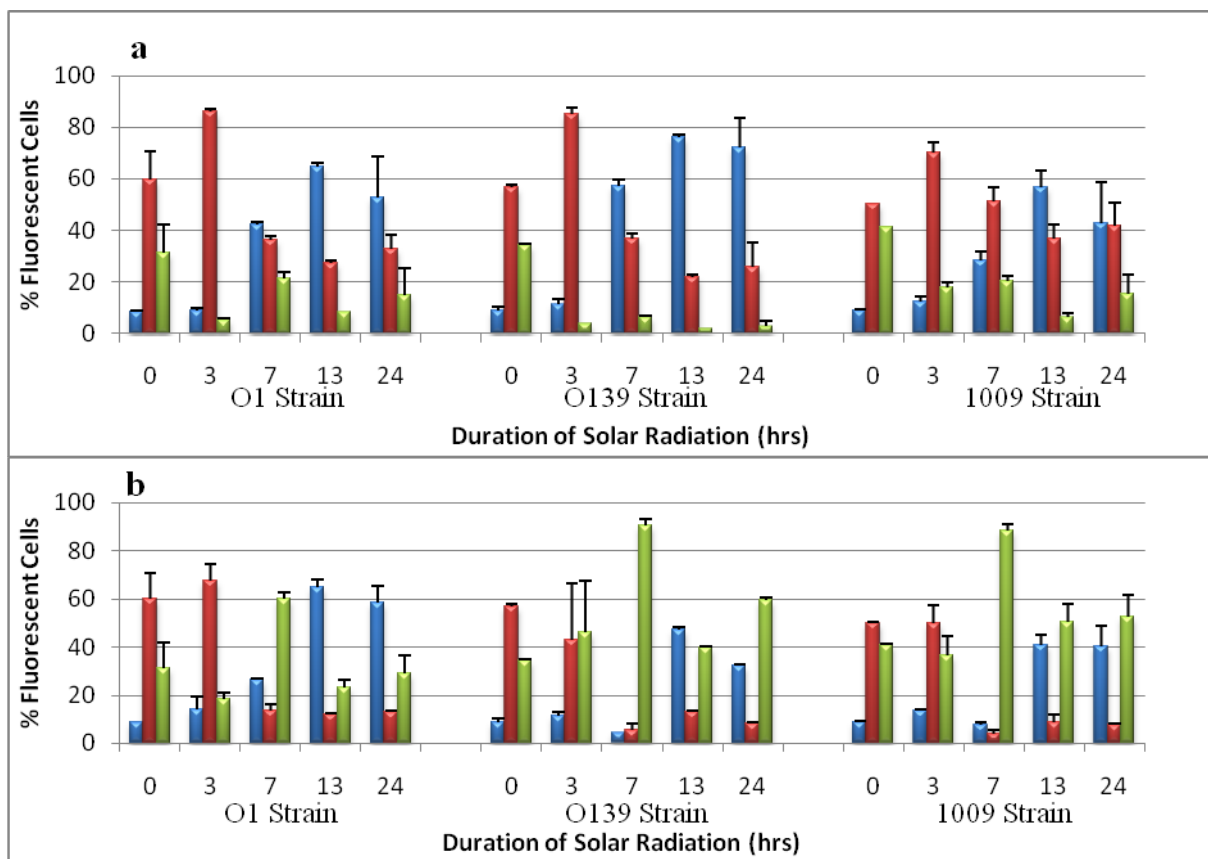
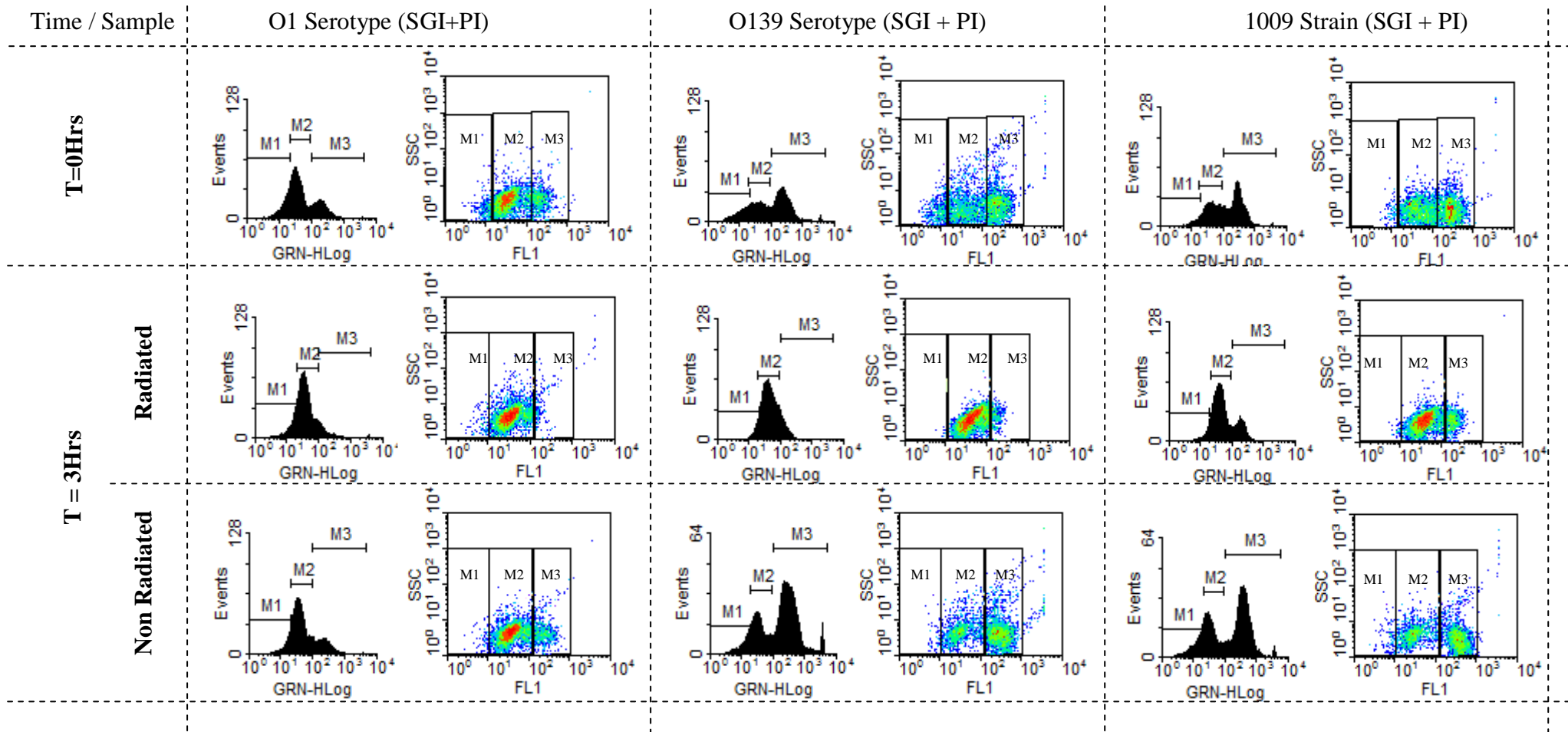


Figure 48: Flow cytometric analysis of green fluorescence histograms after staining 0, 3, 7, 13 and 24hr solar radiated (a) and non-radiated (b) cultures of *V. cholerae* strains O1, O139 and 1009 in ground water at pH 6.5 with a mixture of fluorescent dyes containing SGI and PI. The Red bars indicate percentage of events within the M1 region, the blue bars indicate percentage of events within the M2 region and the green bars indicate the percentage of events within the M3 region. Error bars represent standard deviations of duplicate measurements.

On the other hand at both pH 6.5 and 8.5 the O139 strain had the highest percentage of unstained events while the 1009 had the highest percentage of cells exhibiting the quenching effect. All non-solar exposed samples at the same time point showed a remarkable increase in the percentage of intact (M3) cells regardless of the strain and pH, although the O1 serotype had the lowest percentage at both pHs (Figures 47b and 48b).

After 13 hours of solar radiation the three *V. cholerae* strains exhibited similar staining characteristics regardless of the pH of the ground water. The M1 region accounted for most of the events followed by regions M2 and M3. The solar radiated cultures in ground water at both pH 6.5 and 8.5 showed an increase in unstained events with O139 serotype showing the highest percentage of unstained events followed by O1 serotype and 1009 strain (Figures 47a and 48a). Both the O1 and O139 serotypes showed similar percentages of events exhibiting the quenching effect but the 1009 strain had a slightly higher percentage of cells with similar properties. Then the O1 serotypes at both pHs of ground water had the highest percentage of intact cells followed by the 1009 strain and O139 serotype with the least. As for the unexposed samples, there seemed to be an increase in the percentage of the unstained events for strains O1 and 1009 in ground water at pH 8.5 and a decrease in the percentage of intact cells but the percentage of partially damaged cells remained the lowest. The unexposed O139 *V. cholerae* serotype in ground water at pH 8.5, unlike the other two discussed above, had the highest percentage of intact cells (Figures 47b and 49). However in ground water at pH 6.5 serotypes O1 and O139 showed a similar dominant property characterised by the increase in the percentage of unstained events; 1009 unlike the other strains showed a higher percentage of intact cells (Figures 48b and 50).

After twenty four hours of solar radiation, *V. cholerae* O1serotype and 1009 strain showed similar staining characteristics but the patterns differed based on the pH of the ground water (Figures 49 and 50). In ground water at pH 6.5 these strains had the majority of their events within the M1 region followed by M2 and lastly M3 with the least number of cells. However in ground water at pH 8.5 the majority of the events occurred within the M2 region followed by M1 and finally M3. On the other hand the O139 *V. cholerae* serotype showed similar staining characteristics at both pHs. For this strain, there was a high percentage of unstained events (M1) followed by those that were partially damaged (M2) and eventually those with intact cell walls (M3).



Time / Sample

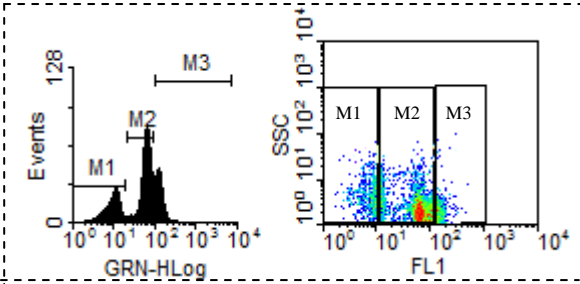
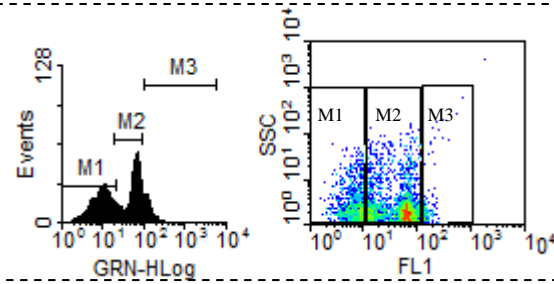
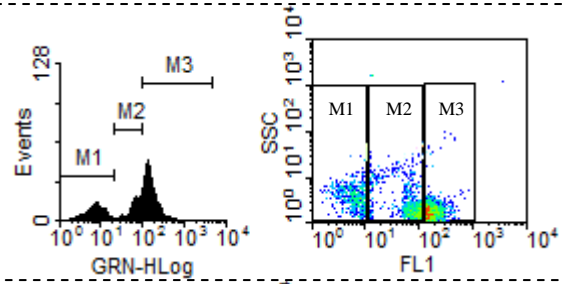
O1 Serotype (SGI+PI)

O139 Serotype (SGI + PI)

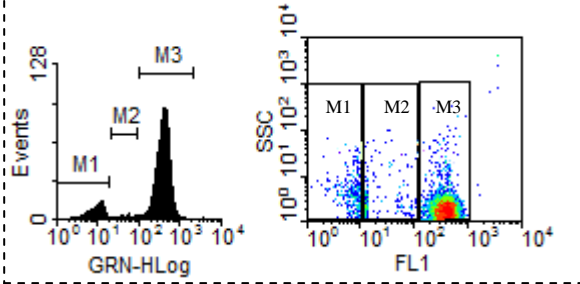
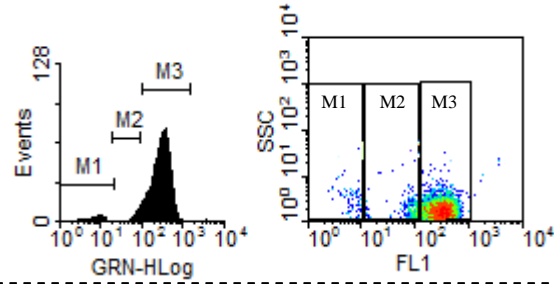
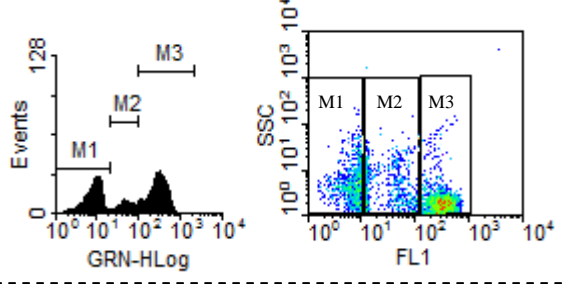
1009 Strain (SGI + PI)

T = 7 Hrs

Radiated

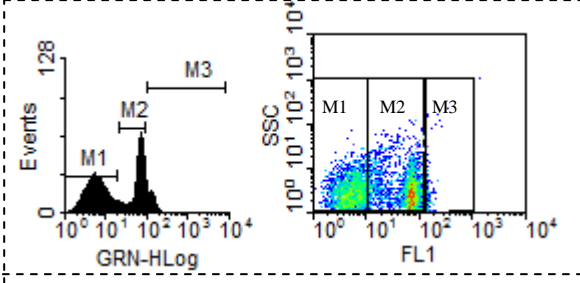
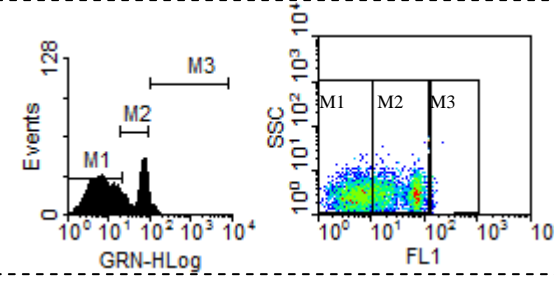
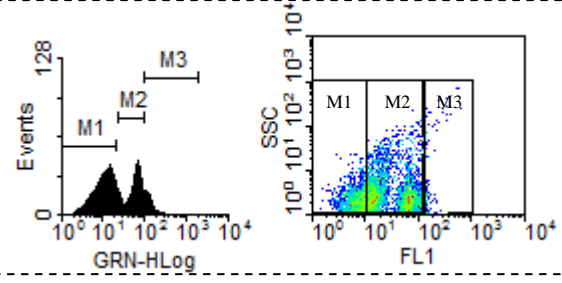


Non Radiated

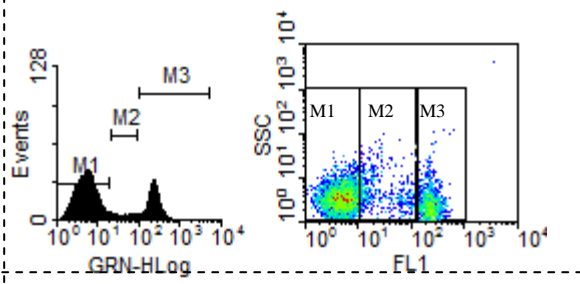
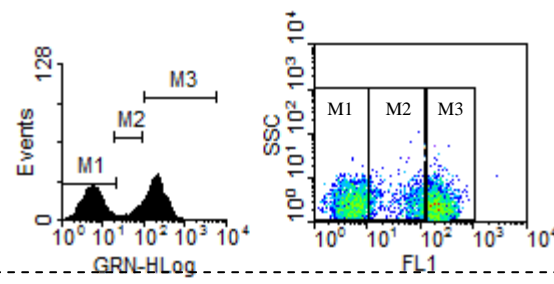
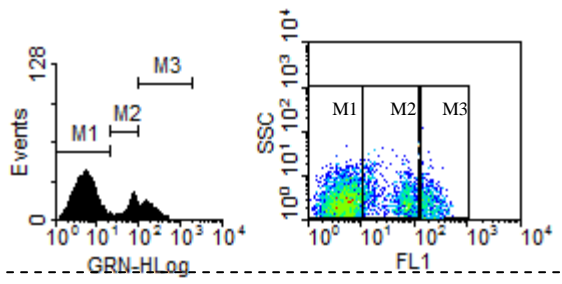


T = 13Hrs

Radiated



Non Radiated



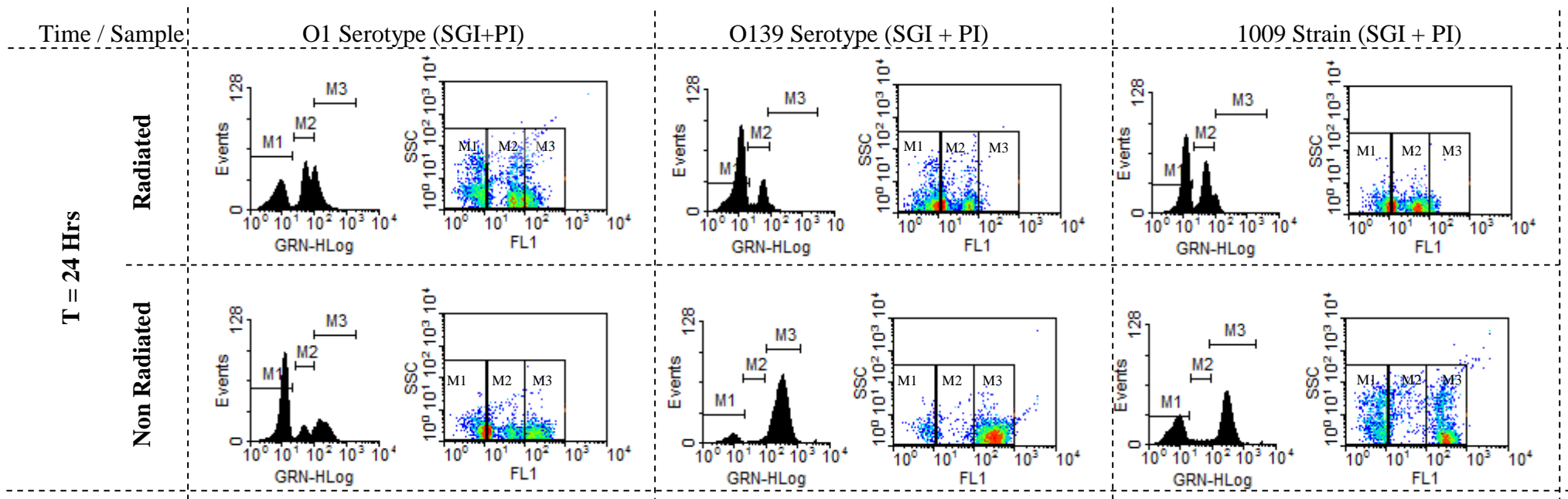
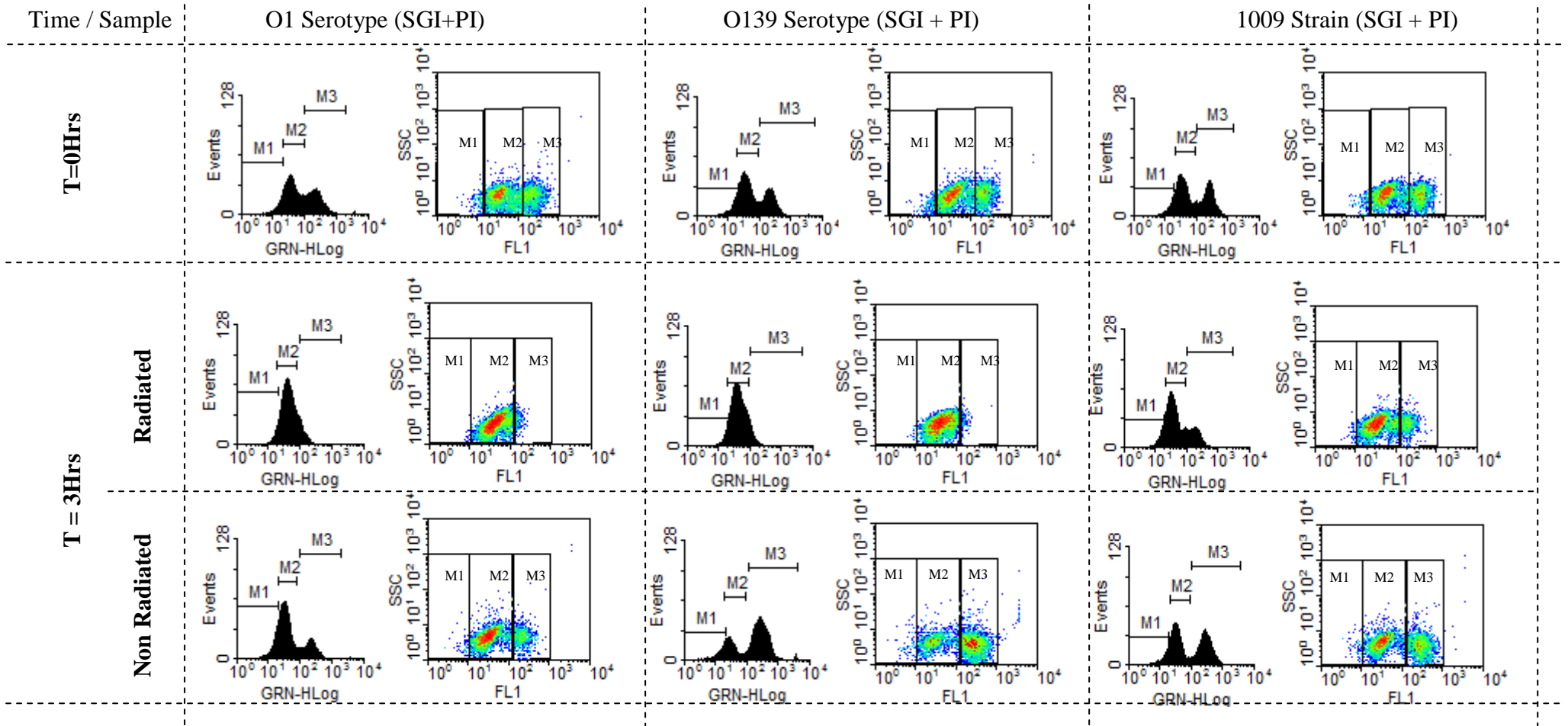
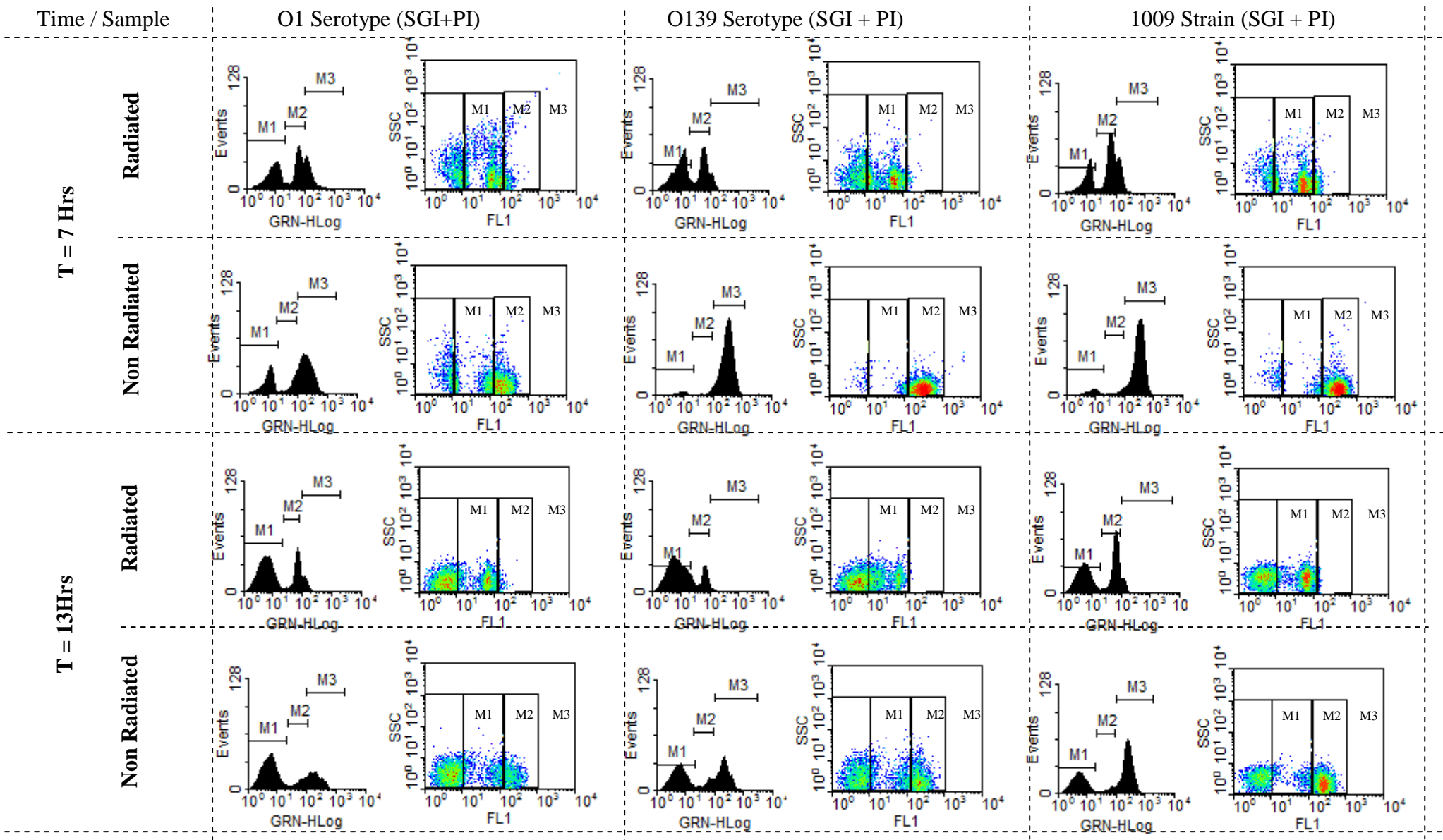


Figure 49: Histograms of green fluorescence intensity (GRN-HLog) and dot plots of FL1, $520 \pm 30\text{nm}$ (GRN fluorescence); SSC (side scatter) resulting from the flow cytometric analysis of 3, 7, 13 and 24hrs solar radiated and non-radiated cultures of *V. cholerae* strains O1, O139 and 1009 in ground water at pH 8.5 after staining with a mixture of SGI and PI fluorescent dyes. Each histogram and dot plot consists of three regions i.e. M1 representing unstained/background fluorescence, M2 comprising of bacterial cells with a compromised cytoplasmic membrane and finally M3 constituting of bacterial cells with intact cytoplasmic membranes. The M1 region in the histogram can be found within the region indicated M1 in the corresponding density plot same applies for M2 and M3. The colours within the density plots represent the relative density of cells in each location. The red colour represents the region with the highest density of cells, followed by green, sky blue and then the royal blue, the cells occurring at the lowest frequency are the navy blue in colour.





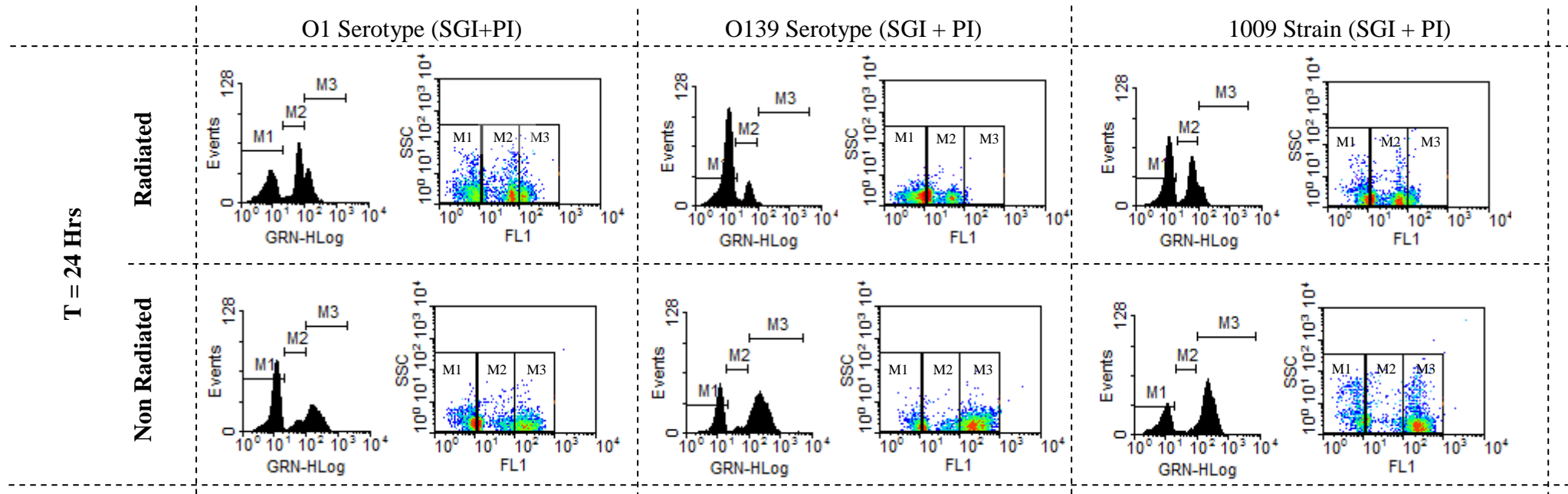


Figure 50: Histograms of green fluorescence intensity (GRN-HLog) and dot plots of FL1, $520 \pm 30\text{nm}$ (GRN fluorescence); SSC (side scatter) resulting from the flow cytometric analysis of 3, 7, 13 and 24hrs solar radiated and non-radiated cultures of *V. cholerae* serotypes O1, O139 and strain 1009 in ground water at pH 6.5 after staining with a mixture of SGI and PI fluorescent dyes. Each histogram and dot plot consists of three regions i.e. M1 representing unstained/back ground fluorescence, M2 comprising of bacterial cells with a compromised cytoplasmic membrane and finally M3 constituting of bacterial cells with intact cytoplasmic membranes. The M1 region in the histogram can be found within the region indicated M1 in the corresponding density plot same applies for M2 and M3. The colours within the density plots represent the relative density of cells in each location. The red colour represents the region with the highest density of cells, followed by green, sky blue and then the royal blue, the cells occurring at the lowest frequency are the navy blue in colour.

3.9.2 Flow cytometric analysis of solar exposed *V. cholerae* strains in LB

V. cholerae serotypes O1, O139 and strain 1009 were exposed to SUVR in LB at pH 8.5 and 6.5 on the 17th of November 2009. On this day the sky was overcast and the maximum temperature recorded at the time of exposure was 17°C and the UVA recorded was 20.41W/m².

Before exposure to SUVR, the majority of the *V. cholerae* cells had intact/uncompromised cytoplasmic membranes as indicated by the flow cytometric analysis of their membrane integrity using a mixture of fluorescent dyes containing SGI and PI (Figures 51, 52, 53 and 54). This was observed regardless of the strain or the pH of LB.

Upon sunlight exposure, the uptake of PI by all the solar exposed *V. cholerae* strains started regardless of the pH of the LB (Figures 53 and 54). This in turn led to the reduction in the percentages of cells with an intact cytoplasmic membrane as indicated by M3. However the extent to which the strains were affected by sunlight exposure differed from one strain to another although in some instances strains showed similar properties and staining patterns.

After three hours of solar exposure, there was an increase in the percentage of cells with compromised cytoplasmic membranes as indicated by the events within the M2 region (Figures 51 and 52). Even though all three strains showed an increase in cells at both pHs evincing the quenching effect, the extent to which this effect happened differed from one strain to the other as well as on the pH of the LB. The O1 serotype exposed to sunlight in LB at pH 8.5 seemed to be the most affected as the majority of its cellular population had compromised cytoplasmic membranes. In contrast the majority of the cellular population for both the O139 serotype and 1009 strain, exposed to sunlight in LB at pH 8.5 and 6.5 had intact cytoplasmic membranes, but there was no detectable increase in biomass formation for any of the strains at any of the pHs. On the other hand, all non-solar exposed samples at the same time point showed a remarkable increase in the percentage of cells with intact cytoplasmic membranes as indicated by the M3 region; this was complimentary to the increase in biomass. But the O1 serotype had the lowest percentage of biomass increase at both pHs. Interestingly there was a slightly higher percentage of intact cells for all the non-solar exposed LB cultures at pH 6.5 than that at pH 8.5 (Figure 51b and 52b).

Seven hours later, there was a decrease in the percentage of both unstained (M1) and intact (M3) cellular events as well as an increase in cellular populations with compromised

cytoplasmic membranes (M2) by only the toxigenic strains i.e. serotypes O1 and O139 in LB exposed to sunlight at pH 8.5 (Figure 51a). The environmental strain (1009) on the other hand showed, at the same pH, an increase in the percentage of cells with intact cytoplasmic membranes as well as a decrease in the percentage of cells whose cell membrane had been compromised (Figure 51a).

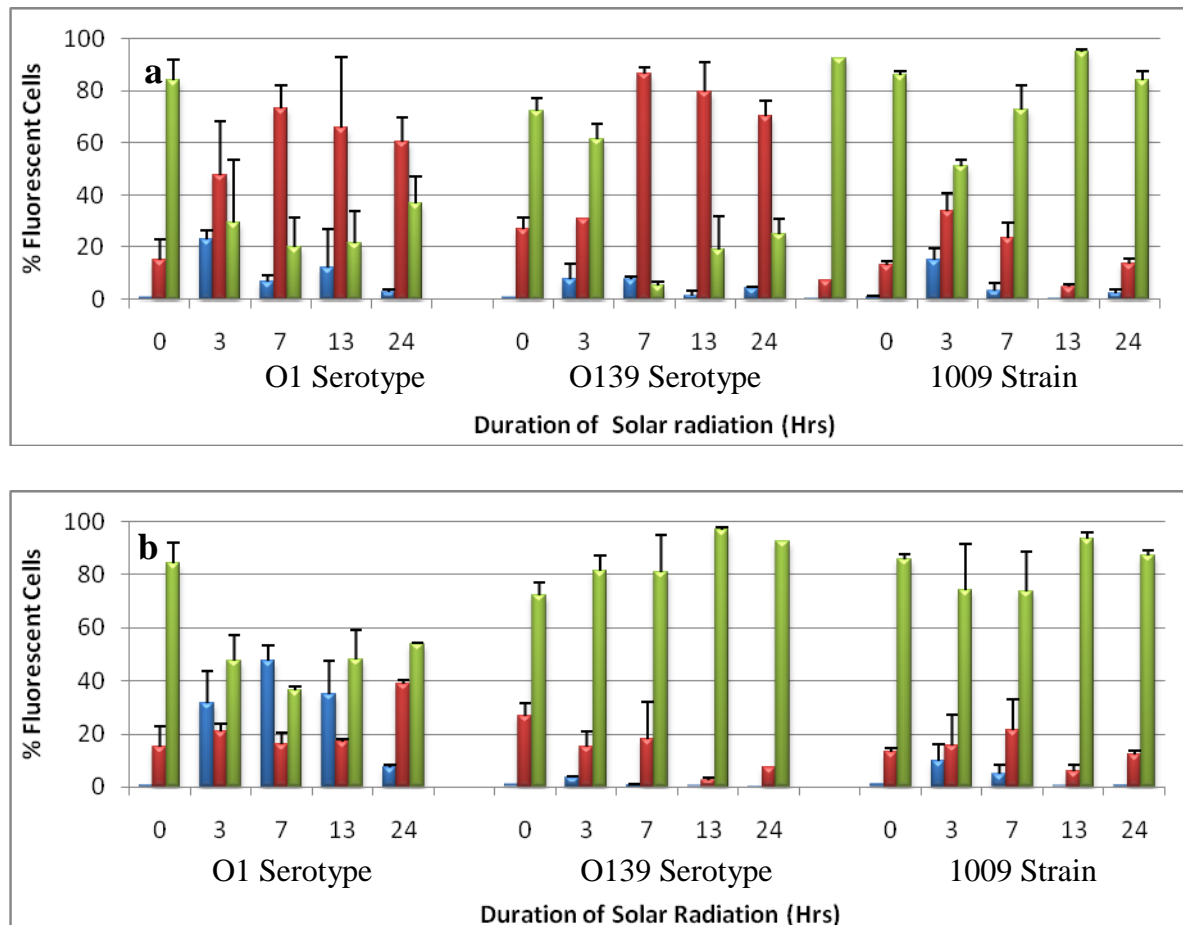


Figure 51: Flow cytometric analysis of green fluorescence histograms after staining 0, 3, 7, 13 and 24hr solar radiated (a) and non-radiated (b) cultures of *V. cholerae* serotypes O1, O139 and strain 1009 in LB at pH 8.5 with a mixture of fluorescent dyes containing SGI and PI. The Red bars indicate percentage of events within the M1 region, the blue bars indicate percentage of events within the M2 region and the green bars indicate the percentage of events within the M3 region. Error bars represent standard deviations of duplicate measurements.

Then at pH 6.5 all three strains had compromised cell membranes as indicated by the percentage of events within the M2 region (Figure 52a).

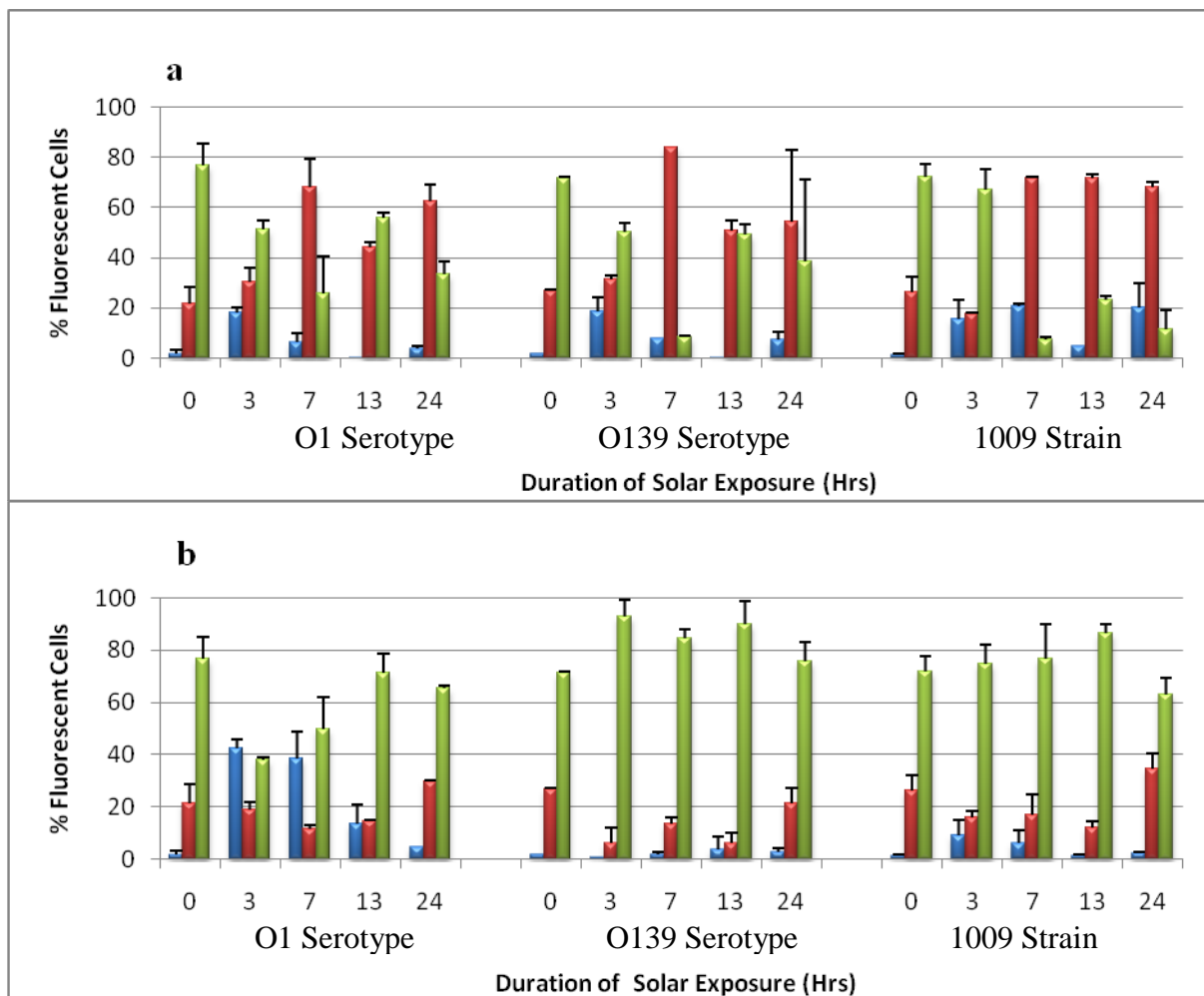
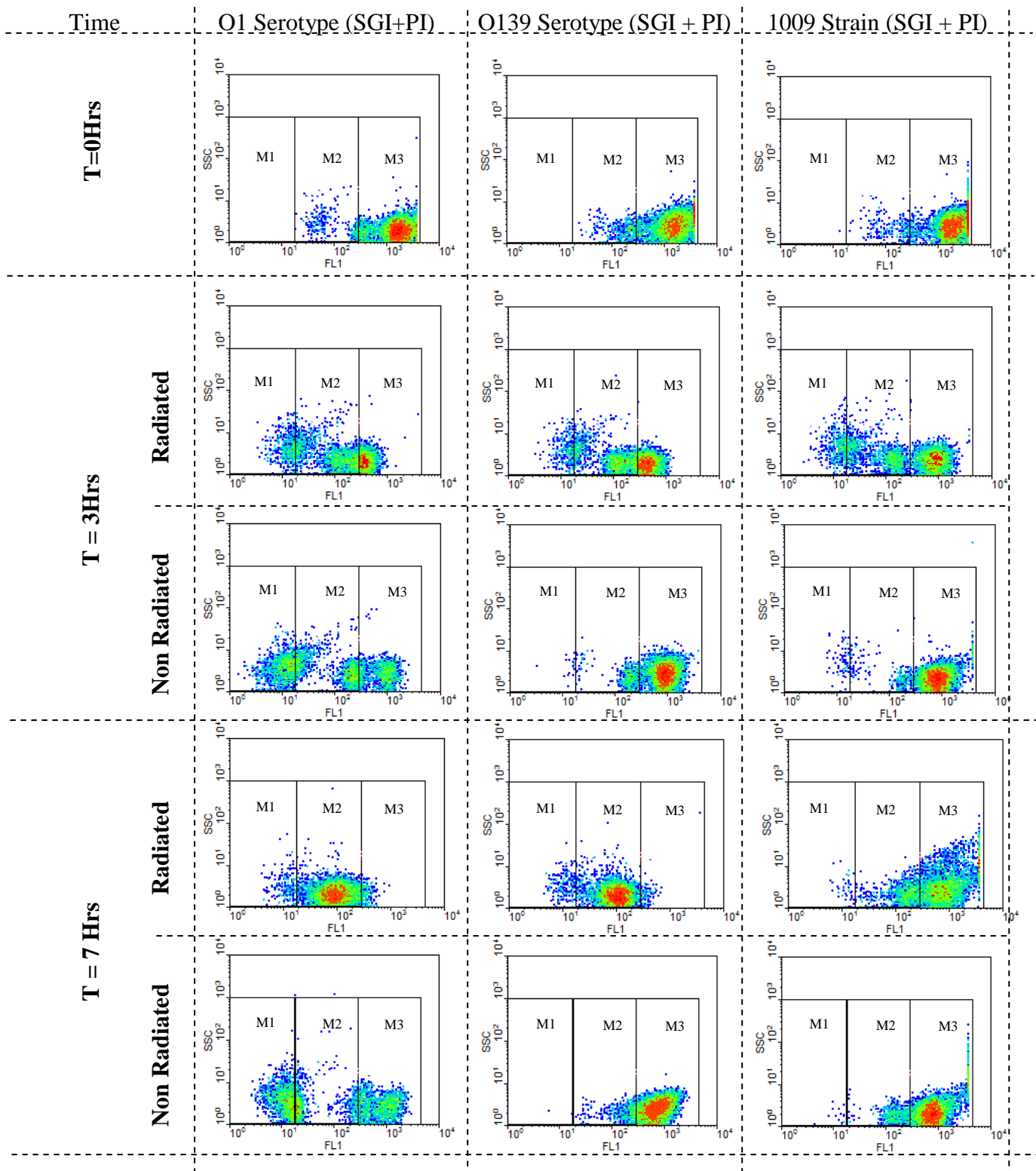


Figure 52: Flow cytometric analysis of green fluorescence histograms after staining 0, 3, 7, 13 and 24hr solar radiated (a) and non radiated (b) cultures of *V. cholerae* serotypes O1, O139 and strain 1009 in LB at pH 6.5 with a mixture of fluorescent dyes containing SGI and PI. The Red bars indicate percentage of events within the M1 region, the blue bars indicate percentage of events within the M2 region and the green bars indicate the percentage of events within the M3 region. Error bars represent standard deviations of duplicate measurements.

There was also a population with intact cytoplasmic membranes as indicated by the percentages within the M3 region. The O1 strains had the highest percentage of cells within the M3 region after solar exposure, however all three strains showed no increase in biomass formation after exposure to sunlight regardless of the pH of LB. On the other hand, all non-exposed cultures of the three strains maintained their membrane integrity as indicated by the percentages of events within the M3 region with the exception of the O1 strain at pH 8.5 (Figure 52b). The non-exposed samples at this time point showed an increase in their biomass

as indicated by an increase in the OD_{600} with the exception of the O1 strain and this time at both pHs.



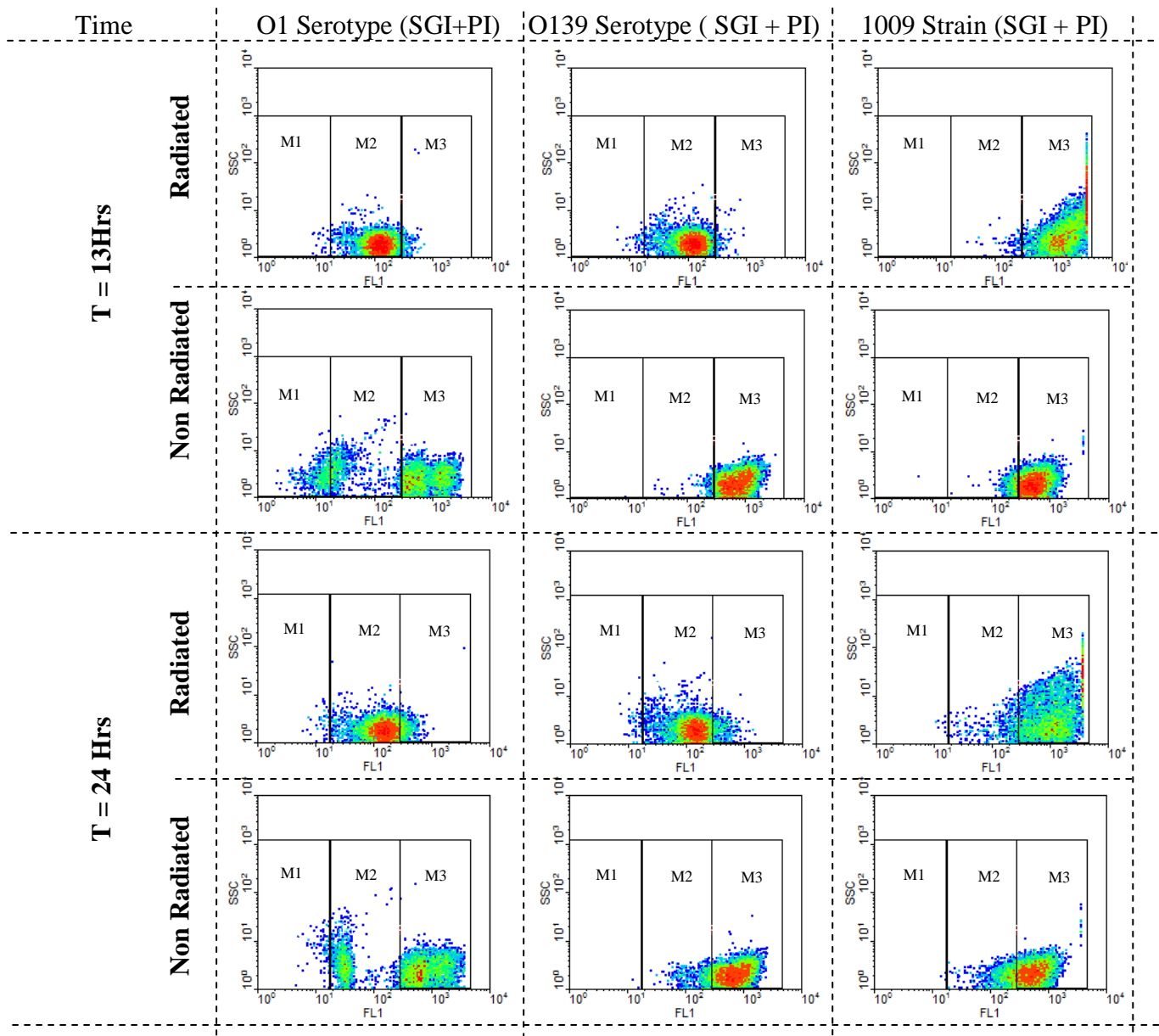
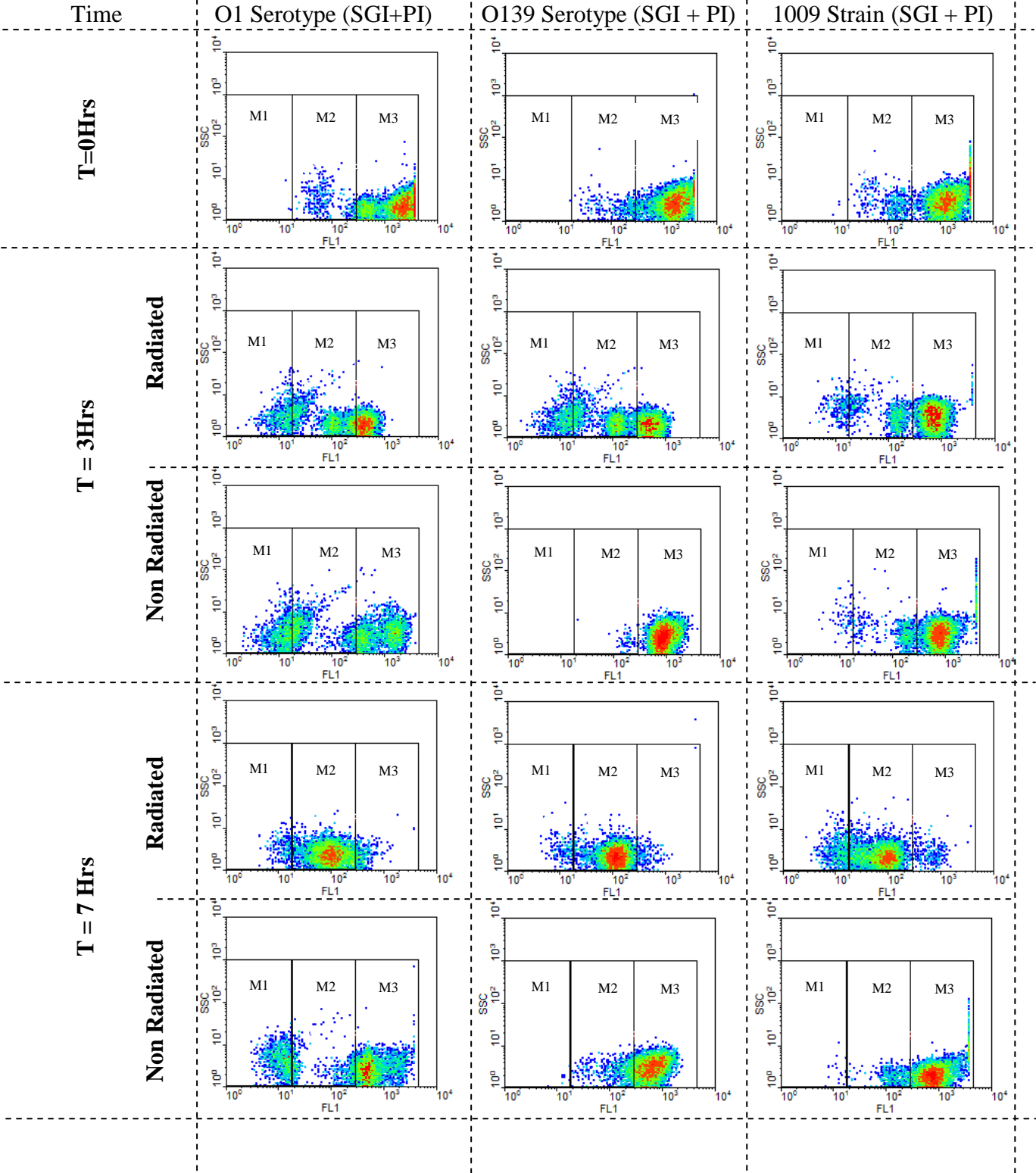


Figure 53: Smoothed density plots FL1, 520 ± 30nm (GRN fluorescence); SSC (side scatter) resulting from the flow cytometric analysis of 3, 7, 13 and 24hrs solar radiated and non-radiated cultures of *V. cholerae* serotypes O1, O139 and strain 1009 in LB at pH 8.5 after staining with a mixture of SGI and PI fluorescent dyes. Each density plot consists of three regions i.e. M1 representing the frequency of unstained/back ground fluorescence, M2 comprising of the frequency of bacterial cells with a compromised cytoplasmic membrane and finally M3 constituting of the frequency of bacterial cells with intact cytoplasmic membranes. The colours represent the relative density of cells in each location within the flow cytometry density plot. The red colour represents the region with the highest density of cells, followed by green, sky blue and then the royal blue, the cells occurring at the lowest frequency are the navy blue in colour.

After 13 hours of solar radiation the majority of the toxigenic *V. cholerae* strains exposed in LB at pH 8.5 continued to exhibit signs of compromised cytoplasmic membranes as indicated by the percentage of events in the M2 regions as well as that in the density plots (Figure 51 and 53). However there was a slight reduction in the percentage of cells with compromised cytoplasmic membranes and a slight increase in the percentage of cells with intact cytoplasmic membranes in comparison to the 7hrs solar exposure at the same pH. And like before (7hrs solar exposure) at pH 8.5, the environmental strain (1009) cell population had intact cytoplasmic membranes, as indicated by the percentage of events within the M3 marker of the green fluorescence histogram, as well as that in the density plot. This was in agreement with the increase in biomass. There was however an increase in the percentage of cell populations with intact cytoplasmic membranes by all three strains in solar exposed LB at pH 6.5. The O1 serotype unlike the other two strains had the majority of its population within the regions M3 as indicated by the percentage in the green fluoresce histogram and density plot respectively (Figures 51a and 53). The solar exposed culture of the environmental strain however had most of its events within the M2 marker which was also comparable to that shown in its respective density plot. The O139 serotype on the other hand had almost similar percentages of cells with a compromised and an intact cytoplasmic membrane as shown by the M2 and M3 markers on the histogram. The non-exposed cultures for all these strains continued to exhibit same properties as before characterized by greater increase in cell population with intact cytoplasmic membrane (Figures 52 and 54). However the O139 serotype and 1009 strain of the non-exposed cultures, at pH 6.5 showed an increase in the biomass as determined by the OD₆₀₀ reading.

At the end of the twenty four hours of solar exposure, the previously observed flow cytometric profile (7 and 13hrs) persisted for all three solar exposed strains in LB at both pHs. However in solar exposed LB at pH 8.5, there was a slight difference in the percentage of cellular events within all the predetermined regions. For instance there continued to be a gradual decrease in cells with compromised cytoplasmic membranes even though this characteristic accounted for the majority of the cellular states for both toxigenic strains (Figure 51a). Although there was a slight increase in the number of cells with intact cytoplasmic membranes at pH8.5 by both toxigenic strains, there was no detectable increase in the OD₆₀₀ reading. The environmental strain on the other hand, under the same conditions, showed a slight reduction in the percentage of cells with intact cytoplasmic membranes although this property accounted for the majority of the cellular population. Then at pH 6.5

there was an increase in the percentage of cells with compromised cytoplasmic membranes as indicated by the M1 marker of the green fluorescence histogram for all three strains. As for the non-exposed samples, there was a slight reduction in the percentage of cells with intact cell however they still accounted for majority of the cell population.



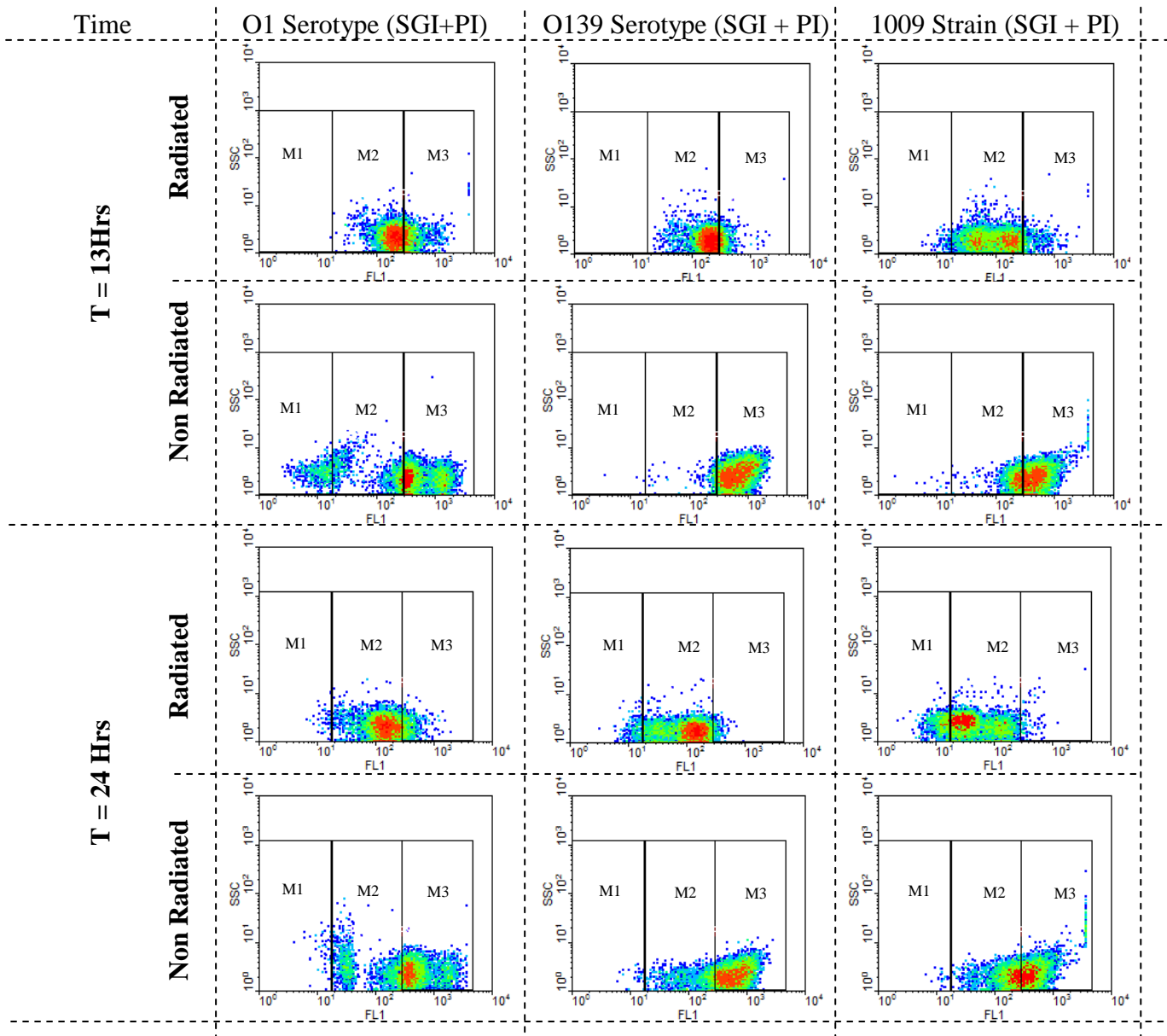


Figure 54: Smoothed density plots FL1, 520 ± 30nm (GRN fluorescence); SSC (side scatter) resulting from the flow cytometric analysis of 3, 7, 13 and 24hrs solar radiated and non-radiated cultures of *V. cholerae* serotypes O1, O139 and strain 1009 in LB at pH 8.5 after staining with a mixture of SGI and PI fluorescent dyes. Each density plot consists of three regions i.e. M1 representing the frequency of unstained/back ground fluorescence, M2 comprising of the frequency of bacterial cells with a compromised cytoplasmic membrane and finally M3 constituting of the frequency of bacterial cells with intact cytoplasmic membranes. The colours represent the relative density of cells in each location within the flow cytometry density plot. The red colour represents the region with the highest density of cells, followed by green; sky blue and then the royal blue, the cells occurring at the lowest frequency are the navy blue in colour.

Chapter 4

4 General Discussion and Conclusion

The WHO and other health related organizations continually report on the transmission of diseases through the consumption of untreated water and its' associated consequences that can ultimately lead to the death of thousands of people *Vibrio cholerae*, a natural habitat of the aquatic ecosystem is known to cause cholera when consumed by drinking untreated water or contaminated food. However, only *V. cholerae* CTX Φ and VPI Φ carrying serotypes (i.e. O1 and O139) are known to cause this deadly disease.

The survival and proliferation of *V. cholerae* within its natural environment is dependent on abiotic factors such as the environment and climate, as well as on biotic factors such as phytoplankton and microbial communities. In this study, we investigated the effect of solar ultraviolet radiation and temperature on the growth of *V. cholerae* and on the secretion of the cholera toxin to assess whether solar disinfection has any effect on the bacterium.

Three *V. cholerae* strains were used in this study. The two toxigenic strains belonging to serotypes O1 (strain 5941) and O139 (strain 12945) were acquired from NCTC (National Collection of Type Cultures), while the third non-toxigenic environmental strain (1009) was isolated from the Vaal River, Gauteng, South Africa. These strains were cultured in a nutrient rich medium represented by LB and a nutrient poor media consisting of ground water. LB is representative of a nutrient rich environment such as that found in the human gut or sewage where *V. cholerae* thrives. The ground water was acquired from Soshanguve, a formal settlement close to Pretoria. The choice of ground water in contrast to laboratory distilled water, bottled water or tap water was based on its significance to resource poor communities that have limited or sporadic access to treated water. The growth of the three *V. cholerae* strains in the two media was first tested in the laboratory at three different pHs, (i.e. pHs 6.5, 7.5 and 8.5). These pHs were chosen based on the closest percentile of the acidity, neutral and alkalinity of the majority of water sources in South Africa (DWA website). Since there was no dramatic observable pH effect during laboratory experiments, only two pHs 6.5 and 8.5 were retained because of their published significance to cholera toxin production and optimal growth conditions. Furthermore, the growth of *V. cholerae* was evaluated at three temperatures, 25°C, 30°C and 37°C under laboratory conditions. It was found that all the *V.*

cholerae strains grew in all three temperatures even though optimum growth and toxin production varied according to the media (section 3.1).

4.1 Growth of *V. cholerae* and Toxin Secretion under Laboratory Conditions

The three *V. cholerae* strains never lost their culturability throughout the entire period of incubation at the three different pHs even though a decline in CFU was observed when grown in ground water. However, their growth pattern did not follow a typical growth curve characterized by lag, log, stationary and death phases. Therefore the GInaFiT tool was used to model their mode of survival in ground water. On the other hand the growth of *V. cholerae* in a nutrient rich media displayed typical growth curves clearly highlighting the impact that added nutrients could have on the growth and proliferation of *V. cholerae*. In their natural environments, eutrophication of rivers and dams provides the nutrients for growth and proliferation of *V. cholerae*. In developing countries eutrophication of water systems is mainly due to human activities such as farming, lack of sewage systems and inadequate waste management handling or treatment. Since the biomass of the microorganisms increased considerably due to the availability of nutrients, an OD rather than plate count was used to measure growth.

The culturability of the *V. cholerae* strains was found to be highly dependent on incubation temperature in both ground water and LB, especially for the toxigenic strains (Figures 11, 13 and 15). Survival of these strains in ground water at 37°C especially under acidic conditions was not optimal for microbial growth as shown in Figure 15. Growth of the microorganisms in both media was best at an incubation of 25°C followed by incubation at 30°C at all pHs. However, the toxigenic strains of *V. cholerae* released more cholera toxin at 37°C in ground water under alkaline conditions as determined by the GM₁ ELISA (Figure 16).

The two toxigenic strains showed different cholera toxin release profiles (Chapter 3, section 3.3.3) suggesting that both serotypes behave differently when exposed to similar environments. Conditions that were less favourable for optimal growth in ground water seemed to support greater toxin secretion (Figure 16). It is possible that those conditions enhanced toxin secretion.

In LB there was an increase in toxin production with a decrease in pH (Figure 12) but the extent to which that happened was temperature and strain dependent. The difference in the

cholera toxin profiles of the two strains suggests they probably have different control mechanism for toxin production under different growth conditions. In addition, it was also observed that increase in biomass did not necessarily translate into increase in cholera toxin release.

4.2 Growth of *V. cholerae* and Toxin Secretion during Exposures to Solar Radiation

Once growth and toxin production patterns for the *V. cholerae* strains were established under laboratory conditions, these parameters were assessed by exposing the bacteria to natural environmental solar ultraviolet radiation (SUVR) and temperature. The lowest levels of SUVR and temperature were recorded in winter. These levels gradually increased throughout spring and peaked in summer and then started to decline during autumn until they reached their lowest levels in winter. There was a wide variation for UVA, UVB and temperature (Figure 22) in the different seasons experienced in South Africa.

The effectiveness of SUVR in reducing the number of *V. cholerae* in ground water as well as in inhibiting biomass turnover when grown in LB depended on the season of the year, on the solar conditions and on the duration of exposure to SUVR. In summer and autumn, the three *V. cholerae* strains grown in water were non-culturable and biomass increased was inhibited by SUVR when compared with days with similar solar conditions during winter or spring. Furthermore, in spite of a decrease in biomass, an increase in the release of cholera toxin was observed during summer and autumn suggesting that the cellular integrity of *V. cholerae* could have also been compromised. The effect of the duration of SUVR exposures on the behaviour of *V. cholerae* in water was also dependent on the seasons. In winter and spring when the intensity of SUVR was much lower, *V. cholerae* was still culturable even after 24 hours of solar exposure in contrast to similar exposures in the summer and autumn where 3 to 7 hours was sufficient to cause non-culturability. These results showed that there is a relationship (perhaps synergy) between the intensity of SUVR and temperature, and culturability of *V. cholerae*. This was, however, strain dependent; the virulent strains were found to be more sensitive to solar exposure in ground water compared to the environmental strain and a shorter period of exposure made them non-culturable. In some instances, regrowth was observed in samples collected overnight suggesting that in the absence of sunlight, *V. cholerae* underwent cellular repair. The GM1 ganglioside cholera toxin ELISA assay showed that for the two *V. cholerae* toxigenic strains, SUVR triggered an increase in

cholera toxin secretion although no culturability or increase in biomass was observed for these samples. The increase in CT secretion by the solar exposed samples could have resulted from the damage sustained by the cytoplasmic membrane due to SUVR. In addition the effect of SUVR on the secretion of CT was influenced by the media in which the toxigenic strains were exposed. Ground water favoured greater toxin release as opposed to LB. It is possible that LB afforded some form of protection (perhaps the bi-carbonate ions) to the microorganisms' cytoplasmic membrane which ground water was not able to.

Although the exact mode of action of SUVR is not well understood, various studies have shown that the dangerous O_2 radicals produced during solar exposures damage the cellular membrane integrity (Falcioni et al., 2008; Wang, Hammes, De Roy, Verstraete, & Boon, 2010). This was confirmed by the flow cytometric studies which showed that the cells were not able to exclude the infiltration of propidium iodide, a fluorescent dye known to enter cells with a compromised cytoplasmic membrane (Falcioni et al., 2008; Wang et al., 2010). The O_2 radicals produced during SUVR exposure appear to stress the microbial cell membranes, since it is the first line of defence against such compounds (Berney et al., 2007; Falcioni et al., 2008). The extent to which the cytoplasmic membrane was disrupted was also strain dependent as indicated by the density plots (Figures 49, 50, 53 and 54). After SUVR exposure, the cytoplasmic membrane was partially damaged and as the time of exposure increased the majority of these cells lost their overall cellular integrity (Figures 49 and 53). However, in some instances the density of cells with an intact cellular membrane increased in absence of SUVR (during the night). When cultured after 24hrs exposure in ground water there was no colony formation. This could possibly indicate that the microorganisms could survive in a viable but non-culturable state when exposed to SUVR in ground water. This could also explain the reason why in some cholera incidents the microorganisms from the environment could not be cultured (M. Du Preez, personal communication). It is likely that the microorganisms present in the contaminated water were in a VBNC state. As they passed through the body systems they fully recovered, multiplied and caused cholera.

SUVR did not affect the culturability of the three *V. cholerae* strains cultured in LB but only prevented them from increasing in biomass. This could have resulted from the presence of hydrogen bicarbonate ions in LB that dampened the effect of solar UVA by reacting with the dangerous free radicals generated from O_2 . Hydrogen bicarbonate ions in the natural environment has been shown to protect biological systems because the ions act as photo absorbers and limit light penetration into the bacterial suspension (Navntoft et al., 2008).

However, compromise of the cytoplasmic membrane of the microorganisms could have been one of the main reasons why there was more cholera toxin available in the environment especially that of the ground water. Cholera toxin was shown to be expressed and released in both ground water and LB regardless of the environmental conditions (Chapter 3 Section 3.7).

In this study the implication of SUVR and temperature for solar disinfection of water suggests that the effectiveness of the SODIS technique is dependent on the amount of SUVR and temperature which in turn was dependent on the season of the year. This agrees with previous reports (Navntoft et al., 2008; Oates, Shanahan, & Polz, 2003). Furthermore, on the basis of these results, it appears that in the natural environment less SUVR during winter enables these microorganisms to recover from the effects of solar radiation, while in spring they are able to multiply due to the increase in temperature. This may explain the lack of cholera incidents during winter and spring. However, due to the high SUVR and higher temperatures in summer and early autumn the microbes decrease in numbers due damage of the cell membrane. This enables the release of more cholera toxin leading to cholera. This analogy could offer some explanation for the possible reasons why cholera incidents and outbreaks in South Africa usually occur during summer and fade during autumn despite the presence of sunlight (Mugero & Hoque, 2001).

Solar conditions also played a major role second to the season of the year. The main driver of these conditions was the cloud systems specifically the dark clouds. The effect of the solar conditions on an overcast day with respect to the experiment done on the 29th of September 2009 did not result in the total loss of culturability (Figure 23). The same was observed in the cultures exposed to natural sunlight in LB on the 17th of November 2009 that resulted in no increase in biomass (Figure 29a and 29b). However SODIS on such days would require more than one days exposure or the use of solar concentrators if possible (Navntoft et al., 2008).

4.3 Conclusion

This study showed that the variation that exists in the levels of SUVR and temperature during the different seasons, over a one year period in Pretoria, South Africa, has implications for the treatment of water using SODIS. SODIS has been proven to be effective against the spread of cholera disease during epidemics in Kenya (Conroy et al., 2001). Some light has also been shed on the probable role that climate may have on the onset of cholera disease. SUVR exposure to a greater extent leads to disruption of *V. cholerae* cellular integrity; in addition it may induce VBNC states. On the other hand SUVR exposure may directly or indirectly induce the secretion of cholera toxin. This depends on the media in which the bacteria are growing and the season of the year.

The results from this study also suggest that the microorganisms may exist in a dormant state. Exposure to solar radiation does, however, compromise their overall integrity and if not sheltered by sediments or phytoplankton which often is the case in their natural habitat their recovery is not assured (Abd, Saeed, Weintraub, Nair, & Sandstrom, 2007).

SODIS can serve as a means of preventing the spread of cholera provided it is used all year round. This study complements the recommendations as well as conclusions stemming from other studies emphasising the need of a 2 day exposure, for total inactivation of microbial matter during days with partial sunlight, such as those experienced during spring, winter and cloudy days. The time required for total inactivation could be reduced if solar concentrators are utilized. However, this would increase the cost of the technology and will not be available in remote areas

4.4 Recommendations

The use of SODIS for disinfecting water should be adopted by communities worldwide especially in areas with the highest burden of water borne diseases such as cholera.

Sensitisation drivers should be employed to disseminate information relating to the use of SODIS as a means of disinfecting water for consumption.

More work is required to further understand the critical role that climate plays in the unfolding of water borne diseases like cholera.

Although SUVR exposure increases the release of cholera toxin the integrity of the cholera toxin after solar exposure needs to be investigated.

References

- Abd, H., Saeed, A., Weintraub, A., Nair, G. B., & Sandstrom, G. (2007). *Vibrio cholerae* O1 strains are facultative intracellular bacteria, able to survive and multiply symbiotically inside the aquatic free-living amoeba *Acanthamoeba castellanii*. *FEMS Microbiol Ecol*, *60*(1), 33-39.
- Acra, A., Jurdi, M., Mu'Allem, H., Karahagopian, Y., & Raffoul, Z. (1989). Sunlight as disinfectant. *Lancet*, *1*(8632), 280.
- Albert, I., & Mafart, P. (2005). A modified Weibull model for bacterial inactivation. *International Journal of Food Microbiology*, *100*(1-3), 197-211.
- Allen, M. J., Edberg, S. C., & Reasoner, D. J. (2004). Heterotrophic plate count bacteria--what is their significance in drinking water? *Int J Food Microbiol*, *92*(3), 265-274.
- Allman, R., Hann, A. C., Manchee, R., & Lloyd, D. (1992). Characterization of bacteria by multiparameter flow cytometry. *Journal of Applied Microbiology*, *73*(5), 438-444.
- Alonso-Sáez, L., Gasol, J. M., Lefort, T., Hofer, J., & Sommaruga, R. (2006). Effect of Natural Sunlight on Bacterial Activity and Differential Sensitivity of Natural Bacterioplankton Groups in Northwestern Mediterranean Coastal Waters. *Applied and Environmental Microbiology*, *72*(9), 5806–5813-5806–5813.
- Aoki, H., Wu, H., Nakano, T., Ooi, Y., Daikoku, E., Kohno, T., et al. (2009). Nanotransportation system for cholera toxin in *Vibrio cholerae* O1. *Med Mol Morphol*, *42*(1), 40-46.
- Arrage, A. A., Phelps, T. J., Benoit, R. E., & White, D. C. (1993). Survival of subsurface microorganisms exposed to UV radiation and hydrogen peroxide. *Applied and Environmental Microbiology*, *59*(11), 3545–3550-3545–3550.

Bailey, C. A., Neihof, R. A., & Tabor, P. S. (1983). Inhibitory Effect of Solar Radiation on Amino Acid Uptake in Chesapeake Bay Bacteria. *Applied and Environmental Microbiology*, 46(1), 44–49-44–49.

Barbesti, S., Citterio, S., Labra, M., Baroni, M. D., Neri, M. G., & Sgorbati, S. (2000). Two and three-color fluorescence flow cytometric analysis of immunoidentified viable bacteria. *Cytometry*, 40(3), 214-218.

Bartram, J., Cotruvo, J., Exner, M., Fricker, C., & Glasmacher, A. (2004). Heterotrophic plate count measurement in drinking water safety management: report of an Expert Meeting Geneva, 24-25 April 2002. *Int J Food Microbiol*, 92(3), 241-247.

Bergquist, P., Hardiman, E., Ferrari, B., & Winsley, T. (2009). Applications of flow cytometry in environmental microbiology and biotechnology. *Extremophiles*, 13(3), 389-401.

Berney, Hammes, F., Bosshard, F., Weilenmann, H.-U., & Egli, T. (2007). Assessment and Interpretation of Bacterial Viability by Using the LIVE/DEAD BacLight Kit in Combination with Flow Cytometry. *Appl. Environ. Microbiol.*, 73(10), 3283-3290.

Berney, Weilenmann, H. U., Simonetti, A., & Egli, T. (2006). Efficacy of solar disinfection of *Escherichia coli*, *Shigella flexneri*, *Salmonella Typhimurium* and *Vibrio cholerae*. *Journal of Applied Microbiology*, 101(4), 828-836.

Boyle, M., Sichel, C., Fernández-Ibáñez, P., Arias-Quiroz, G. B., Iriarte-Puñá, M., Mercado, A., et al. (2008). Bactericidal Effect of Solar Water Disinfection under Real Sunlight Conditions. *Applied and Environmental Microbiology*, 74(10), 2997–3001-2997–3001.

Caldwell, M. M., Bjorn, L. O., Bornman, J. F., Flint, S. D., Kulandaivelu, G., Teramura, A. H., et al. (1998). Effects of increased solar ultraviolet radiation on terrestrial ecosystems. *Journal of Photochemistry and Photobiology B: Biology*, 46, 40-52.

Carlucci, A. F., & Pramer, D. (1959). Factors Affecting the Survival of Bacteria in Sea Water. *Applied Microbiology*, 7(6), 388–392-388–392.

Cerf, O. (1977). A REVIEW Tailing of Survival Curves of Bacterial Spores. *Journal of Applied Microbiology*, 42(1), 1-19.

Cholera - Wikipedia, the free encyclopedia. (2010). Retrieved 8 November, 2010, from http://en.wikipedia.org/wiki/Cholera#cite_note-65

Conroy, R. M., Elmore-Meegan, M., Joyce, T., McGuigan, K. G., & Barnes, J. (1996). Solar disinfection of drinking water and diarrhoea in Maasai children: a controlled field trial. *The Lancet*, 348(9043), 1695-1697.

Conroy, R. M., Meegan, M. E., Joyce, T., McGuigan, K., & Barnes, J. (1999). Solar disinfection of water reduces diarrhoeal disease: an update. *Archives of Disease in Childhood*, 81(4), 337-338.

Conroy, R. M., Meegan, M. E., Joyce, T., McGuigan, K., & Barnes, J. (2001). Solar disinfection of drinking water protects against cholera in children under 6 years of age. *Arch Dis Child*, 85(4), 293-295.

Coutard, F., Crassous, P., Droguet, M., Gobin, E., Colwell, R. R., Pommepuy, M., et al. (2007). Recovery in culture of viable but nonculturable *Vibrio parahaemolyticus*: regrowth or resuscitation? *ISME J*, 1(2), 111-120.

Czechowska, K., Johnson, D. R., & van der Meer, J. R. (2008). Use of flow cytometric methods for single-cell analysis in environmental microbiology. *Current Opinion in Microbiology*, 11(3), 205-212.

David A. Relman, M. A. H. E. R. C., Alison & Mack, R. (2009). *Microbial Evolution and Co-Adaptation: A Tribute to the Life and Scientific Legacies of Joshua Lederberg*. Washington, D.C.: The National Academies Press.

Diffey, B. L. (1991). Solar ultraviolet radiation effects on biological systems. *Phys Med Biol*, 36(3), 299-328.

Diffey, B. L., & Roscoe, A. H. (1990). Exposure to solar ultraviolet radiation in flight. *Aviat Space Environ Med*, 61(11), 1032-1035.

Downes, A., & Blunt, T. P. (1877). Researches on the Effect of Light upon Bacteria and other Organisms. *Proceedings of the Royal Society of London*, 26, 488-500.

Echeverria, P., Harrison, B. A., Tirapat, C., & McFarland, A. (1983). Flies as a source of enteric pathogens in a rural village in Thailand. *Applied and Environmental Microbiology*, 46(1), 32-36-32-36.

Elasri, M. O., & Miller, R. V. (1999). Study of the Response of a Biofilm Bacterial Community to UV Radiation. *Applied and Environmental Microbiology*, 65(5), 2025-2031-2025-2031.

ESR LTD. (2001). *Vibrio cholerae* [Electronic Version]. Retrieved 12 Aug 2010, from <http://www.nzfsa.govt.nz/science/data-sheets/vibrio-cholerae.pdf>

Falcioni, T., Papa, S., Campana, R., Manti, A., Battistelli, M., & Baffone, W. (2008). State transitions of *Vibrio parahaemolyticus* VBNC cells evaluated by flow cytometry. *Cytometry Part B: Clinical Cytometry*, 74B(5), 272-281.

Frost, W. H. (1976). Cholera: synopsis of clinical aspects and principles of treatment. *Canadian Medical Association Journal*, 115(5), 401-403-401-403.

Fujioka, R. S., Hashimoto, H. H., Siwak, E. B., & Young, R. H. (1981). Effect of sunlight on survival of indicator bacteria in seawater. *Applied and Environmental Microbiology*, 41(3), 690-696-690-696.

Gaffga, N. H., Tauxe, R. V., & Mintz, E. D. (2007). Cholera: a new homeland in Africa? *Am J Trop Med Hyg*, 77(4), 705-713.

Gasol, J. M., Zweifel, U. L., Peters, F., Fuhrman, J. A., & Hagstrom, A. (1999). Significance of Size and Nucleic Acid Content Heterogeneity as Measured by Flow Cytometry in Natural Planktonic Bacteria. *Appl. Environ. Microbiol.*, 65(10), 4475-4483.

Geeraerd, A. H., Herremans, C. H., & Van Impe, J. F. (2000). Structural model requirements to describe microbial inactivation during a mild heat treatment. *International Journal of Food Microbiology*, 59(3), 185-209.

Geeraerd, A. H., Valdramidis, V. P., & Van Impe, J. F. (2005). GInaFiT, a freeware tool to assess non-log-linear microbial survivor curves. *International Journal of Food Microbiology*, 102(1), 95-105.

Goel, A. K., Jain, M., Kumar, P., Bhadauria, S., Kmboj, D. V., & Singh, L. (2008). A new variant of *Vibrio cholerae* O1 El Tor causing cholera in India. *J Infect*, 57(3), 280-281.

Heaselgrave, W., Patel, N., Kilvington, S., Kehoe, S. C., & McGuigan, K. G. (2006). Solar disinfection of poliovirus and *Acanthamoeba polyphaga* cysts in water - a laboratory study using simulated sunlight. *Letters in Applied Microbiology*, 43(2), 125-130.

Herz, K., Vimont, S., Padan, E., & Berche, P. (2003). Roles of NhaA, NhaB, and NhaD Na⁺/H⁺ Antiporters in Survival of *Vibrio cholerae* in a Saline Environment. *Journal of Bacteriology*, 185(4), 1236–1244-1236–1244.

Hewitt, C. J., Caron, G. N.-V., Nienow, A. W., & McFarlane, C. M. (1999). Use of multi-staining flow cytometry to characterise the physiological state of *Escherichia coli* W3110 in high cell density fed-batch cultures. *Biotechnology and Bioengineering*, 63(6), 705-711.

Joux, F., Jeffrey, W. H., Lebaron, P., & Mitchell, D. L. (1999). Marine Bacterial Isolates Display Diverse Responses to UV-B Radiation. *Applied and Environmental Microbiology*, 65(9), 3820–3827-3820–3827.

Kalbfleisch, J. D., & Prentice, R. L. (1980). *The Statistical Analysis of Failure Time Data*. New York: Wiley.

Kamiya, E., Izumiyama, S., Nishimura, M., Mitchell, J., & Kogure, K. (2007). Effects of fixation and storage on flow cytometric analysis of marine bacteria. *Journal of Oceanography*, 63(1), 101-112.

Kassen, R., & Bataillon, T. (2006). Distribution of fitness effects among beneficial mutations before selection in experimental populations of bacteria. *Nat Genet*, 38(4), 484-488.

Kirschner, A. K. T., Schlesinger, J., Farnleitner, A. H., Hornek, R., Süß, B., Golda, B., et al. (2008). Rapid Growth of Planktonic *Vibrio cholerae* Non-O1/Non-O139 Strains in a Large Alkaline Lake in Austria: Dependence on Temperature and Dissolved Organic Carbon Quality. *Applied and Environmental Microbiology*, 74(7), 2004–2015-2004–2015.

Kramer, G. F., Baker, J. C., & Ames, B. N. (1988). Near-UV stress in *Salmonella typhimurium*: 4-thiouridine in tRNA, ppGpp, and ApppGpp as components of an adaptive response. *Journal of Bacteriology*, 170(5), 2344–2351-2344–2351.

Lawless, J. F. (2002). *Statistical Models and Methods for Lifetime Data*. New York: Wiley.

McGuigan, K. G., Joyce, T. M., Conroy, R. M., Gillespie, J. B., & Elmore-Meehan, M. (1998). Solar disinfection of drinking water contained in transparent plastic bottles: characterizing the bacterial inactivation process. *Journal of Applied Microbiology*, 84(6), 1138-1148.

Merrell, D. S., Tischler, A. D., Lee, S. H., & Camilli, A. (2000). *Vibrio cholerae* Requires rpoS for Efficient Intestinal Colonization. *Infection and Immunity*, 68(12), 6691–6696-6691–6696.

Midgley, M. (1987). An efflux system for cationic dyes and related compounds in *Escherichia coli*. *Microbiol Sci*, 4(4), 125-127.

Morris, D. P., Zagarese, H., Williamson, C. E., Balseiro, E. G., Hargreaves, B. R., Modenutti, B., et al. (1995). The Attenuation of Solar UV Radiation in Lakes and the Role of Dissolved Organic Carbon. *Limnology and Oceanography*, 40(8), 1381-1391.

Morris, J. G., Szein, M. B., Rice, E. W., Nataro, J. P., Losonsky, G. A., Panigrahi, P., et al. (1996). *Vibrio cholerae* O1 can assume a chlorine-resistant rugose survival form that is virulent for humans. *The Journal of Infectious Diseases*, 174(6), 1364-1368.

Mugero, C., & Hoque, A. (2001). Review of cholera epidemic in South Africa, with focus on Kwazulu-natal Province. Retrieved 20 September, 2010, from <http://www.kznhealth.gov.za/cholerareview.pdf>

Nackerdien, Z. E., Keynan, A., Bassler, B. L., Lederberg, J., & Thaler, D. S. (2008). Quorum Sensing Influences *Vibrio harveyi* Growth Rates in a Manner Not Fully Accounted For by the Marker Effect of Bioluminescence. *PLoS ONE*, 3(2), e1671-e1671.

Navntoft, C., Ubomba-Jaswa, E., McGuigan, K. G., & Fernández-Ibáñez, P. (2008). Effectiveness of solar disinfection using batch reactors with non-imaging aluminium reflectors under real conditions: Natural well-water and solar light. *Journal of Photochemistry and Photobiology B: Biology*, 93(3), 155-161.

Nebe-von-Caron, G., Stephens, P. J., Hewitt, C. J., Powell, J. R., & Badley, R. A. (2000). Analysis of bacterial function by multi-colour fluorescence flow cytometry and single cell sorting. *Journal of Microbiological Methods*, 42(1), 97-114.

Oates, P. M., Shanahan, P., & Polz, M. F. (2003). Solar disinfection (SODIS): simulation of solar radiation for global assessment and application for point-of-use water treatment in Haiti. *Water Res*, 37(1), 47-54.

Ogg, J. E., Ryder, R. A., & Jr, H. L. S. (1989). Isolation of *Vibrio cholerae* from aquatic birds in Colorado and Utah. *Applied and Environmental Microbiology*, 55(1), 95–99-95–99.

Oliver, J. D. (2005). The viable but nonculturable state in bacteria. *Journal of Microbiology (Seoul, Korea)*, 43 Spec No, 93-100.

Osei, F. B., & Duker, A. A. (2008). Spatial dependency of *V. cholera* prevalence on open space refuse dumps in Kumasi, Ghana: a spatial statistical modelling. *International Journal of Health Geographics*, 7, 62-62.

Parisi, A. V. (2005). Physics concepts of solar ultraviolet radiation by distance education. *European Journal of Physics*, 26, 313-320.

Patrick, M. H., & Rahn, R. O. (1976). Photochemistry of DNA and polynucleotides: photoproducts. *Photochemistry and Photobiology of Nucleic Acids*, II, 35-95.

Peterson, K. M. (2002). Expression of *Vibrio cholerae* virulence genes in response to environmental signals. *Curr Issues Intest Microbiol*, 3(2), 29-38.

Qiu, X., Sundin, G. W., Chai, B., & Tiedje, J. M. (2004). Survival of *Shewanella oneidensis* MR-1 after UV Radiation Exposure. *Applied and Environmental Microbiology*, 70(11), 6435–6443-6435–6443.

Sachidanandham, R., Gin, K. Y.-H., & Poh, C. L. (2005). Monitoring of active but non-culturable bacterial cells by flow cytometry. *Biotechnology and Bioengineering*, 89(1), 24-31.

Safapour, N., & Metcalf, R. H. (1999). Enhancement of Solar Water Pasteurization with Reflectors. *Applied and Environmental Microbiology*, 65(2), 859–861-859–861.

Sinton, L. W., Finlay, R. K., & Lynch, P. A. (1999). Sunlight Inactivation of Fecal Bacteriophages and Bacteria in Sewage-Polluted Seawater. *Applied and Environmental Microbiology*, 65(8), 3605–3613.

Skorupski, K., & Taylor, R. K. (1997). Cyclic AMP and its receptor protein negatively regulate the coordinate expression of cholera toxin and toxin-coregulated pilus in *Vibrio cholerae*. *Proc Natl Acad Sci U S A*, 94(1), 265-270.

Smith, R. J., Kehoe, S. C., McGuigan, K. G., & Barer, M. R. (2000). Effects of simulated solar disinfection of water on infectivity of *Salmonella typhimurium*. *Letters in Applied Microbiology*, 31(4), 284-288.

Srivastava, P., Fekete, R. A., & Chattoraj, D. K. (2006). Segregation of the Replication Terminus of the Two *Vibrio cholerae* Chromosomes. *Journal of Bacteriology*, 188(3), 1060–1070.

Steen, H. B. (2000). Flow cytometry of bacteria: glimpses from the past with a view to the future. *Journal of Microbiological Methods*, 42(1), 65-74.

Toth, B., & Dose, K. (1976). Photochemically induced cross-links between DNA and alcohol dehydrogenase or salmine, respectively. *Radiat Environ Biophys*, 13(2), 105-113.

Ubomba-Jaswa, E., Boyle, M. A. R., & McGuigan, K. G. (2008). Inactivation of enteropathogenic *E. coli* by solar disinfection (SODIS) under simulated sunlight conditions. *Journal of Physics: Conference Series*, 101, 012003-012003.

Unknown. (2010a). South Africa's weather and climate - SouthAfrica.info. Retrieved 07 September 2010, 2010, from <http://www.southafrica.info/travel/advice/climate.htm>

Unknown. (2010b). Weather Station History : Weather Underground. Retrieved 07 September 2010, 2010, from <http://www.wunderground.com/weatherstation/WXDailyHistory.asp?ID=I00017B6>

Vives-Rego, J., Lebaron, P., & Nebe-von Caron, G. (2000). Current and future applications of flow cytometry in aquatic microbiology. *FEMS Microbiol Rev*, 24(4), 429-448.

Walberg, M., Gaustad, P., & Steen, H. B. (1999). Uptake kinetics of nucleic acid targeting dyes in *S. aureus*, *E. faecalis* and *B. cereus*: a flow cytometric study. *Journal of Microbiological Methods*, 35(2), 167-176.

Wang, Y., Hammes, F., De Roy, K., Verstraete, W., & Boon, N. (2010). Past, present and future applications of flow cytometry in aquatic microbiology. *Trends in Biotechnology*, 28(8), 416-424.

Weinbauer, M. G., Wilhelm, S. W., Suttle, C. A., & Garza, D. R. (1997). Photoreactivation compensates for UV damage and restores infectivity to natural marine virus communities. *Applied and Environmental Microbiology*, 63(6), 2200–2205-2200–2205.

WHO. (1996). *Guidelines for Drinking-Water Quality, Health Criteria and Other Supporting Information*. Geneva Switzerland: World Health Organization. Document Number)

WHO. (2002). Ultraviolet radiation: global solar UV index An educational tool to reduce risks of skin cancer and cataract. Retrieved 27 October, 2009, from <http://www.who.int/mediacentre/factsheets/fs271/en/print.html>

WHO. (2006). *Weekly epidemiological record*. Geneva, Switzerland: World Health Organization. Document Number)

Wyss, O. (1956). Microbial Adaptation. *Industrial & Engineering Chemistry*, 48(9), 1404-1406.

Xu, H. S., Roberts, N., Singleton, F. L., Attwell, R. W., Grimes, D. J., & Colwell, R. R. (1982). Survival and viability of nonculturable *Escherichia coli* and *Vibrio cholerae* in the estuarine and marine environment. *Microbial Ecology*, 8(4), 313-323.

Xue, Y., & Nicholson, W. L. (1996). The two major spore DNA repair pathways, nucleotide excision repair and spore photoproduct lyase, are sufficient for the resistance of *Bacillus subtilis* spores to artificial UV-C and UV-B but not to solar radiation. *Applied and Environmental Microbiology*, 62(7), 2221–2227-2221–2227.